

---

# Application of sediment budget analysis to an alpine torrential system

Hazard assessment of a subcatchment of the Riou Bourdoux system, southern France

---



---

D. F. Jager  
November 2001  
Department of Physical Geography  
Faculty of Geographical Sciences  
Utrecht University

Supervisor  
Dr. H. van Steijn

---

## Preface

I would like to thank the following persons for their support during the many, many months of I've struggled with this report.

For their company and efforts during and after the fieldwork, I would like to thank Petra Spee, Saskia Visser and Anneke de Joode. Special thanks to Anneke and Saskia for their personal encouragements in the last few years..

My thanks also go out to Dr. H. van Steijn for his professional support during the fieldwork and his unrelenting patience in the years after.

On a more personal note, I would like to thank my family and especially Tessa van Keeken for their support during the moments when the prospect of ever finishing this report was very grim indeed.

Finally (but foremost) I would like to thank God for granting me the patience and perseverance I needed for the accomplishment of this work.

## Abstract

In the summer of 1997 a research was undertaken in a subcatchment of the Riou Bourdoux system near Barcelonnette, Alpes de Haute-Provence, France. This torrential system is notorious for its high process activity, especially concerning laves torrentielles (debris flows), which occasionally pose a severe risk to infrastructure and residences in the area. In order to make predictions about the size and frequency of occurrence of these events and to assess process-activity in general, a sediment budget analysis according to Reid & Dunne (1996) is applied.

During the research the relative importance of active processes in the subcatchment was successfully determined. Some quantitative estimates about the volumes of transported and stored sediment on the hillslopes by the different processes were made (in order-of-magnitude). Since the frequency and magnitude of some processes were undeterminable, a complete sediment budget could not be constructed.

The investigated subcatchment is, in its present state, unable to produce a lave torrentielle mobile enough to reach to valley river. Only a subcatchment investigated by Spee & Visser (1999) is able to produce these events.

The results of the investigation were used to create a GIS model, which accurately simulates debris flow propagation through the drainage network of the subcatchment.

# Contents

<b>1</b>	<b>Introduction</b>	<b>7</b>
1.1	Framework and purpose of the research	7
1.2	Problem and hypothesis	8
1.3	Study area	10
1.3.1	Geology	10
1.3.2	Geomorphology	12
1.3.3	Climate	15
1.3.4	Vegetation	16
1.3.5	Studied subcatchment	17
<b>2</b>	<b><i>Theoretical background</i></b>	<b>18</b>
2.1	Introduction to sediment budget analysis	18
2.2	Hillslope processes	20
2.2.1	Erosion on hillslopes by raindrops and flowing water	20
2.2.2	Mass wasting	26
2.2.3	Debris flows	29
2.3	Storage elements	34
2.3.1	Colluvial storage	35
2.3.2	Channel storage	36
2.4	Sediment budget analysis (linkages)	38
<b>3</b>	<b><i>Methods</i></b>	<b>39</b>
3.1	Construction of a sediment budget	39
3.2	Mapping techniques	40
3.2.1	Geomorphological mapping	41
3.2.2	Thematic mapping	42
3.2.3	Map construction	42
3.2.4	Mapping debris flow and channel features	43
3.2.5	Mapping old debris flow deposits	44
3.2.6	Identification of debris flow source zones and colluvial storages	45
3.2.7	Channel process measurements	46
3.3	Hydrological measurements	50
3.3.1	Rainfall measurements	50
3.3.2	Infiltration capacity measurements on crucial landscape..	52
3.3.3	Discharge measurements	56
3.3.4	Suspended sediment load measurements	59
3.4	Methods to determine the shear strength of Terres Noires	60
3.4.1	Direct shear test	60
3.4.2	Stability analysis	61
3.5	Dating techniques	62
3.5.1	Dendrochronology	62
3.5.2	Lichenometric dating	63
<b>4</b>	<b><i>Results</i></b>	<b>64</b>
4.1	Detailed description of study area	64
4.1.1	Upper debris slopes	64
4.1.2	Morainic ‘threshold’	65
4.1.3	Old landslide	66
4.1.4	Terres Noires slopes	68
4.1.5	Linkages	68

4.2	Hydrological results	70
4.2.1	Rainfall characteristics	70
4.2.2	Saturated conductivity and sorptivity	71
4.2.3	Discharge and suspended load of the Riou Bourdoux	73
4.3	Debris flow and channel process results	74
4.3.1	Debris flow characteristics	74
4.3.2	Channel process activity	78
4.4	Other results	79
4.4.1	Shear strength of Terres Noires	79
4.4.2	Landslide and debris-flow frequencies	80
<b>5</b>	<b><i>Debris-flow model of the Riou de la Pare catchment</i></b>	<b>81</b>
5.1	A partial sediment budget for the Riou de la Pare catchment	81
5.2	PCRaster modeling	83
5.3	Model construction	85
5.3.1	Initial assumptions and values	86
5.3.2	Sediment production	87
5.3.3	The debris-flow ‘trigger’	89
5.3.4	Debris-flow initiation	90
5.3.5	Debris-flow propagation	91
5.3.6	Debris-flow routing	92
5.4	Model results	93
<b>6</b>	<b><i>Discussion</i></b>	<b>95</b>
6.1	Hydrological interpretations	95
6.1.1	Methodological discussion	95
6.1.2	Rainfall-runoff relationship	97
6.2	GIS-model discussion	98
6.3	Long-term catchment development	100
<b>7</b>	<b><i>Conclusions</i></b>	<b>106</b>
	<b><i>References</i></b>	<b>108</b>

### ***List of tables***

Table 1.1	Mean monthly precipitation and temperature data...	16
Table 2.1	Intensity of erosion processes in the rill... (Van Asch, 1996)	22
Table 2.2	Classification scheme of Varnes (1975)	27
Table 4.1	Rainfall amount at various altitudes in the Riou Bourdoux catchment	70
Table 4.2	The duration and amount of a few rain-events registered...	71
Table 4.3	Sorptivity and $K_{sat}$ of the 4 different sites...	72
Table 4.4	Qualitative indications of overland flow based...	72
Table 4.5	Calculated discharges and sediment load for every measurement	73
Table 4.6	Summary of the characteristics of the analyzed debris flow deposits	75
Table 4.7	Summary of all observed initiation, deposition and junction angles	78
Table 4.8	Qualitative comparison between discharge and cross-section...	78
Table 4.9	Measured diameter (thalli) of the lichens...	80
Table 5.1	The different landscape-units with the corresponding “erosion”-values	87
Table 5.2	Slope-angle classes	88
Table 6.1	Measured amount of sediment load compared to the relative amount of...	98

**List of figures**

Figure 1.1	Location of the Riou Bourdoux catchment	7
Figure 1.2	Structural scheme of the French-Italian Alps	11
Figure 1.3	Approximate location of various geological units (Cl. Kerckhove, 1969)	12
Figure 1.4	The Southern French Alps from the end... (Jorda, 1994)	13
Figure 1.5	Slope orientation and solar radiation (Douguedroit, 1976)	15
Figure 1.6	Photographs showing the Riou Bourdoux system	17
Figure 2.1	Flowchart of linkages (Reid & Dunne, 1996)	19
Figure 2.2	The effect of rainsplash erosion in combination with slope gradient	21
Figure 2.3	Photograph showing typical rill erosion	22
Figure 2.4	Slope contours	23
Figure 2.5	Gully pattern development on concave slopes (Faulkner, 1995)	25
Figure 2.6	Transport mass of soil... (Jahn, 1981)	27
Figure 2.7	Features of a slump (Selby, 1993)	28
Figure 2.8	St.Venant elastoplastic solid (Selby, 1993)	28
Figure 2.9	Stress-strain curves (Selby, 1993)	28
Figure 2.10	Typical morphology of hillslope debris flow... (Blijenberg, 1998)	30
Figure 2.11	Flowchart of debris-flow initiation according to Blijenberg (1998)	31
Figure 2.12	Flowchart for predicting deposition of debris flows (Benda & Cundy, 1990)	33
Figure 2.13	Geometry and terminology of stream junction (Benda & Cundy, 1990)	34
Figure 3.1	Examples of increasingly complex flowcharts... (Reid & Dunne, 1996)	40
Figure 3.2	Section of the Riou de la Pare flowing through debris-flow deposits...	44
Figure 3.3	Photograph and sketch of the investigated channel-midsection...	47
Figure 3.4	Schematic representation of the main channel of the Riou Bourdoux...	49
Figure 3.5	Rain gauges used during the fieldwork	50
Figure 3.6	Infiltration envelope	52
Figure 3.7	A researcher handling the ground bore	53
Figure 3.8	Inversed augerhole method (Kessler & Oosterbaan, 1974)	53
Figure 3.9	A) Drawing of the sudden input tracer method...	57
Figure 3.10	Shear strength versus normal stress for a specimen with cohesion	60
Figure 3.11	Example of curved trees found in the Riou Bourdoux catchment	62
Figure 3.12	Relation between the age of the lichen... (Orombelli & porter, 1983)	63
Figure 4.1	Block diagram of the investigated area (De Jooode, 2000)	64
Figure 4.2	Photograph of two gullies in the upper debris slopes	65
Figure 4.3	Photograph showing the debris slopes and morainic threshold...	65
Figure 4.4	Debris flow / avalanche track at observation point 37	67
Figure 4.5	Photograph of the 2 <sup>nd</sup> order channel near observation point 6...	69
Figure 4.6	Graph showing the relationship between rainfall and altitude...	70
Figure 4.7	Graph showing the relationship between measured discharge...	73
Figure 4.8	Flow-path of the observed small-scale debris flow...	74
Figure 5.1	Flow-chart of the sediment budget recommended for...	81
Figure 5.2	Overview of the imported PCRaster maps	84
Figure 5.3	New simplified river-pattern	86
Figure 5.4	Location of the different landscape-units	88
Figure 5.5	Flow-chart depicting the sediment production of the model	89
Figure 5.6	Flow-chart of the initiation of debris flows in the PCRaster model	90
Figure 5.7	Flow-chart of the entire debris flow routing model	93
Figure 5.8	Results of time-step 50	93
Figure 5.9	Graph showing the mass-balance difference at each time-step	94
Figure 6.1	Graph showing the discharge and rainfall data against time	97
Figure 6.2	Graph showing the sediment load versus discharge	97
Figure 6.3	Orientation of the three subcatchments	101
Figure 6.4	Insolation-controlled process response of a hypothetical south-exposed...	101
Figure 6.5	Outflow-point of the Riou Chamous at the confluence point	102
Figure 6.6	Schematic longitudinal profile of in-channel gullying at the confluence point	104

# 1 Introduction

## 1.1 Framework and purpose of the research

This report is part of the result of a research undertaken in the Riou Bourdoux catchment, Ubaye valley, Alpes de Haute-Provence, France (figure 1.1). It was conducted by four students during a period of eight weeks in the summer of 1997. The research forms an integral part of the MSc-program of Physical Geography at Utrecht University, The Netherlands.

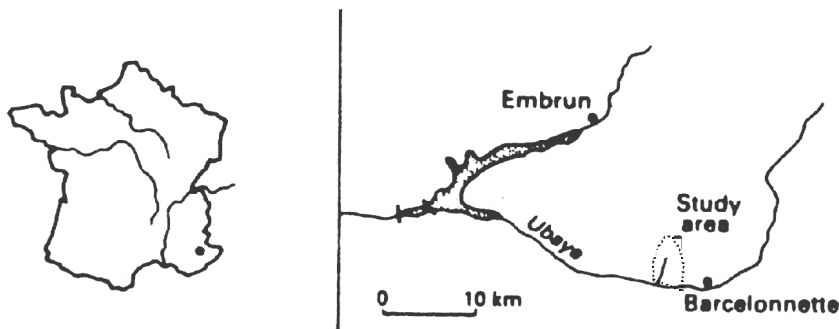


Figure 1.1 Location of the Riou Bourdoux catchment in France.

Certain parts of the French Alps, including the valley of the Ubaye, and indeed many valleys in many alpine mountain regions are severely exposed to hazards from torrential systems. These systems usually consist of steep tributary catchments. General aspects of such systems are a complex internal structure with regard to morphology, activity of geomorphologic processes and hydrological behaviour. The geomorphic processes comprise a multitude of hillslope and channel processes. These different processes, especially with regard to erosion, operate either discontinuously through time in (large) fluxes or they operate continuously and more slowly over longer time-scales. The former is known as discrete and the latter as chronic (erosion) processes (Reid & Dunne, 1996). The interaction between these processes obviously results in the high complexity of such systems and moreover, anthropogenic influence on these systems raises the complexity even further.

The specific problems concerning torrentiality in the Ubaye valley are the result of several unique factors. These factors include the presence of highly erodable black marls (i.e. the 'Terres Noires'), the nature of present-day precipitation patterns, the history of glaciation, and man's extensive influence in the region. These will be explained in the next section. These factors have resulted in an area dominated by torrential systems. The Riou Bourdoux catchment is the largest of these systems within the Ubaye Valley.

Possibly the most important and dangerous form of sediment transport processes in systems as the Riou Bourdoux, is the 'lave torrentielle'. This is a typical, highly mobile debris flow (a channel process) capable of reaching the floor of the Ubaye Valley. This may result in damage to houses, infrastructure and possibly the damming of the Ubaye itself causing severe flooding. Research on alluvial fans in the valley of the Ubaye has revealed 'laves

torrentielles' activity throughout much of the Holocene (Jorda, 1983; Jorda, 1987), with an increase in recent centuries by man's influence (deforestation, cattle grazing, etc).

Although much is being done to prevent damage caused by such systems, in many cases the risk they pose cannot be fully controlled. This is because on one hand activity in such systems may continue, although at a reduced intensity or frequency of occurrence. On the other hand the occurrence of high-magnitude, low-frequency events may still raise the potential hazard of such systems because this may simply not be envisaged by present damage prevention plans. This has certainly been shown to occur on a large-scale the last few years in several European countries (Spain, 1996 and Italy, 1998). In the Ubaye valley as well, there was the blocking of the main road by a 'lave torrentielle' in august 1996. These examples show that these systems can still be hazardous and as such new attention to hazard assessment must be given.

The purpose of this study is to obtain detailed knowledge about process activity in general and debris flows in particular, including their spatial and temporal variation, within a subcatchment of the Riou Bourdoux system. The study will be focused upon the identification of storage elements, serving as possible initiation sites of debris flows, and on debris flow routing, for identifying possible paths and deposition sites. Further attention in the research will also be given to the specific conditions required to initiate a debris flow and upon developing a GIS<sup>1</sup> model that can predict the occurrence and the routing of debris flows.

## 1.2 Problem and hypothesis

In order to obtain the information about process-activity, several questions about sediment production and transportation processes on slopes and in channels, and about the specific conditions required for the formation of a debris flow have to be answered. The following research objectives were formulated for this purpose:

### 1.2.1 Concerning hillslope processes<sup>2</sup>:

- Which processes are present in the subcatchment? And where are these processes located within this catchment?
- Which processes are most important in delivering sediment to the gullies and channels or storage elements on the slopes?
- How much sediment is produced, transported and stored on hillslopes?

### 1.2.2 Concerning channel<sup>3</sup> processes:

- Which processes are active in the channels?
- Which processes are most important in transporting sediment out of the catchment?
- How much mobile sediment is stored on the channel-floor and how much sediment is transported?

---

<sup>1</sup> A GIS model is model which can process and transform spatial data for a particular set of purposes with the aid of computer based databases and tools (Burrough, 1986)

<sup>2</sup> In this report a hillslope includes channels up to 2<sup>nd</sup> order (gullies)

<sup>3</sup> Channels refer to channels of 3<sup>rd</sup> order and higher

*Concerning debris flow initiation:*

- What are the strength characteristics of slope materials at possible initiation sites? (cohesion, angle of internal friction)
- What are the infiltration capacities of these materials?
- What is the slope gradient at known initiation sites?
- Under what conditions does an active debris flow incorporate sediment, which is stored in the gullies and channels? (Discharge, type of sediment, gradient)

*Concerning the deposition of debris flows:*

- Where can deposits of debris flows be found?
- What are the lithological, morphological and sedimentological characteristics of the debris flow deposits?
- What role do specific channel features play in the deposition of debris flows?

In order to unravel the very complicated nature of this large torrential system, an approach using sediment budget analysis (Reid & Dunne, 1996) has been selected. This approach allows for the identification of the most important elements of the system, with regard to sediment production and transport. It also reveals the functional relationships between these elements. This approach appears to give estimates about quantities of mobilized material and frequencies of events that are better than order-of-magnitude (Reid & Dunne, 1996).

This approach, which is fully explained in the next chapter, will be linked with two models. One for predicting the initiation of debris flows, a model by Blijenberg (1998). The other for predicting the routing of debris flows through a catchment, a model by Benda and Cundy (1990). These models are explained in chapter 2.

The linking of the sediment budget analysis with these two models will result in a sediment budget of a subcatchment (section 1.3.5) within the Riou Bourdoux system. From this linkage the proportion of debris flows in the sediment budget, as an erosion- as well as a transportation-process, will be estimated. Together with estimates of frequency of occurrence and possible deposition sites, an attempt will be made to develop a debris flow routing model. This 'initiation and routing' model will be incorporated as a computer-model in a GIS.

This report first describes the specific geological and topographical characteristics of the Barcelonnette Basin in general and gives an overview of the investigated subcatchment within the Riou Bourdoux system in particular. Following, the theoretical aspects of sediment budget analysis and the hillslope and channel processes are given in chapter 2. Chapter 3 gives a description of all the applied methods, both field and laboratory, and the way in which their results are used in the sediment budget. Next, in chapter 4, a detailed description of the study area and the results of the applied methods and the constructed sediment budget are shown. Chapter 5 describes the development (and results) of the debris-flow routing model made in a GIS based on this sediment budget. Finally, the results are discussed in chapter 6 and a conclusion is given in chapter 7.

Many links to the reports of Spee & Visser (1999) en De Joode (2000) are made throughout this report. These are the three other students with whom the author cooperated during the fieldwork. In this report special emphasis is placed on mapping techniques, the

specific hydrological processes working within the Riou Bourdoux catchment and the construction of the GIS model. For a detailed analysis of hillslope processes the reader is referred to De Joode (2000). The report of Spee & Visser (1999) tackles the activity and frequency of processes and the modeling of a sediment budget in a GIS.

### 1.3 Study area

The study area (appendix A1) lies within the Barcelonnette Basin, situated in the middle-part of the Ubaye Valley (figure 1.1). The area is situated 5 kilometers west-northwest of the town of Barcelonnette (some 140 km northwest of Nice).

The basin stretches approximately 15 km from east to west and some 10 km from north to south. The altitude varies between about 1100 m (a.s.l.) at the valley floor to approximately 3100 m at the summits. Within the basin there is a high concentration of torrential systems and large landslides indicating numerous unstable areas. This instability of the landscape can be explained by the interaction of various unfavourable factors. These are not only the combination of geological, geomorphological, climatological and hydrological characteristics, but equally important are the anthropogenic influence and changes of land use in the history of the valley.

#### 1.3.1 Geology

The western French Alps stretch from Lake Geneva to the Mediterranean Sea. The Alps are subdivided into a number of structural units, which are grouped into two zones:

1. The external zone, being the western outer edge of the Alps, and
2. The internal zone, being the eastern interior of the Alps (figure 1.2).

The Barcelonnette Basin is situated in a part of the internal zone, called the Embrunais. The Embrunais is located between the Pelvoux and Argentera massifs, which are composed of crystalline rock. Due to extensive folding and difference in uplift of the crystalline subsurface (being low around the present Durance and Ubaye valleys), and subsequent erosion, a large 'window' in the rock units developed surrounding the Barcelonnette Basin. This 'window' of Barcelonnette predominantly exposes autochthonous bedrock, called the 'Terres Noires'. The Terres Noires is a highly erodible black marl from the Oxfordian (Jurassic period). This rock-type is located at the base of every slope within the Basin. In the center of the basin, around Barcelonnette, it reaches fairly high upslope (some 1500 to 2000 m a.s.l.).

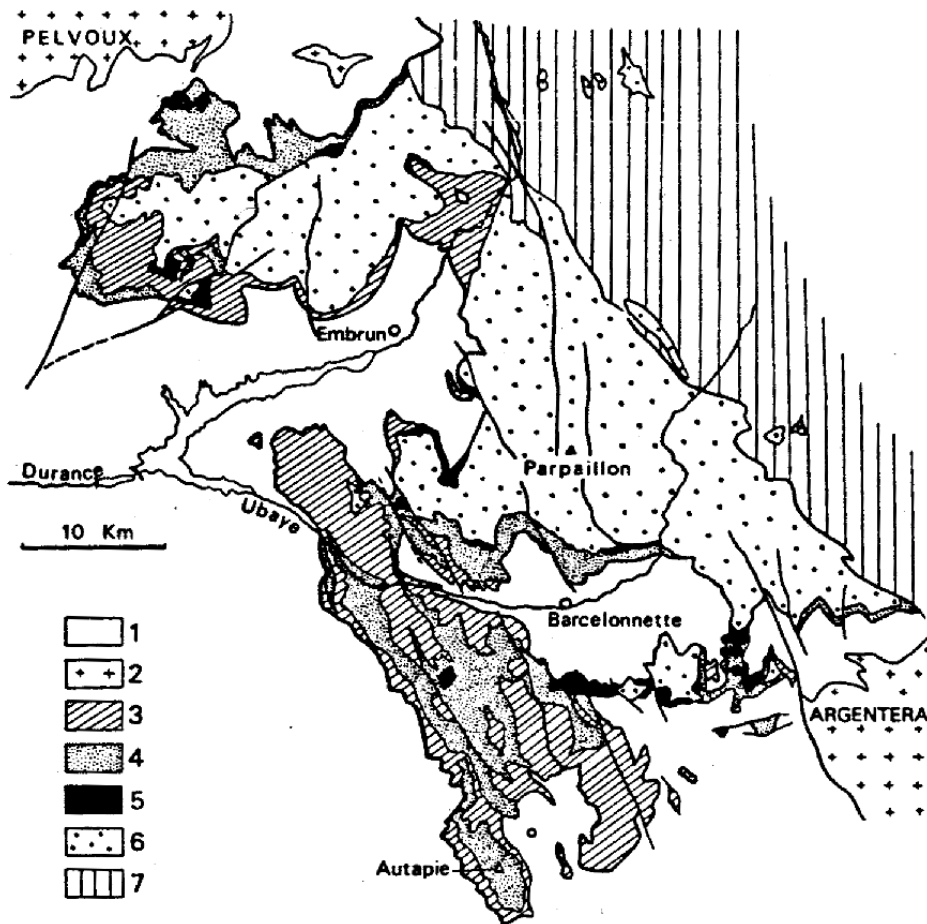


Figure 1.2 Structural scheme of the French-Italian Alps (internal zone: Embrunais). 1. Zone Dauphinoise; 2. Massifs cristallins externs; 3. Écailles subbriançonnaises associées au Flysch de l'Autapie; 4. Flysch de l'Autapie; 5. Écailles subbriançonnaises et briançonnaises associées au Flysch du Parpaillon; 6. Flysch du Parpaillon; 7. Zone briançonnaise (Debelmas, 1974).

On this base of marls two nappes are situated (Debelmas, 1970 & 1974). During the Late-Eocene uplifting occurred in the zone Piémontaise. This is an area to the east of the basin in the internal zone. This uplift resulted in the thrusting of a non-autochthonous nappe on top of the black marls. This nappe is known as the 'nappe de l'Autapie' and consists of flysch (mainly schists and limestones).

During the Late-Oligocene, Early-Miocene another nappe moved westward from the Piémontaise zone. This unit also consists of flysch deposits (limestone and sandstone) and is called the 'nappe du Parpaillon'. Both nappes are referred to as the 'Flysch à Helminthoïdes'. These pre-Quaternary geological units: the Terres Noires and the Flysch à Helminthoïdes are approximately located around and within the study-area as shown in figure 1.3.

For a more detailed description of the geology of the study area the reader is referred to Spee & Visser (1999).

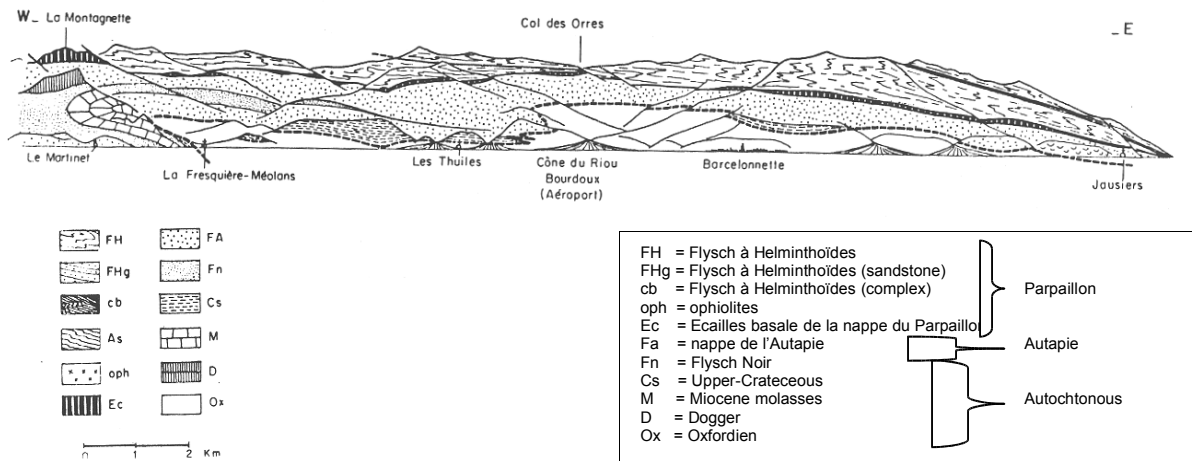


Figure 1.3 Approximate location of the various geological units in and around the study-area (Cl. Kerckhove, 1969).

### 1.3.2 Geomorphology

The present appearance of the Riou Bourdoux catchment has developed under influence of several geomorphological processes superimposed in time and space, and active since the Pleistocene (figure 1.4). Of importance are:

- The presence of glaciers (during the Pleistocene),
- The impact of periglacial conditions on transforming slopes (during the Pleistocene and on higher slopes during the Holocene),
- Incision and erosion by running water during the Holocene
- Consecutive transformations of slopes by mass-movements
- The influence of man since the Subborreal.

#### Pleistocene

During the several glacial periods of the Pleistocene, many of the alpine glaciers in the Alps expanded into the lower parts of the river valleys. During the last glacial period, the Würm, the Ubaye valley was also glaciated (Jorda, 1988). This passage of the Ubaye valley glacier significantly modified the existing morphology. It caused considerable erosion, creating a U-shaped valley with a broad valley bottom and very steep slopes along its edges.

The glacier also deposited much moraine material. These moraine deposits occupy a large part of the slopes within the Barcelonnette window. Their thickness appears to be up to 20 to 30 meters in some places. These deposits were formed below and on the edges of the valley-glacier that reached to a maximum of about 2000 m a.s.l.

On the glacier-free upper-slopes conditions arose for the action of periglacial processes. Of importance in high-mountain areas are frost weathering, solifluction, frost creep and cirque formation.

Cirques produce their own moraines and especially where valley-glaciers and cirques meet, the largest amount of moraines can usually be found (Summerfield, 1992). Due to the shape of several subcatchments, indicating possible ancient cirques, this might also hold true for the Riou Bourdoux system.

During the glacial periods, frost weathering on the upper-slopes may have had considerable influence, which in turn produced even more debris. This debris was transported down-slope to the edge of the glacier, where it fed the side-moraine deposits.

Frost weathering is very effective with diurnal freeze-thaw cycles, the presence of moisture, a minimum temperature of -5°C and rapid freezing conditions (Summerfield, 1992). This seems to suggest that during the glacial periods, frost weathering on surfaces not covered by the ice (above 2000 m) was effective mostly on south-exposed slopes (i.e. adrets) (including the slopes of the Riou Bourdoux) and in summer months.

So during the last glacial period, predominant glacier activity scoured cirques and the valley floor and deposited large amounts of moraines on the valley-slopes at an altitude around 2000 m a.s.l.

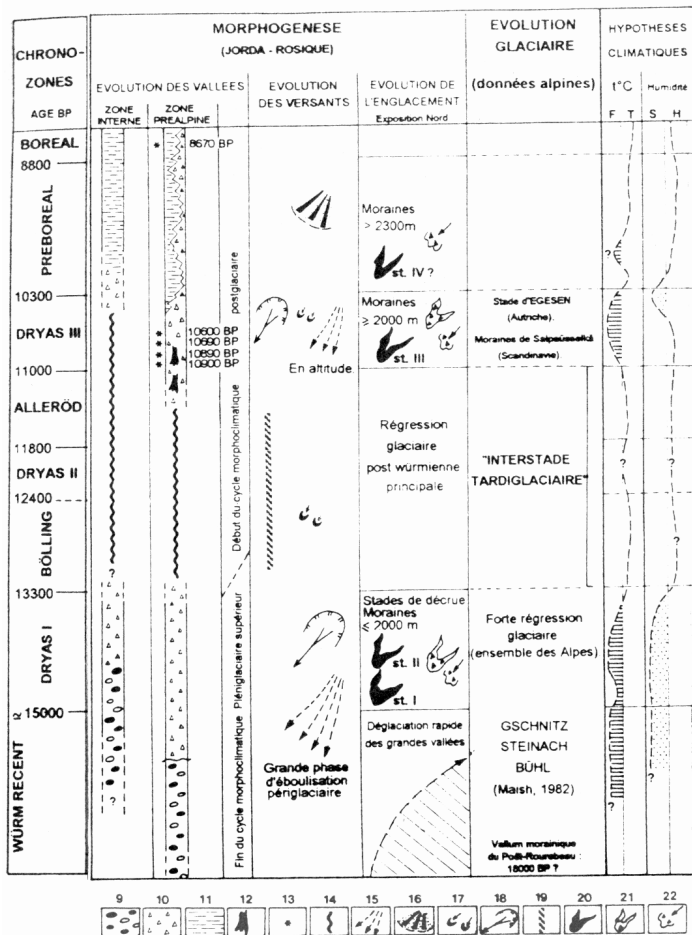


Figure 1.4 The southern French Alps from the end of the upper Pleniglacial to the beginning of the Holocene (Chronostratigraphy Morphogenesis). 9: fluvioglacial deposits; 10: torrential deposits; 11: silty alluvial and colluvial deposits; 12: fossil trunks (pinus sylvestris); 13: C-14- dates; 14: period of vertical incision; 15: periglacial rock fall; 16: colluviation; 17: landslide; 18: incision of torrential basins; 21: rock glaciers; 22: cryo-nival acc., flowing rock mass (Jorda & Rosique, 1994).

**Holocene**

After the retreat of the glacier from much of the Ubaye valley, marking the beginning of the Holocene, a situation of high slope instability had developed. Three factors can be assigned to be the cause of this instability.

The glacial erosion of the valley-slopes caused strong oversteepening (due to U-shaped valleys) and subsequent instability of the oversteepened slopes. Moreover, on the rims of the U-shaped valley large deposits of loose side-moraines where present providing readily erodable material. The instability of this situation was increased by fluvial erosion of the newly exposed Terres Noires at the valley bottom, which probably resulted in undercutting of valley-slopes and hence further oversteepening.

As a result of the oversteepened topography and the high erodability of the Terres Noires, many mass-wasting processes have been active alongside intensive fluvial erosion within the Barcelonnnette Basin during the Holocene, resulting in the quick widening of the valley.

Another factor may also have been responsible for the unstable situation of the region in the Holocene. This factor is the *pressure release process* (Summerfield, 1992). Rock beneath a thick overburden (like a glacier) is under considerable stress. As the burden is removed, in the Ubaye valley during the retreat of a valley glacier, the rocks near the surface will undergo expansion or dilation, which promotes the development of joints. These joints usually develop in relation to the original crystallization, or stratification, or perpendicular to the direction of stress. This may provide lines of weakness along which exfoliation (i.e. the spalling off of thin sheets of rock) and granular disintegration can occur. As Terres Noires is a soft and non-resistant rock-type, it is reasonable to assume that this process very likely occurred at a large-scale within the basin although no research has confirmed this. Still, this process might have further enhanced the instability of the slopes at the beginning of the Holocene. Finally, the soft character of the Terres Noires itself may also have been a great (direct) influence on the occurrence of large mass movements.

The Holocene can be subdivided into five different periods: The Pre-boreal, Boreal, Atlanticum, Subboreal and Subatlanticum (figure 1.4). According to Jorda (1983, 1987, 1988) one type of mass-wasting, the 'lave torrentielle', has especially been active during the transition between the Würm and the Holocene (Jorda & Rosique, 1994). During this transition period there was still little to no vegetation and erosional processes had not yet reworked the oversteepened topography. Its activity continued into the Pre-boreal and Boreal periods till the Early-Atlanticum. These 'laves torrentielles' have been responsible for the bulk of the Quaternary deposits at the valley bottom (Jorda, 1983 & 1987), especially at the base of the Riou Bourdoux torrential system. These deposits are practically all in the shape of alluvial fans and are fed by various streams, which indent the slopes of the main valley. Other deposits at the valley floor are flood and river deposits from the Ubaye or some of the larger tributaries, like the Bachelard.

The Late-Atlanticum and Subboreal appear to have been more stable periods, during which stream and river incision and soil formation on the alluvial fans was taking place.

The Subatlantic saw a major difference when compared to the rest of the Holocene due to the advancing anthropogenic influence on the landscape. The Barcelonnette Basin has been and still is a remote valley. Inhabitants of the valley had been largely dependent on local timber for housing and fuel. Other influences comprise extensive grazing and some localized agricultural activities.

Large-scale deforestation resulted in intensive reactivation of mass-wasting processes. Reforestation started one hundred years ago, but there still are many large-scale mass-movements active in the region, which are being monitored closely. There is concern that the present-day stability is not likely to be preserved, because crucial areas, formerly more or less unaffected, are showing signs of increasing erosion.

### 1.3.3 Climate

The Barcelonnette Basin has a Sub-Mediterranean climate with a marked alpine climatic influence. This means that the summers are warm and dry and the winters will be

cool (at higher altitudes cold) and wet, with part of the precipitation as snow (Henderson-Sellers & Robinson, 1994).

An aspect of the regional climate is that for a rise of 100 m in altitude, the average yearly precipitation will increase with 35 mm and temperature will decrease by 0.8°C (Descroix, 1985). The average annual rainfall at the bottom of the Ubaye valley is approximately 750 mm (source: RTM-average annual stats). Around the summits (circa 2800 m) annual rainfall may reach 1500 mm (ONF, 1976). Most of this precipitation falls in spring and autumn. Summers are punctuated by brief stormy showers and the winters present a minimum of showers. Furthermore, over periods of several years it is observed that there is a large variability of rainfall from one year to another.

25% of the precipitation falls as snow (Avocat, 1970) in the months of December till March. How long the snow will remain, is dependent upon the orientation of the slopes. On the 'adrets', the south-orientated slopes, the snow will melt earlier in the season and it will melt much faster than on the 'ubacs' (i.e. the north-exposed slopes). This is due to the higher surface temperatures on the adrets caused by the reception of more solar radiation (figure 1.5).

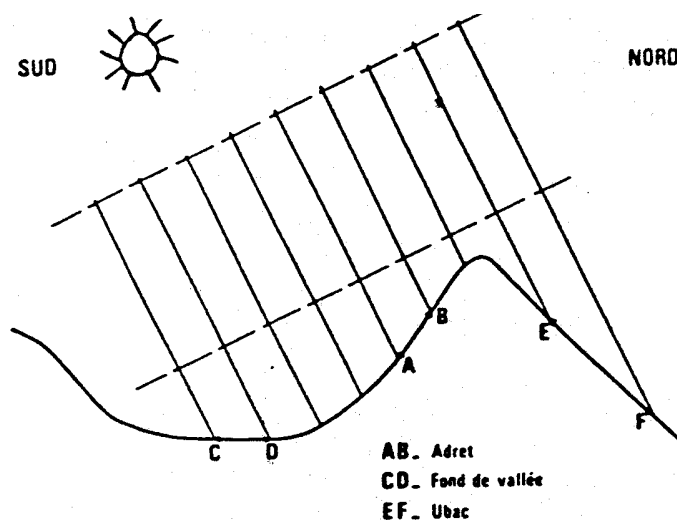


Figure 1.5 Slope orientation and solar radiation. The adret receives more radiation per m<sup>2</sup> (8-10 x more) than the ubac (Douguedroit, 1976).

This rapid snowmelt may result in high discharges within short periods of time (Ward and Robinson, 1990). This occurs mostly from April to June. When the discharge of a river exceeds five times the average discharge, it is called a 'cruet'. The slopes of the Riou Bourdoux catchment have a southeast, south to southwest aspect. This means that in spring the snow on these slopes will melt fast and the probability of a cruet increases. Also the typical high-intensity rainstorms in the summer can cause high discharges. These cruet are especially important for the transport of sediment through gullies and streams.

In table 1.1 the mean monthly temperatures for Barcelonnette are shown. These temperatures however vary significantly depending on the orientation of the slopes and on the altitude. Air-temperature generally decreases with increasing altitude. Ground-temperatures however vary significantly depending on the orientation of the slopes, with

adrets being much warmer throughout the year although no exact measurements exist for the slopes of the Riou Bourdoux system.

Month	Jan.	Feb.	Mar.	Apr.	May.	June	July	Aug.	Sept	Oct.	Nov.	Dec.
Precip. (mm)	66.9	62.5	61.7	49.7	59.5	67	46.3	55.3	61.6	86.7	92.1	64.8
Temp.(°C)	-1.7	0.2	3.2	6.4	11.0	14.0	16.5	16.0	13.2	2.3	2.3	-0.9
Tmin(°C)	-8.5	-6.6	-3.6	-0.8	3.4	6.3	7.9	7.6	5.4	-3.4	-3.4	-7.0
Tmax(°C)	4.9	7.1	10.1	18.6	18.6	21.7	25.0	24.4	21.0	8.9	8.9	5.2

Table 1.1 Mean monthly precipitation and temperature data for the period 1956-1979 for the station Barcelonnette/St.Pons (1130 m. a.s.l.) (Avocat, 1970).

#### 1.3.4 Vegetation

The vegetation in the Barcelonnette Basin can be subdivided into three distinct zones. This zonation is based upon the model presented by Ellenberg (1986). It has to be noted that this natural zonation is distorted due to afforestation and other anthropogenic influences (Ballandras, 1996).

Barcelonnette lies at an altitude of 1140 meters. This is within the montane zone, which is characterized by extensive growth of (silver) firs. If local climatic conditions are favourable, i.e. slightly warmer, also oak and birch trees can be present. However, due to the above-mentioned afforestation of the area, this zone is now largely represented by pine forests (*Pinus sylvestris*). The montane zone reaches to an altitude of about 1800 meters (on the adrets) in this part of the Alps.

Above this zone, the narrow sub-alpine zone can be found. This comprises predominantly closed pine forests interspersed with areas only having some spread tree-growth. Since pine trees represent both montane and sub-alpine zones, the distinction between these zones within the Barcelonnette Basin is not always clear. These forests have almost all been replanted, and appointed as protected national forests.

Above the tree line, the sub-alpine zone goes over into the alpine zone. The alpine zone is divided into four different sub-zones, namely (increasing from lower to higher altitudes) the shrubs and thicket zone, the dwarf-shrubs zone, the alpine-meadow zone and the sub-nival zone with its pioneer vegetation. The upper boundary of this zone is at approximately 2800 m. (a.s.l.). The alpine zone is extensively used as pasture grounds for cattle and sheep in summer.

The nival zone is the zone above the firn line. The crests around the Barcelonnette Basin however rarely exceed this height, so this zone is practically absent.

#### 1.3.5 Studied subcatchment

The area, studied in detail in this report, is a subcatchment within the Riou Bourdoux system (figure 1.6). The major stream draining this subcatchment is named the 'Riou de la Pare'. Hence, this investigated subcatchment will from here on be referred to as the *Riou de*

*la Pare catchment*. The studied catchment (delineated in red in Appendix A1) is located between the Riou Guérin- and the Riou Chamous-catchments (both subcatchments within the Riou Bourdoux system). The latter have been extensively studied by Spee & Visser (1999).

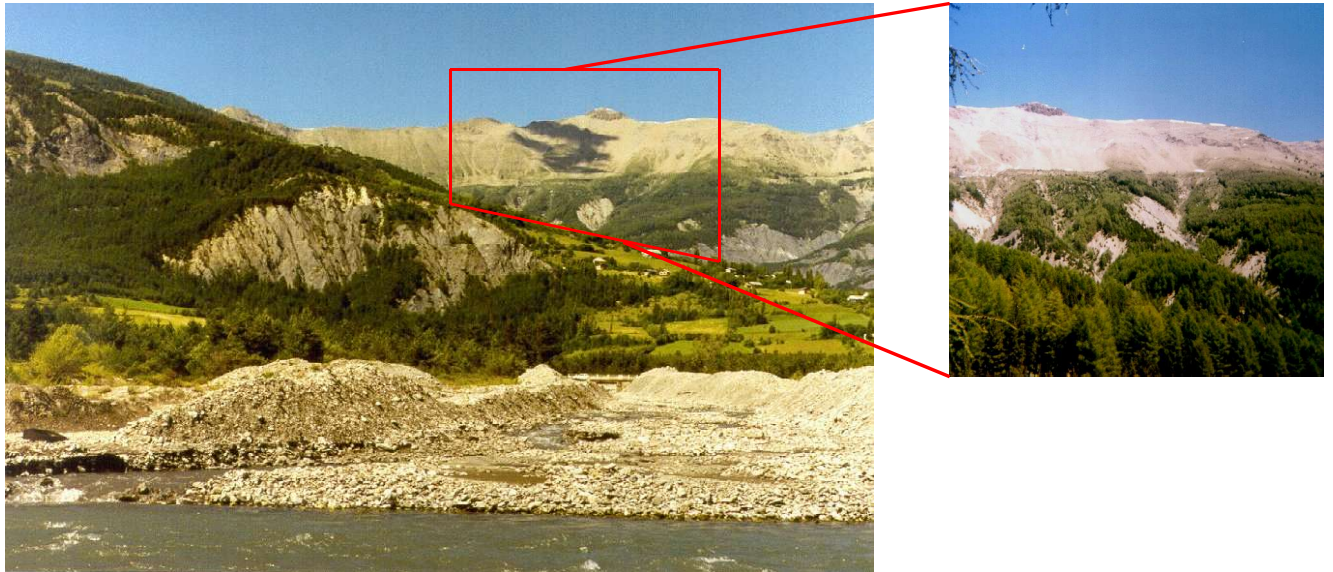


Figure 1.6 Photographs showing the Riou Bourdoux system (left) with a close-up of a part of the investigated sub-catchment (right).

From a preliminary investigation of the topographical map and aerial photographs, the following can be observed. The Riou de la Pare catchment is predominately south-exposed, hence being an adret. The catchment has steep slopes. A marked flattening of the relief can be observed around 2100 m (appendix A1), probably indicating the bulk of the moraine deposits. The tree-line is located around 2000 m. The altitude of the catchment ranges from 1500 m near the confluence point of the Riou de la Pare, the Riou Guérin and the Riou Chamous to approximately 2800 m around the summits.

The catchment is densely covered with forest. However, large un-vegetated areas can be observed in many different locations in the subcatchment, most of which are connected to large ravine- and gully-systems (badlands).

## 2 Theoretical background

### 2.1 Introduction to sediment budget analysis

A sediment budget is an accounting of the sources and disposition of sediment as it travels from its point of origin to its eventual exit at the mouth of a drainage basin (Reid & Dunne, 1996). To construct a sediment budget for a drainage basin, the temporal and spatial variations of transport and storage processes must be integrated. This is done through the solution of three requirements (Swanson et al, 1982), namely:

- 1) Recognition and quantification of transport processes,
- 2) Recognition and quantification of storage elements, and
- 3) Identification of linkages among transport processes and storage elements.

In this study an approach to these requirements is made. Since this study is based on a short-term analysis of a catchment (using some rapid surveying methods and estimates) it is not possible to do exact calculations. Field studies like these are useful in preparation to long-term monitoring programs (Swanson *et al*, 1982; Reid & Dunne, 1996). In many cases the purpose is to determine the order of magnitude, as is the case in this study and hence an approximate budget gives satisfying results.

To quantify and relate the major processes responsible for the generation and transport of sediment is difficult because the processes are either slow and continuous, like creep, or discreet and both are highly variable in time and space (Dietrich & Dunne, 1978). In a forested mountainous landscape rapid transport of sediment by landslides and debris flows is of great importance and these processes are also variable in time and space. Other processes that have shown to be important in (wet) forested drainage basins are soil creep, biogenic transport, sheetwash and rainsplash erosion (on unvegetated surfaces, either natural or due to deforestation), and gully erosion (Swanson et al, 1982; Selby, 1993).

To simplify the quantification of a sediment budget, it is necessary to estimate the relative importance of these types of hillslope-transport processes and their distribution within the basin (Swanson et al, 1982).

Dietrich & Dunne (1978) and Lehre (1981) found that in mountainous catchments debris flows are big contributors to the sediment transport. In the area investigated in the present study, the Riou Bourdoux catchment, it is assumed that most of the sediment stored in 1<sup>st</sup> and 2<sup>nd</sup> order channels is ultimately transported downstream by debris flows (Benda, 1990; Benda & Cundy, 1990). Debris flows are important agents of landform development by the erosion and transport of sediment (Dietrich & Dunne, 1978). Determining the frequency of debris flows has been a continuous problem in mountainous catchments (Dietrich & Dunne, 1978). By constructing a sediment budget based on the debris-flow contributing hillslope processes in the study area, an attempt is made to determine the possible size and frequency of debris flows (see section 2.2.3).

Linkages among processes and storage elements establish the general form of a sediment budget, which can be expressed in a flow diagram (Figure 2.1).

The causal linkages in the budget of the study area will be identified. These linkages will highlight the effect of successive transfers on the characteristics and quantity of the sediment that is moved (Swanson et al, 1982). This identification requires intensive field investigations, and is necessary to estimate the frequency of debris flows, to define the magnitude and location of sediment storages and to recognise subtle features such as colluvium-filled hollows or the effect of wash processes (Dietrich & Dunne, 1978).

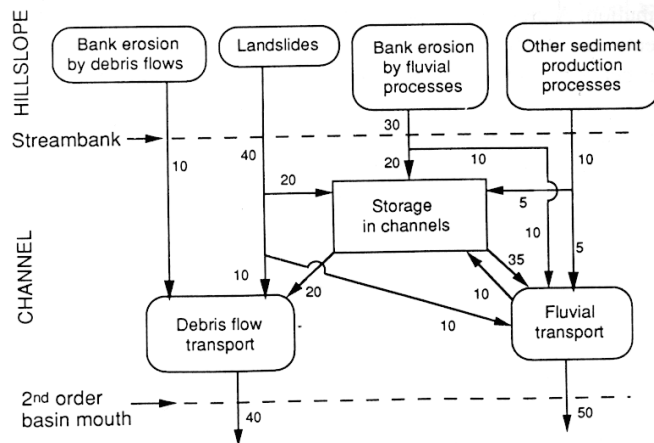


Figure 2.1 Flowchart of the linkages among processes and storage elements establishing the general form of a sediment budget (Reid & Dunne, 1996).

Since geomorphic processes are highly variable in time and space, data from short-term monitoring at a few localities are not easily extrapolated to compute the sediment budget for a catchment (Dietrich & Dunne, 1978). The only way to generalise from a few measurement sites to a landscape is to develop predictive models for the relation of each transport process to its controls (Swanson et al, 1982). It is assumed that the landscape can be divided into several landscape-units, each having a dominant transport process. By combining all landscape-units of the catchment with the predictive models (extrapolation), a total sediment budget can be created.

According to this approach of sediment budgeting one has to assume that the basin is in approximate steady state. Over longer time periods, with changes of climate and human impact, this will certainly not be true. Hence, it is important to consider the longer-term changes that have occurred in mountain drainage basins (Boelhouwers, 1996).

In the case of this study a sediment budget is constructed for present conditions, based on the results of two months of investigation. The conditions (climate and vegetation) are assumed to be constant over time (i.e. the last 100 years) and the area is in approximate steady state.

As can be seen in figure 2.1 the processes within a catchment can be subdivided into hillslope processes and channel processes. Hillslope processes produce sediment, which is either stored on the hillslope itself or in a 1<sup>st</sup> or 2<sup>nd</sup> order channel. The sediment remains in these channels until it is removed by a scouring debris flow. This means that any fluvial transport occurring in these channels is neglected. Debris flows are thus regarded as the major contributors of sediment to 3<sup>rd</sup> or higher order channels. In these 3<sup>rd</sup> order channels fluvial processes become increasingly important in storing and transporting sediment (Benda & Cundy, 1990; Benda & Dunne, 1987; Reid & Dunne, 1996).

## 2.2 Hillslope processes

An important step in the simplification of a sediment budget to a form that can be examined in the field is the recognition of the dominant hillslope processes. Since it is beyond the scope of this research to discuss all processes active within the Riou de la Pare catchment, only those are discussed that have proved to be most important (based on the field investigation) in contributing to the sediment budget of the catchment. Analysis of the processes which are not addressed here, was either restricted due to the time-scale of operation, like creep, or processes proved insignificant compared to the activity of other processes in the same location.

After preliminary research (literature) and the conducting of fieldwork the following major contributing processes were found (see section 4.1): Sheetwash and rainsplash erosion, rill and interrill erosion, gully erosion, (soil-)creep, landslides, debris flows and channel transport and storage. Weathering processes are also active on the Terres Noires and Flysch slopes, but this process is of little relevance to the present state of instability within the catchment. A more detailed investigation into the active weathering processes in the Riou Bourdoux catchment is given by Spee & Visser (1999).

The processes will be divided into two groups of erosion and/or transport processes. The first group consists of processes that affect hillslopes by raindrops and flowing water. The other group is the mass wasting of soils. Because of the special importance of debris flows within the Riou Bourdoux catchment, this process is discussed in a separate section.

### 2.2.1 Erosion on hillslopes by raindrops and flowing water

#### Sheetwash and rainsplash

Detachment, transport and deposition are the basic processes that act upon slopes. Detachment occurs when the erosive forces of raindrops or running water exceed the resistance of the soil against erosion. The detached soil can be transported by water. This transport is generated by three wash processes: rainsplash erosion, slope wash and solute transport. Together these processes are called wash processes.

Rainsplash erosion and slope wash are only effective on slopes covered with soil or sediments; solute transport can be effective on both soil and rock slopes. Deposition occurs when the transport capacity is no longer enough to keep the sediments in transport. These wash processes are driven by the hydrological processes of precipitation and runoff, generated by rainfall or snowmelt (van Asch, 1992). The water is flowing over the surface of a slope and is stored in depressions or infiltrates into the soil. The proportion of precipitation that flows over the surface instead of infiltrating depends on intensity and duration of the rain, and on the infiltration capacity of the slope material (Summerfield, 1992). The infiltration capacity is influenced by different characteristics of the surface, like mean particle size, percentage of organic compounds and intensity of animal activity.

Where precipitation intensity or meltwater supply is larger than the infiltration capacity of the surface, part of the water will flow over the slope as infiltration excess (Hortonian) overland flow. Saturation overland flow occurs where a combination of rainfall intensity and

duration causes saturation of the soil. Common places of this type of overland flow are locations where the ground water table is close to the surface. Saturation overland flow is often associated with snowmelt (Ward & Robinson, 1990).

According to Reid & Dunne (1996) sheetwash erosion is only effective on surfaces where overland flow occurs regularly. Because the Riou Bourdoux catchment is largely vegetated with an extensive forest cover and in other places by grassland, overland flow is restricted to the unvegetated badlands and roads. As will be shown in this report, sheetwash by overland flow on badlands quickly changes to rill and interrill erosion patterns. So true sheetwash is restricted to roads, where the compacted surface leads to lowered infiltration rates and hence overland flow. Because there are only few roads within the Riou Bourdoux catchment and their down-slope sides are usually bordered by grassland or forest, inhibiting erosion, true sheetwash is not important in this sediment budget.

Rainsplash erosion is the process of loosening particles on the soil surface by the impact of raindrops. This process is fuelled by the kinetic energy of raindrops, as a result of their mass and velocity, which is partly transferred to the surface upon impact. The mechanism of rainsplash is an effective erosion process on locations lacking vegetation (Selby, 1993). Both slope gradient and surface characteristics influence the effectiveness of rainsplash erosion.

The process is more effective on steep slopes with a sandy soil, since cohesion causes a decrease of the impact of falling raindrops (Summerfield, 1992) and because erosion on steep slopes is accelerated due to a higher downward component of movement (figure 2.2). Since these factors are spatially variable, rainsplash also has a variable spatial pattern (Terry, 1996).

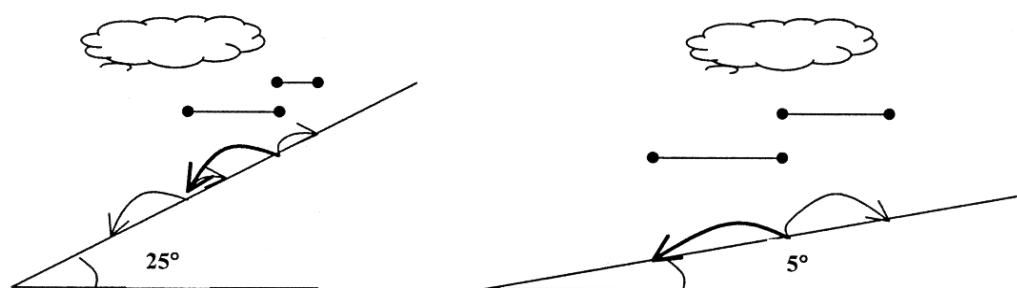


Figure 2.2 The effect of rainsplash erosion in combination with slope gradient. Although, effectively, less rain will fall per  $m^2$  on steeper slopes (with vertical falling rain), reducing rainsplash intensity, De Villiers (1990) showed that the local influence of topography results in an obliquely falling rain *towards the sloped surface*, increasing this intensity again. So in general, splash effectiveness increases with slope gradient.

Rainsplash erosion can cause a decrease in infiltration capacity by the falling apart of aggregates and by filling small hollows with the detached particles resulting in the formation of a pavement or surface layer (Kutilek & Nielson, 1994). Therefore, the combination of rainsplash and slope wash is a very effective erosion mechanism.

Rainsplash can produce sediment, which can ultimately be transported by overland flow. Formulae to calculate this are given in De Joode (2000), which will not be used in the present study.

Solute transport is a difficult factor to determine, because solution mostly does not remove the whole weathered rock, but only a part of it. The residual differs in density, but mostly not in thickness making it difficult to determine the total effect of solute transport on a slope. Therefore solute transport will not be included in the calculation of erosion by wash processes.

### Rill and interrill erosion

Water can flow concentrated over the surface. After continued concentrated flow rills having a width and depth of a few centimetres can eventually develop. These rills develop on unvegetated surfaces and the process is called rill erosion (figure 2.3). They are usually discontinuous and may have no connection to a stream-channel system. They can be formed and obliterated by a single storm (Selby, 1993).

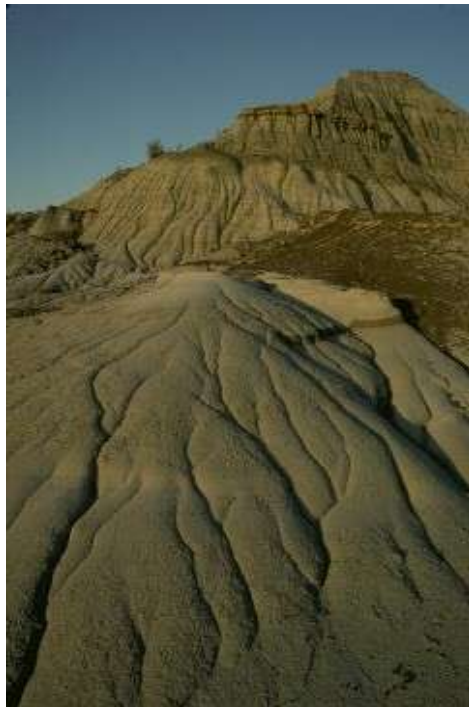


Figure 2.3 Photograph showing typical rill erosion

Rills are both collection areas for inter-rill sediment and transport agencies for those removed sediments from rill walls and floors. Rill erosion is then the primary agent for sediment transport on slopes with little vegetation (Morgan, 1977 op cit. Selby, 1993).

In between rills, interrill erosion can occur, predominantly caused by rainsplash detachment and transport. Sediment supply from the interrill area to the rills is important for the amount of sediment that can be eroded from these rills by overland flow. If the erosive forces of the flow are large enough, the sediment will be transported by rill erosion. Table 2.1 gives an overview of the intensity of the different processes.

Area	Process	Agens	Intensity
<b>Rill</b>	Detachment	Raindrops	-
		Overland flow	+
	Transport	Raindrops	-
		Overland flow	+
<b>Interrill</b>	Detachment	Raindrops	+
		Overland flow	-
	Transport	Raindrops	+
		Overland flow	-

Table 2.1 Intensity of erosion processes in the rill and interrill-area (reproduced after Van Asch, 1996). A '+' indicates a high and a '-' a low process intensity

If there is much more supply of sediment into the rills than is eroded by concentrated overland flow, rills can disappear because of sedimentation. On the other hand, it is possible that a rill will widen and deepen and develops into a gully and hence becoming a permanent

part of the drainage network. The slope contour is of importance during this development (figure 2.4). At a convex plan sheet flow will diverge and erosion will be minimised, while on a concave slope profile the flow will concentrate and rill erosion will become more effective. On concave slopes rills may thus form the heads of natural drainage systems.

A first step in evaluating rill and interrill erosion is to identify the types of sites subject to Hortonian overland flow. The Terres Noires, present in the study area, are known for their high susceptibility to surface wash (rill and interrill) erosion (Antoine et al, 1995; Oostwoud Wijdenes & Ergenzinger, 1998), producing easily entrainable sediment. Other slope-surface lithology may also exhibit wash erosion, which can be identified by geomorphological mapping.

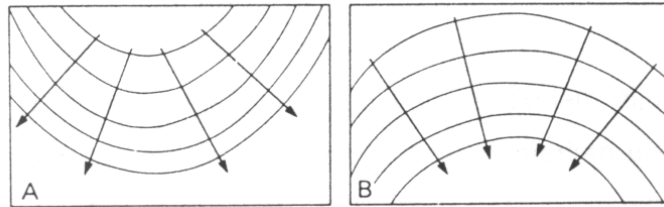


Figure 2.4 Slope contours. A showing a convex plan, B a concave plan.

Most calculations for quantifying rill and interrill erosion are based on the Universal Soil Loss Equation (USLE) (Van Asch, 1996; Reid & Dunne, 1996). This equation uses many parameters, most of which are determined in laboratory experiments. It was thus not feasible to quantify this erosion process in this study. The recognition of areas showing wash erosion is however important, because this process is related to other processes like debris flows (see section 2.2.3).

### Gully Erosion

A gully is a recently extended drainage channel that transmits ephemeral flow, has steep sides, a steeply sloping or vertical head scarp, a width greater than 0.3 m, and a depth greater than about 0.6 m (Selby, 1993). The longitudinal profile of a typical gully shows a gradient near its head steeper than the mountain slope, but less steep near the base, where deposition of the eroded material takes place. Because they are very rapidly developed erosional forms, gullies are usually not regarded as features of normal erosion, but as a result of sudden natural or anthropogenic influenced changes in the environment (Selby, 1993). Gullies are grouped into three classes.

I. The first class of gullies is governed by concentrated surface flow as the primary process of formation. This class will be addressed as *gully type 1* following Faulkner (1995). This class can be further subdivided into two separate groups.

- a) Gullies of the first group are those, which can form at any break of slope or break in vegetation cover when the underlying material is mechanically weak or unconsolidated where surface wash processes are active (Selby, 1993). These gullies are therefore common in, among other, colluvium, debris from mass movements and moraine deposits, which were abundantly found in the study area (appendix B1 & B2).

A large rill at these sites may so deepen and widen its channel that at some point it is classified as a gully and becomes a permanent feature on the hillslope. At each point a small headscarp forms and as this retreats headwards a trench is left down-valley

with a debris fan spreading out from its toe to form a small alluvial fan. Deposition of material within the gully can be attributed to infiltration of runoff into the underlying colluvium, hence reducing transport capacity and causing deposition. This leads to a reduced gradient causing even more deposition (Faulkner, 1995).

This group of gullies can thus be independent of an existing drainage pattern and usually has a discontinuous character.

- b) The other group of this gully class comprises gullies that develop in weak argillic rocks, such as argillites, phyllites, mudrocks, and shales. These gullies are often channels through which debris flows and mudflows, with very high sediment discharges, drain unstable catchments (Selby, 1993). The Terres Noires are such a rock type, and observations show extensive gullying occurs on slopes in this rock type (Antoine *et al*, 1995; Oostwoud Wijdenes & Ergenzinger, 1998). Gullies developed in this type of substrate are usually continuous.

II. The second class of gullies comprises those, which are initiated by subsurface flows in natural pipes, with subsequent collapse of the roof of the pipe (Selby, 1993) or by “spring sapping” (Faulkner, 1995). This type will be named *gully type 2* (Faulkner, 1995). The process of formation is primarily driven by snowmelt and long-duration low-intensity rainfall.

Piping is common in the walls of gullies and in the heads of landslides where the confined flow in soils is suddenly accelerated and seepage pressures permit particles to be washed out of the soil (Selby, 1993). This class of gullies can also be associated with convex slopes where an impermeable substrate is capped by a permeable one. Throughflow within the permeable substrate is deflected towards the surface in mid-slope generating a spring, which promotes gullying (Faulkner, 1995; Summerfield, 1992).

These gullies usually have a continuous character due to a sustained supply of subsurface water and are thus connected to the drainage pattern. The sustained flow results in a continuous fluvial action, causing these gullies to produce much sediment (Faulkner, 1995).

III. In this report a third class of gullies is recognized. This gully type is controlled by changes in local erosion base level (Oostwoud Wijdenes & Bryan, 1994) and will be referred to as *gully type 3*. The (sudden) changes in base level may be natural or anthropogenic. Natural factors may, for example, be large landslides, blocking a channel in which a small lake will then form. Anthropogenic factors may be in the form of sediment retaining structures.

Both a lowering and a rising base level may promote gullying. In order to attain a new profile in equilibrium with the changed erosion base, the channel cuts headwards into its existing profile, hence initiating gullying *within a channel*.

Although actual field situations may not strictly follow the above-mentioned division, this general picture of hillslope gully formation will be expected to occur within the Riou Bourdoux catchment.

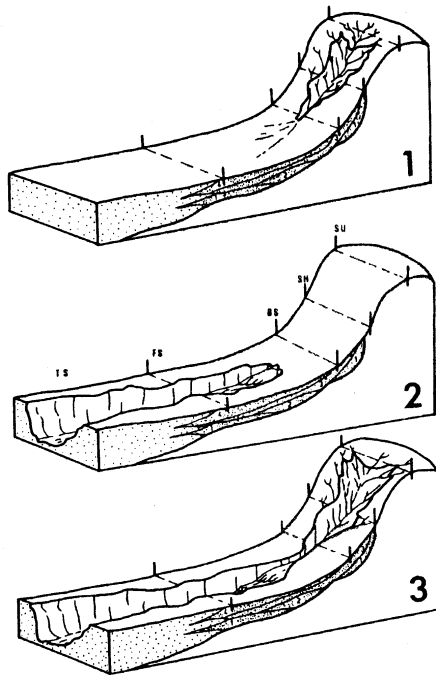


Figure 2.5 Gully pattern development on concave slopes (Faulkner, 1995). 1: *Gully type 1*. 2: *Gully type 2*. 3: Interaction of both gully types on one slope.

Faulkner (1995) showed that *gully type 1* and *gully type 2* may also be located at specific locations within a drainage basin. *Gully type 1*, especially group *a*, usually forms in the higher and steeper locations within a catchment, where vegetation is more sparse and overland flow more effective. *Type 2* forms on the lower reaches of the hillslopes where more throughflow reaches the surface. This spatial variation of gully formation on a slope is illustrated in figure 2.5.

Gullying in channels nearly always starts for one of two reasons: Either there is an increase in the amount of flood runoff, or the flood runoff remains the same but the capacity of water courses to carry the flood waters is reduced. The most common causes of increases in runoff or

deterioration in channel stability within the Riou Bourdoux catchment may be changes in vegetation cover (especially logging), climatic change with accompanying variations in rainfall periodicity and intensity, and changes in the local base level.

The capacity of a stream channel depends on the cross-sectional area, the slope, gradient, and roughness. Changes in these factors can easily disturb the equilibrium between channel geometry and the processes of erosion and deposition, which have moulded it. The relationship between the velocity of water in a channel and the geometry of the channel are expressed in Manning's equation:

$$V = \frac{1}{n} \cdot R^{\frac{2}{3}} \cdot S^{\frac{1}{2}} \quad (2.1)$$

Where:

- $V$  = average velocity of flow (m/s)
- $n$  = a roughness coefficient, known as Manning's  $n$
- $S$  = average gradient of the channel (m/m)
- $R$  = hydraulic radius (m) (expressed as  $A/P$ , with  $A$  = the cross-section area of a stream,  $P$  = the wetted perimeter)

Once gullying starts the gullied channel has a more angular and deep shape than the original bed (i.e.  $R$  increases). The gullied channel is usually rough and irregular so the value of  $n$  increases. The value of  $n$  varies much less in relation to  $R$ . For the velocity to remain constant the gradient must, therefore, decrease and this is what usually happens. The gradient of the floor of the gully is flatter than that of the original streambed ( $S$  decreases). The head of the gully then works back upstream and the height of the gully head

progressively increases. As the head gets higher (or the velocity increases) gullying is likely to become more rapid.

Attempts are frequently made to control gully erosion by building dams of concrete, stone and wood. But most dams are liable to decay, to be bypassed or undermined, and in many cases they do not modify the basic cause of gully erosion (Selby, 1993). In terms of the Manning's equation: increasing surface roughness decreases flow-velocity. On valley-floors this is largely attained by increasing vegetation cover.

The contribution of gullies to a sediment budget is difficult to determine. Gullies that are incorporated into the channel system are more influenced by local base level, channel scouring and bank collapse, while the contribution of discontinuous hillslope gullies is predominately controlled by head-cut retreat and wash erosion on the side-slopes and by storage within the gully-system. Both, however, need detailed measurement programs in order to evaluate their significance in the budget (Oostwoud Wijdenes & Bryan, 1994). Detailed monitoring was beyond the scope of this research. Moreover, almost all formulas for calculating gully retreat (and hence erosion rates) are based on lowland (hillslope) gullies (Reid & Dunne, 1996). Gully restriction dams further complicate gully erosion rate calculation. Therefore, the contribution of most hillslope gullies to the sediment budget was undeterminable.

Experiments in an experimental catchment near Digne, 35 km southwest of Barcelonnette, show that sediment production due to gully erosion (including other wash processes) on the typical steep and bare slopes of the Terres Noires, amounts to more than  $100 \text{ t}\cdot\text{ha}^{-1}\cdot\text{y}^{-1}$ . This value was used in the sediment budget constructed by De Joode (2000) (see section 5.1), but has not been used in this report.

Gullies were however carefully mapped due to their significance in the assessment of the present stability of the Riou Bourdoux catchment.

### 2.2.2 *Mass wasting*<sup>4</sup>

Mass wasting, the downslope movement of soil or rock material under the influence of gravity without the direct aid of other media such as water, air or ice is classified by several authors (Varnes, 1958, 1975; Hutchinson, 1988). The classification of Varnes (1958, 1975) is often used (Selby, 1993; van Asch, 1992). Although it has its drawbacks, Varnes's scheme and terminology (1975) will be followed in this report. Table 2.2 shows this scheme.

This table shows landslide types only and excludes creep and frozen ground phenomena. Since creep, landsliding and debris flows were found to be important in the Riou Bourdoux catchment (see chapter 4) these processes will be discussed here.

---

<sup>4</sup> This section is taken in short from De Joode (2000).

Type of Movement	Type of Material					
	Bedrock		Soils			
			coarse		fine	
FALLS		ROCKFALL	DEBRIS FALL		EARTH FALL	
TOPPLES		ROCK TOPPLE	" TOPPLE	"	TOPPLE	
SLIDES	rotational	few units	" SLUMP	"	SLUMP	" SLUMP
	translational	many units	" BLOCK GLIDE	"	BLOCK GLIDE	" BLOCK GLIDE
		" SLIDE	"	SLIDE	"	SLIDE
LATERAL SPREAD		" SPREAD	"	SPREAD	"	SPREAD
FLAWS		" FLOW (deep creep)	"	FLOW (soil creep)	"	FLOW
COMPLEX		Combination of 2 or more types				

Table 2.2 Classification scheme of Varnes (1975).

Creep

In this report the term creep is the general term for a group of processes, which causes the imperceptible but continuous movement of rock debris and soil down a slope in response to gravity (Whittow, 1984). Indicators of the probability of creep are terracettes, bent trees, soil accumulations upslope of retaining structures, cracks in soils and old landslides (Selby, 1993).

Creep rates are usually measured by the displacement of pins, blocks or tubes, placed in the soil or the displacement of marked particles on the soil-surface. From these measurements creep rates (at the surface) can be estimated. Common creep rates in vegetation-covered soil are between 0.1 and 15 mm/year. On exposed talus slopes, or in cold climates where freeze-thaw processes are common, higher rates up to 0.5 m/year have been recorded (Selby, 1993).

The mass transport of soil by creep (S) is dependent partly on the creep rate (d), which includes slope gradient, but even more on the creep depth (h) and profile as shown in figure 2.6 and the following equation:

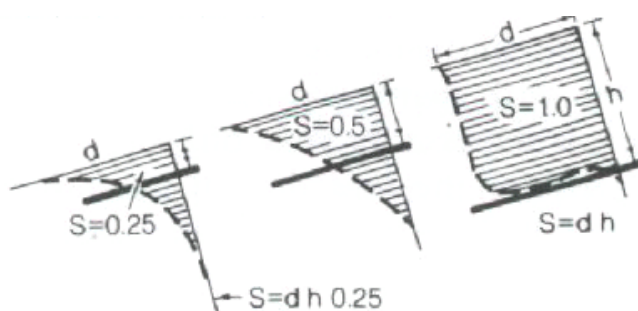


Figure 2.6 Transport mass of soil calculated in accordance with the observed creep profile (after Jahn, 1989).

$$S = d \cdot h \tag{2.2}$$

(expressed as volume per year) (Selby, 1993).

Since most creep processes are usually imperceptible and only observable in long-term measurements, it proved impossible to determine creep rates in this short-term study.

Landslides

The gravity driven downslope movement of sediment or rock ‘en masse’ is called slide or slump depending on the morphometry of the slip face. A slip face of a slide is straight, a slump has a curved failure plane (Selby, 1993) and can be defined as a rotational slide. Slumps are common in soft rocks such as shales, mudstones, and over-consolidated clays (Selby, 1993).

Slides or translational slides usually are shallow features and their length is commonly large compared with their depth. The straight failure plane develops along a boundary between materials of different permeability or density. If impervious strata are overlain by porous strata, heavy rainfall can cause saturation of the upper strata, which means loss of shear strength and eventually failure.

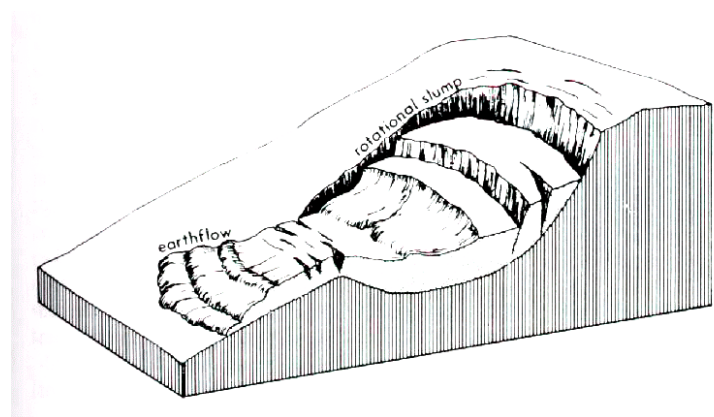


Figure 2.7 Features of a slump (Selby, 1993).

The water cannot penetrate into the underlying impermeable strata and will flow over these strata causing failure along this plane (Selby, 1993). This process is very likely to occur within the Riou Bourdoux catchment, because on many localities within the catchment moraines cover the more impervious Terres Noires.

One type of mass movement can lead to a failure of another kind. Often, complexes of different kinds of mass movement will occur (Figure 2.7).

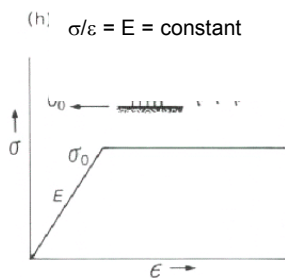


Figure 2.8 St. Venant elastoplastic solid. Stress ( $\sigma$ ) divided by strain ( $\epsilon$ ) is constant ( $E$ ).  $E$  is known as Young's modulus and is a characteristic of material (Selby, 1993)

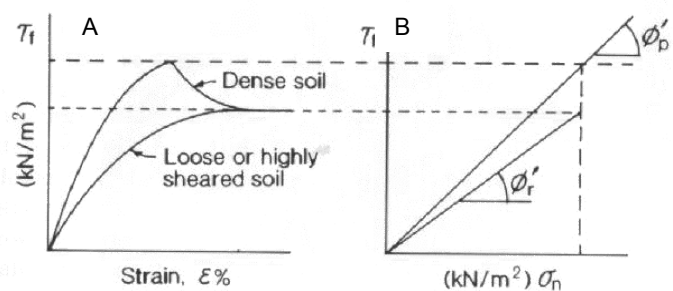


Figure 2.9 A) Stress-strain curves and B) strength envelopes for peak (p) and residual (r) strength. In figure B) the angle of internal friction is indicated (Selby, 1993).

The materials in which landslides occur show elasto-plastic behaviour (figure 2.8). This means that the material is elastic for stresses less than the yield stress and therefore it will return to its former character after deformation. For stresses equal to yield stress the material is plastic and after the maximum shear strength is reached the material will slide

along one or more failure planes. When stress is increasing, first the material will be deformed and cracks will develop. This continues until a critical stress (equal to the peak strength of the material) is reached and one or more slip planes will form along which the sediment will move downslope. Eventually the sediment will settle down at residual strength (van Asch, 1992) (Figure 2.9).

A decrease of shear strength or an increase of shear stress can cause instability of a slope. The components which contribute to (effective) shear strength ( $\tau_f$ ), namely (effective) cohesion ( $c'$ ), normal stress ( $\sigma_n$ ), pore-water pressure ( $u$ ) and angle of friction (with respect to effective stress) ( $\phi'$ ) are directly or indirectly influenced by, for example, effects of pore water, changes in slope angle or vegetation. Effective shear strength at any point in the soil is given by the Coulomb equation as:

$$\tau_f = c' + (\sigma_n - u) \cdot \tan \phi' \quad (2.3)$$

Detailed explanation of this equation is given in De Joode (2000). To determine the strength of the Terres Noires direct shear tests are done on material found in the Riou Bourdoux catchment (see section 3.5).

In the French Alps the larger landslides in Terres Noires show intermittent activity with periods of rest of about 5 to 12 years. Observations of soil moisture profiles indicated that only under conditions of rain of long duration or prolonged periods of snow melt a critical saturation height can be reached, leading to instability (van Asch & van Steijn, 1991).

Small slides can however be triggered by individual storms. These slides are also common along the base of slopes where the hillslope soil is undermined by streams and gullies (Dietrich & Dunne, 1978). This effect is observed in the Terres Noires slopes in the Riou Bourdoux catchment.

### 2.2.3 Debris flows

As mentioned in the previous chapter, debris flows and in particular the 'laves torrentielles' (i.e. the more mobile, channelled debris flows capable of reaching the Ubaye river) are of special interest in the Barcelonette Basin.

#### Characteristics

A debris flow system can mostly be subdivided into three basic zones; a source area, a transport zone (a channel or gully) and a deposition zone (figure 2.10).

Debris flow deposits are easily recognised in the field because of the typical morphology of the two latter zones: a long and small, ribbon-like channel bordered by lateral levees which meet downslope in a lobate or tongue-shaped terminal deposit. They behave like a visco-plastic or viscous flow and are gravity driven. Debris flows usually occur in periodic surges or waves lasting a few minutes (Coussot & Meunier, 1996; Blijenberg, 1998)

and commonly have velocities between 1 and 10 m/s (Coussot & Meunier, 1996). In areas where slope angles are relatively low, the flow path may exhibit a meandering pattern.

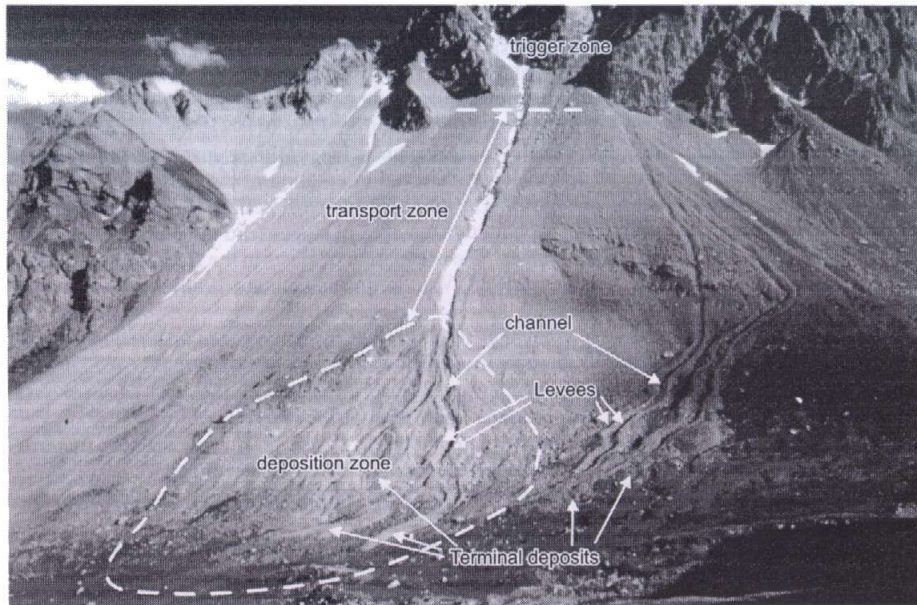


Figure 2.10 Typical morphology of a hillslope debris flow and debris-flow terminology (Blijenberg, 1998).

Debris flow deposits display a wide range in grain size distribution, from clay particles to large boulders (Coussot & Meunier, 1996), although a bimodal distribution (Blijenberg, 1998) can mostly be identified, with one mode in the silt and the other in the coarse

gravel fractions. Although the deposits show poor sorting, some sorting may be present in the levees. The coarsest debris is mostly accumulated in front of the deposit and on the outer edges of the levees.

Debris flows exist on different scales, from micro-scale ( $<1 \text{ m}^3$ ) up to large (or mega-) scale ( $>10^5 \text{ m}^3$ ). In the southern French Alps especially medium-scale ( $10^3$ - $10^4 \text{ m}^3$ ) debris flows occur. Therefore, in this report the accent will be on these medium-scale debris flows. On the hillslopes in the upper parts of the Riou Bourdoux catchment also small-scale debris flows have been investigated (see section 4.3 and Spee & Visser, 1999).

Typical debris flow source areas are described by Hovius (1990) for the Bachelard valley, near Barcelonnette, as spoon- or funnel-shaped concave parts of slopes. The slopes of these source areas are between  $33$  and  $38^\circ$  or even steeper. For the initiation of debris flows steep slopes, high pore-water pressure and the availability of sediment, which can be mobilised, are required.

Connection of the source area to the stream network also plays a vital role, for further transport of the debris flow. The orientation of possible source areas is also important in this respect. Small-scale debris flows triggered in typical source areas may not continue through a channel, if the angle at which the hillslope debris flow enters the drainage network is too great (Benda & Dunne, 1987). Debris flow trigger zones, capable of producing 'larger flows', are thus more or less aligned with a channel that acts as its transport zone.

Several authors have tried to explain the mechanisms of initiation. Three of these mechanisms will be mentioned here.

## Initiation

Johnson (1970) describes a mechanism for the initiation of debris flows by the transformation of landslides into a debris flow by dilatancy or liquefaction during movement. Dilatancy is the tendency of tightly packed sediment to expand under shear due to an influx of water from an external source. The process of liquefaction is generated without an external source of water. During collapse of the grains into tighter packing, overpressure is developed (van den Berg & van Gelder, 1999).

A second mechanism is the damming of water behind an accumulation of debris (Costa, 1984). In between outcrops, narrow zones can exist at which debris accumulates. During an extreme rainstorm the debris, if abundantly available, can be washed away and transform into a debris flow (Luckman, 1992).

The last mechanism is based on the model for debris flow initiation of Takahashi (1981) and was modified by Postma (1988) and Blijenberg (1998). During high-intensity rainstorms within the alpine source areas, overland flow transporting fine material or micro-scale debris flows (MDF) occurs. The muddy flow has a higher density compared to water and has a higher viscosity. Downslope, coarse debris can be found in hillslope gullies. The high viscous mud (or when there is an abundant supply, even water (overland flow) itself) can run over and enter the pores of the coarse debris on the gully floor. Through saturation of this coarse debris or by loading, failure of the debris will occur and the mixed material will then continue to move as a debris flow (Blijenberg, 1998) (figure 2.11).

In this report it is assumed that the model of Blijenberg (1998) is most valid for the investigated subcatchment. This assumption will be checked in the field, including the validity of the other two methods. Debris flow source areas can thus be identified as steep locations, having an abundant presence of colluvium, on slopes which are prone to surface wash erosion (rill erosion). On these slopes a sufficiently fine matrix must be present which can be incorporated into overland flow. Gullies must be present to connect the trigger hollows to the drainage network.

The triggering of debris flows will thus depend largely on the presence or absence of overland flow. The occurrence of overland flow can be calculated with surface infiltration formulas and precipitation data (see section 3.4.2). This will only indicate whether possible overland flow occurs, and not whether a debris flow is actually triggered.

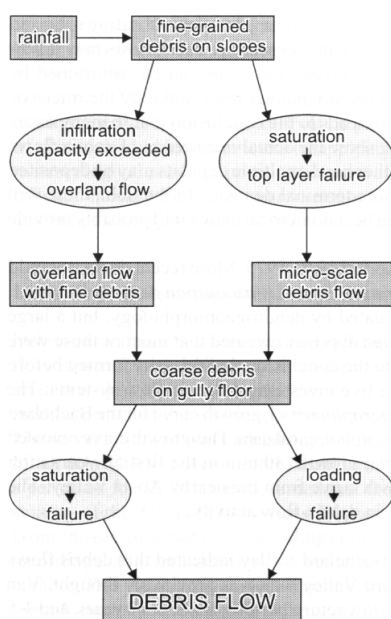


Figure 2.11 Flowchart of debris-flow initiation according to Blijenberg (1998).

## Erosion

Once initiated, the volume of debris flows may increase by scouring colluvium from the bed of gullies and channels during its movement down-slope. This increase primarily takes place in the steeper 1<sup>st</sup> and 2<sup>nd</sup> order channels (Benda & Dunne, 1987; Benda & Cundy,

1990). Benda & Cundy (1990) found on the Oregon Coast range a critical channel gradient of  $10^\circ$  above which debris flows scour a channel to its bed, although this value may be different in the Barcelonnette Basin. The total volume of a debris flow reflects thus two components. One part is the sediment that has failed during the triggering process of the debris flow; the other part is the sediment that is incorporated into the debris flow during its movement. Coussot and Meunier (1996) suggest that the largest part of the volume of a debris flow is derived from this incorporated colluvium.

This colluvium can eventually reach the basin outlet mainly as a result of the debris-flow process (Benda, 1990). While stored in headwater channels, the colluvium shows practically no signs of fluvial sorting (i.e. it has the same grain-size distribution as colluvium on slopes unaffected by streamflow). Possible explanations for this lack of fluvial sorting are the following:

- Small landslides cause instant delivery of thick colluvial wedges to the narrow channels. The stream power in these channels is insufficient to clear all debris, before a new large input of material occurs, resulting in a net storage.
- The presence of large boulders and woody debris (in the stored colluvium) reduces channel gradients due to an increased channel roughness (see equation 2.1).
- The channels only drain small catchments. The water flow depth (and thus velocity) in the streams is therefore not high enough to adequately erode sediments.

The incapacity of normal stream flow to erode and transport material from 1<sup>st</sup> and 2<sup>nd</sup> order channels, combined with the erosional processes of debris flows, results in a system of aggradation and degradation for these channels. From the moment a debris flow travels through the channel, most stored sediment is eroded and transported to higher order channels. After this event, aggradation will take place; all kinds of processes produce sediment to the channel, which is stored until it is removed by another debris flow (degradation). The time period over which the colluvium is stored in the channel depends on the frequency of debris flow occurrence.

#### Size and frequency estimation

Because debris flows are thus an important erosion and transport process in forested, mountainous areas, it is important to make an accurate estimate of their frequency and volume.

In the Riou Bourdoux catchment small- to medium-scale debris flows occur in zero and/or first order channels. The contribution of these debris flows to the sediment budget can be determined by measuring the volume of the deposit. The total volume of a debris flow can be determined by multiplying the length of a deposit by its average cross-sectional area.

The contribution of the medium-scale debris flows deposited in higher order channels, is more complex to estimate. Since much of the volume of these debris flow deposits represents remobilised channel sediments, the actual volume of sediment production from debris flows is much lower than the volume of their deposits (Benda & Dunne, 1987). The calculation of the contribution of these medium-scale debris flows is very difficult because they erode all evidence of other hillslope processes. Reid & Dunne (1996) tried to solve this problem by comparing the volume of the debris flow deposit with the volume of immobilised

sediment in neighbouring channels. The frequency may sometimes be determined from aerial photographs. It is evident that debris flow frequency usually decreases with increasing channel order and that debris flows in 3<sup>rd</sup> or higher order channels become increasingly depositional in character (Reid & Dunne, 1996).

Debris flows found in the French Alps are controlled by precipitation (van Asch & van Steijn, 1991; Coussot & Meunier, 1996). Because the initiation process of debris flows is still difficult to quantify, threshold hydrological conditions under which debris flows are likely to occur are usually used as predictors (Coussot & Meunier, 1996; Selby, 1993).

If debris availability is not the limiting factor, debris flows are triggered if a certain precipitation intensity threshold is exceeded according to Caine (1980). Caine found a curve of minimum rainfall intensity ( $i_r$  in mm/hr):

$$i_r = 14.82 \cdot D^{-0.39} \quad (2.4)$$

$D$  is the rainfall duration in hours. Instead of rainfall intensity Innes (1983) used total rainfall in a period ( $i_t$  in mm) to construct a curve for debris flow triggering:

$$i_t = 4.94 \cdot D^{0.50} \quad (2.5)$$

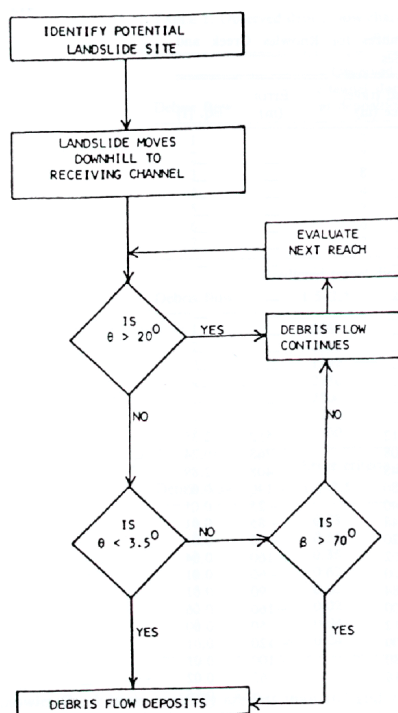


Figure 2.12 Flowchart for predicting deposition of debris flows (Benda & Cundy, 1990).

According to Blijenberg (1998) the curve of Caine is more valid for the Bachelard valley. In this study it is supposed that the curve of Caine (1980) is also valid for the triggering of debris flows in the Riou Bourdoux catchment.

High-intensity rainstorms with durations of 5 to 10 minutes (and an intensity of 50-100 mm/hr) appear to be able to initiate debris flows. Blijenberg (1998) found a threshold value (i.e. a function of slope gradient) of minimally 45-55 mm/hr during a few minutes for the initiation of micro-scale (<1 m<sup>3</sup>) debris flows on steep slopes in flysch deposits. Van Asch & van Steijn (1991) found a recurrence interval of 4 to 10 years for medium scale debris flows in the French Alps. However, for small-scale debris flows Blijenberg (1998) identifies frequencies of 1.6 to 6.6 years for the Bachelard valley.

### Routing and deposition

For predicting the position of debris flow deposits the empirical model of Benda & Cundy (1990) is used (Figure 2.12). The model is based on two criteria for deposition: channel slope and tributary junction angle. If the gradient of the channel through which the debris flow is travelling has declined to a certain critical angle (in the case of Benda & Cundy, 1990, a critical angle of  $3.5^\circ$ ) the debris will be deposited. This is also the case where a flow enters a tributary with a certain critical junction angle (Benda & Cundy, 1990:  $70^\circ$  or more) (figure 2.12). The junction angle ( $\beta$ ) is defined as the upstream angle between the tangent lines of two intersecting channels (figure 2.13). Benda and Dunne (1987) found that debris flows deposit a portion of their sediment on debris fans at tributary junctions. If the junction angle is too great, the debris flow will not be able to 'make the turn' and come to a complete halt by partly smashing in to the opposite valley wall.

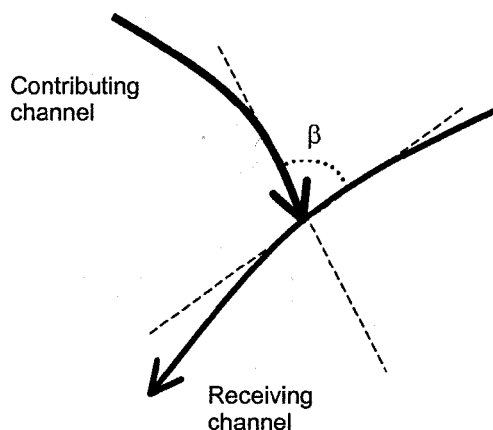


Figure 2.13 Geometry and terminology of stream junction.  $\beta$  refers to the junction angle (Benda & Cundy, 1990).

In this model the rheological properties (sediment size and water content) of debris flows are not required, since they appear to be relatively constant inside a catchment (Benda, 1990).

In this report this model will be assumed valid and the critical slope and junction angle will be determined for the investigated subcatchments of the Riou Bourdoux.

A problem, which may arise with its application, is the assumption of the uniform rheological properties. Due to the many different lithology types present in the study area, the colluvium at trigger sites may also show this variation, which may result in debris flows with different grain-size distributions, size and flow behaviour (Selby, 1993). Another factor is the water content, which may vary between debris flows and which affects flow behaviour. Because the model disregards the momentum of debris flows, prediction of the routing of the more fluid debris flows becomes difficult.

Another possible problem in the application of this model is due to the fact that many of the (1<sup>st</sup> and 2<sup>nd</sup> order) channels in the investigated subcatchments have small debris-retention dams. As indicated by Benda & Cundy (1990), the model does not account for (artificial) stair-stepped channels.

## 2.3 Storage elements

In sediment budgeting often a steady-state equilibrium condition is assumed. The inputs are assumed to be equal to the outputs, and the sediment pathways within the basin are not considered (Sutherland, 1990). In recent years it has been proven that large

proportions of sediment produced by erosion, mass wasting, and other processes within a basin are stored for significant amounts of time within the basin (Phillips, 1991).

Material produced on hillslopes will be transported to low order channels. In the Riou Bourdoux catchment these first- and second-order channels comprise approximately 70% of the cumulative channel length in which this colluvium is concentrated. Such low order channels can store colluvium for centuries (Benda & Dunne, 1987). Only during extreme conditions this sediment is transferred by debris flows to higher-order valley floors. If not directly transferred to the basin outlet, this sediment is stored here as *alluvium* (in-channel storage).

Although there is continuous sediment influx to higher-order channels by soil creep, slope wash, bank erosion and small-scale debris flows (from streamside slopes), the portion of episodic channelled debris flow transport causes unsteady sediment supply. Benda and Dunne (1987) use the term *waves* to indicate that there exist in the channel network unsteady and non-uniform variations of transport and storage volumes that may travel or remain stationary.

There is a lag between upslope erosion and basin sediment output, which is a function of the residence time of the various reservoirs of the basin (Sutherland, 1990). Variations in sediment output are caused by remobilisation of previously stored sediments (Sutherland, 1990). Since these changes in storage are difficult to determine, changes in sediment production may be offset or overshadowed and therefore influence sediment yield estimates. Phillips (1991) found that storage might be more sensitive to environmental changes than sediment yield.

### 2.3.1 Colluvial storage

Colluvium is the sediment stored on a hillslope, which is produced on the same slope (Whittow, 1984). Practically any concave section of a hillslope, independent of its process of formation, can act as a storage location for colluvium. Usually colluvium is stored at the foot of slopes, in hollows and (dis-)continuous gullies. In this report sediment having a hillslope source, which is stored in low-order channels (up to 2<sup>nd</sup> order), is also regarded as colluvium. The sediment is produced by weathering or supplied by processes like creep, debris flows, landslides and sheet wash (see section 2.2), although some colluvium may also be relict from the Pleistocene, when sediment production processes were more active. As mentioned earlier, colluvium can be recognized by its particle-size distribution, since no fine sediment is washed out yet (Benda & Dunne, 1987).

The thickness of colluvium can vary considerably, depending on the rate at which colluvium is produced, the frequency of scouring debris flows and the maximum volume of the “colluvial reservoir”.

### 2.3.2 Channel storage

Channel alluvium represents a reservoir of sediment that has been eroded and deposited within a drainage basin. Channel storage can be defined as the difference between sediment yield from the basin outlet and sediment delivered to the channel from upstream subcatchments (Sutherland, 1990).

In-channel storage or alluvium includes transitory channel deposits, channel fill and accretion deposits, which can be found in higher order channels (from 3<sup>rd</sup> order upward) and at their margin locations. The main channel of the Riou Bourdoux is a 3<sup>rd</sup> order channel, in which fluvial processes, next to debris flows, may be important in influencing channel storage (and thus catchment sediment yield; Reid & Dunne, 1996). This may be largely due to the increasing volume of sustained river flow (due to an increasing number of contributing tributaries) (Benda & Dunne, 1987). Moreover, a decreasing channel gradient and an increasing width, slows down debris flows to the point of deposition, reducing their impact.

Because debris flows from 1<sup>st</sup> and 2<sup>nd</sup> order channels deliver most sediment for storage in the main channel of the Riou Bourdoux, the character of sediment delivery is predominately episodic. The frequency and size of these events is determined by the frequency and size of the debris flows.

In between aggrading debris-flow events, the Main Channel may have time to “clean up” the riverbed (degradation) by fluvial processes (Benda & Dunne, 1987). However, some of the more fluid *laves torrentielles* are capable of reaching the Ubaye (traversing the entire main channel of the Riou Bourdoux), depositing only little sediment in the channel as levees.

The sudden change in sediment supply is often accompanied by an adjustment in channel morphology (Dietrich *et al*, 1989). Changes in channel form cause changes in storage volume and location, with recovery rates on the order of decades or longer (Wolman and Gerson, 1978). Width and slope-gradient of the channel are two important variables that influence in-channel sediment storage. Reductions in width of the channel result in high values of stream power and sediment transport (Sutherland, 1990). Therefore changes in channel cross-sectional area and net change in bed elevation can be used to document net changes in channel storage volumes (Sutherland, 1990).

Sediment yield from the Main Channel (of the Riou Bourdoux) to the basin outlet is thus dependent upon the frequency of the *laves torrentielles*, capable of reaching the Ubaye, and the intensity of fluvial processes able to transport stored sediment. The fluvial transport processes comprise two elements: suspended load and bedload transport (Reid & Dunne, 1996). In order to assess the storage capacity of the Main Channel, the order-of-magnitude of bedload transport has to be determined.

Most mountain rivers are characterized by very high variations of water and sediment discharges. In these circumstances bed load transport takes place mainly during flood waves of short duration and with a rapid increase of the water levels (Georgiev, 1990). River flow in these conditions is unsteady and non-uniform with relatively high velocities.

Several formulas exist for estimating bedload transport amounts based on channel morphology (Khosrowshahi, 1990; Georgiev, 1990). The application of these formulas to steep gravel-bedded mountain channels can, however, be entirely inappropriate, due to the

fact that the formulas are based upon stable channel reaches exhibiting constant discharge (Georgiev, 1990; Reid & Dunne, 1996).

Other methods for estimating fluvial transport include in situ volumetric measurements of bed load and total sediment discharge estimations based on suspended load concentration records. The former method involves placing weirs or digging sediment traps in the channel of interest and monitoring changes (Georgiev, 1990; Sutherland, 1990). The latter method requires long-term suspended load data and a strong correlation between bedload and suspended load (Khosrowshahi, 1990). Since both methods have inherent problems, and require long-term monitoring, they cannot be used in this research.

A factor greatly influencing sediment storage and transport processes in the Main Channel are the sediment-retention dams built by the RTM. A total of 33 dams have been built in the last 100 years (pers. com. RTM, 2001). These dams inhibit normal fluvial processes by widening the channel and reducing the channel gradient, resulting in a lower stream power and a higher storage capacity. These dams trap any sediment until the reservoirs behind the dams are completely filled; after which an artificial stepped channel-profile has resulted. This stepped profile retards even more the transport of bedload to the basin outlet (although when all storage capacity of dams are full, this might increase again). Due to these dams the Main Channel cannot erode into its sediment, so no lengthening or undercutting of slopes occurs promoting stabilization of the riverbanks and general channel aggradation.

The Main Channel is also subject to 'repair works' by the RTM. These repair works include the "cleaning up" of the alluvial riverbed by bulldozers each spring. Part of the sediment is pushed to the edges of both sides of the channel, resulting in an artificially enlarged and heightened stream-bank, approximately 3 meters in height. This bank holds back much debris coming from the surrounding Terres Noires slopes. This repair work has been going on for so long, that vegetation has started growing on these banks (several 20-year old trees were observed), and bank erosion can be neglected. Another part of the alluvium is occasionally "mined" for road repair works within the Riou Bourdoux catchment.

It is evident that under the present circumstances, the stream power of the Riou Bourdoux is artificially so reduced that fluvial process-activity is likely to be at a minimum. Storage in the Main Channel is thus likely to increase (assuming that debris flow activity remains constant).

Because the present-day risk of *laves torrentielles* activity has to be determined, the "repair works" of the RTM must be considered as a part of the process activity in the Main Channel.

In situations as described above, one can do little more than assess the process-activity through determining the infill-rate of the reservoirs behind dams, or monitoring change in channel geometry (Reid & Dunne, 1996).

## 2.4 Sediment budget analysis (linkages)

The general form of a sediment budget is established by the linkages among storage elements and transport processes, which can be expressed in a flow diagram (Swanson et al. 1982). A linkage can be defined as the relative (sediment) contribution from one process to the next, which is expressed as a percentage based on process size and frequency. In this study a flow chart, like figure 2.1, is recommended to simplify the complexity of the investigated area.

The composition of the stored sediment is dependent on the active processes and the residence time. The different types of channel transport (in suspension, as bed load or in debris flows) will influence particle-size distribution. Debris flows will either erode or deposit within channels mostly indiscriminate of particle size, while suspended and bed load mobilise finer material more easily. However, the types of hillslope-transport processes and their distribution within the basin are also important, since these processes influence the input of certain grain-size fractions to the streams, thus influencing channel sediment mobility. The proportion of sediment transferred by a channel process is also partly dependent on residence time, because after longer time more large particles are reduced by weathering to fine sediment that can be transported as suspended load than after a shorter period.

To construct a valuable flow chart for sediment budgeting it is thus important to accurately determine the contribution of transport processes and the residence time of storage elements.

## 3 Methods

### 3.1 Construction of a sediment budget

The construction of a sediment budget for the Riou de la Pare catchment is based on the method described by Reid and Dunne (1996). They developed the following procedure:

- Step 1. Define the problem
- Step 2. Acquire background information
- Step 3. Subdivide area
- Step 4. Interpret aerial photographs
- Step 5. Conduct fieldwork
- Step 6. Analyse data
- Step 7. Check results

The first two steps have been done before the investigated area was visited. The most important points of this preliminary investigation are described in the introduction and chapter 2 of this report. These results are used in preparation for the fieldwork. Since detailed aerial photographs of the catchment were not available, step 4 was skipped. Step 3 also proved difficult to achieve, due to step 4 and the absence of a suitable viewpoint to overview the entire study area. The division was made with the aid of the topographical map.

Step 5 (the fieldwork) was carried out in a period of 8 weeks. During the first weeks the fieldwork area had been explored. During this step active erosion and sediment transport processes were identified, and their distribution and (relative) importance defined. Relatively insignificant processes are considered only briefly during the fieldwork to ascertain their order-of-magnitude. The research was then focused on accurately defining the rates of the processes that have the highest contribution to the sediment budget (Reid & Dunne, 1996). Locations of storages are identified, and the estimated storage-volumes were calculated.

From the problem defined (see introduction), it is assumed that debris flows are the main sediment transport process in the main channel of the Riou Bourdoux catchment. In the investigated area debris flows also seem to be one of the most important erosion and transportation processes. Therefore, focus is on this phenomenon. The probable mechanism responsible for debris flow initiation in the Riou Bourdoux catchment is determined. Furthermore, the depositional characteristics of debris flows, based on the model of Benda & Cundy (1990) (see section 2.2.3) are determined for the studied area.

A preliminary flowchart is constructed for better understanding of the active processes and their interactions. This can be done at any desired level of complexity (figure 3.1). If estimates of process rates are made, these can be incorporated into the flowchart to identify the most important processes and interactions. Estimates of process rates usually require field measurement of the volume or depth of sediment displaced and the age of activity (Reid & Dunne, 1996). During background work (step 2) the types of data needed to

compute rates using predictive equations for erosion or sediment transport are identified, and some of these data will need to be measured in the field.

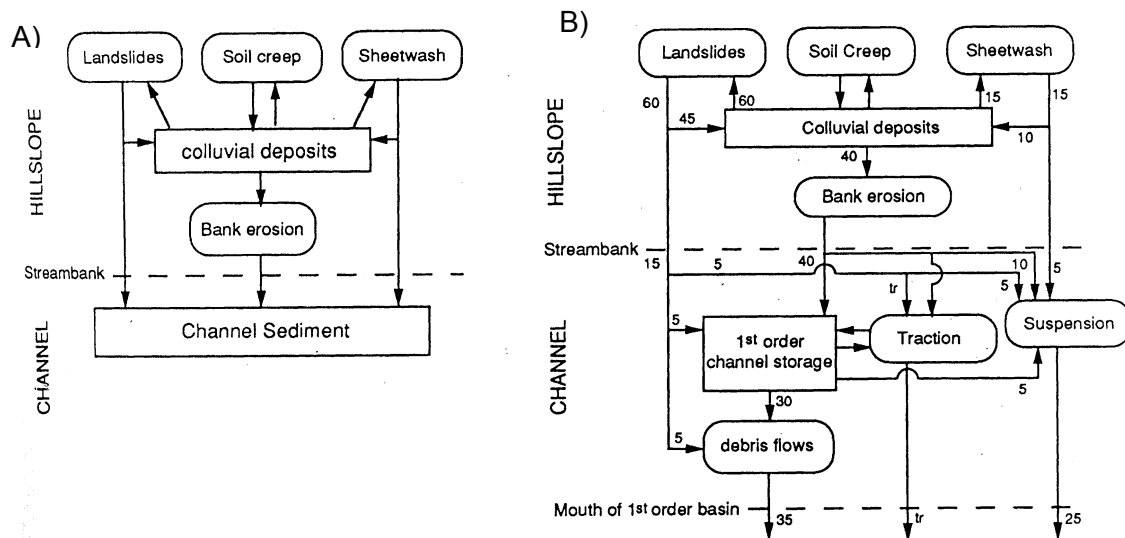


Figure 3.1 Examples of increasingly complex flowcharts for a hypothetical first-order basin. A) Hillslope transport processes and storage, and their relation to sediment delivery. B) Example of quantification of sediment transfers (values in  $t \cdot km^2 \cdot yr^{-1}$ ) (Reid & Dunne, 1996).

During the analysing step (6) data from maps, published reports, and fieldwork, collected at different scales and in different formats, must be reconciled. A common method for combining data sets is to divide the study area into grid cells and to characterise each grid cell. Finally, these “overlays” can be combined.

Long-term (> 30 years) averages of process rates must often be estimated from available short-term data, and this may require, for this study, analysis of weather records. Calculations using predictive equations (see chapter 2: angle of internal friction, debris flow initiation) must also be carried out (De Joode, 2000). The accuracy of estimated rates can be assessed by evaluating the accuracy of component measurements, comparing estimates using different techniques, or testing the sensitivity of calculated results to likely uncertainties in the component data (Reid & Dunne, 1996).

In step 7 the results are compared to those from other studies in areas with the same characteristics. This was not possible for the Riou Bourdoux catchment, because comparative research in catchments with similar characteristics has not been undertaken.

### 3.2 Mapping techniques

Before fieldwork was conducted the Riou Bourdoux catchment was subdivided into several subcatchments; three of which were investigated in 1997 (chapter 1). The Riou Guérin and the Riou Chamous subcatchments have been analysed by Spee & Visser (1999). The Riou de la Pare catchment (appendix A1) is analysed in this report and in De Joode (2000).

In order to obtain a clear picture on the spatial distribution of geomorphological processes and their deposits and interactions, detailed mapping of the study area was

necessary. A geomorphological map in black and white (Salomé & Beukenkamp, 1989) was available for the study area. However, its scale (1:25.000) and the high process activity in the area made it preferable to map the chosen subcatchments within the Riou Bourdoux system anew. In the following sections the different techniques used for mapping are explained.

### 3.2.1 *Geomorphological mapping*

The legend used as a base for mapping the geomorphological features of the study area was adopted from Cools & Den Hoed (1984). This legend has been developed and tested especially for the basin of Barcelonnette (Salomé & Beukenkamp, 1989), so it could be used without alteration.

Detailed geomorphological mapping was carried out based on a system of observation points (Van Zuidam & Cancelado, 1987). At these observation points several landscape characteristics were noted with the aid of a checklist, the so-called “field-observation-form” (appendix A2). This form contains all the important aspects needed for insight into the process activity at a certain location and of the investigated subcatchment as a whole. Mapping of the study area involved traversing the entire area and mapping all relevant geomorphological features. Following the procedure described by Salomé & Beukenkamp (1989), in the field the observed geomorphological features were mapped on (a photocopy of) the 1:10.000 base map of France (I.G.N. 1982 / 1983). Observation points were chosen in such a way that a representative distribution was obtained. Since some sites are more complex than others, a clustering of observation points is not unusual. The location and results of the observation points are shown in appendix A2 and A3 respectively.

The identified geomorphological units were interpolated afterwards with the help natural boundaries easily identifiable in the field and on existing topographic maps (Cooke & Doornkamp, 1990). Since aerial photography could not be used, feature-boundaries had to be drawn directly in the field. In order to accomplish this, the surroundings of the observation points were interpreted as well, with instant boundary drawing on the “field map”. Because some areas within the subcatchment were very difficult to reach (due to dense vegetation or steep slopes), observation from a distance (with the use of a standard pair of binoculars) was necessary. Although this method is less accurate than point observation, it proved satisfactory when combined with pre-existing topographic features indicated on the detailed topographic base map (I.G.N. 1982 / 1983). The application of this method also means that several observations gathered for “boundary drawing” are not represented in the results of the observation points (appendix A3).

The geomorphological units were identified based on the interpretation of the data provided by the observation points in combination with indications given in standard literature on geomorphological mapping. Since an explanation of the characteristics of every legend-unit mapped would be too lengthy a discussion, it is omitted here. The used literature is summed here: Selby (1993), Bunza & Karl (1975), Cools & Den Hoed (1984) & Whittow (1984).

The mapping of the area was towards recognising crucial processes in the sediment budget (Reid & Dunne, 1996). Thus cols, watersheds, and several other similar features were excluded from the maps to improve simplicity and legibility.

Two geomorphological features, which were abundantly present in the study area, are also not shown on the geomorphological map. These are the features creep and terracettes. Creep is present on practically all the slopes in the study area and all slopes in moraine material above the tree-line exhibit terracettes. These processes were not mapped, due to the fact that they would render the map illegible.

### 3.2.2 *Mono-thematic mapping*

In combination with the geomorphological map, three monothematic maps were created. These maps are a vegetation map, a surface lithological map and a slope map (appendix B2-B4). These are needed to produce a landscape-unit map (Reid & Dunne, 1996), which shows areas of relative uniform slope, vegetation and surface lithology, which are important factors in controlling erosional processes. This landscape-unit map is created in a GIS by overlaying (chapter 5).

The vegetation and surface lithology map were created with the data gathered from the observation points. The slope map was solely created in a GIS. For all three maps, the legends were created specifically for this study, so that the required range of displayed variation was obtained.

### 3.2.3 *Map construction*<sup>5</sup>

From the observation points and the produced “field map” (showing all major feature-boundaries) the geomorphological, lithological and vegetation map were thus produced. Maps are nowadays often created with the aid of a Geographical Information System (GIS). Although a GIS is not simply a computer system for making maps, it can create maps at different scales, in different projections, and with different colours. But most importantly, it is an analytical tool capable of performing many analytical operations on spatial data, which can be presented as maps (Burrough, 1986). Since several analyses were necessary on the gathered spatial data (maps), it was decided to produce all maps with the aid of a GIS.

A GIS project can be organized into a series of logical steps, each building upon the previous one.

Step one involves determining the objectives of the project. In this report, the main objectives are to accurately produce all desired maps in presentable form and to develop a debris flow routing model in GIS. For this purpose, two major GIS programs were used. For the conversion of “field maps” into digital maps (spatial GIS data), the ARC/INFO® GIS package was used.

---

<sup>5</sup> This section is taken in short and with adaptation from Spee & Visser (1999).

The making of the *routing*-model was carried out using the PCRaster environmental software package (© Department of Physical Geography, Utrecht University, The Netherlands). The construction of this model is described in chapter 5.

Since this research is a preliminary investigation of the Riou Bourdoux system, the results of both the maps and the model may be of interest to future researchers and also to the agency "Restauration des Terrains en Montagne (RTM), a subdivision of the Office National Forestière (ONF), of the Département des Alpes de Haute-Provence, France.

The next step is to build the database. This is the most critical and time-consuming part of the GIS project. The completeness and accuracy of the database determines the quality of the analysis and final products. To develop a digital database the following steps have to be made: 1) determine the study area boundary; 2) determine the coordinate system to be used; 3) establish which data layers (or coverages) are needed; 4) determine what features are present in each layer; 5) determine what attributes each feature type needs and 6) determine how to code and organise the attributes.

The description of the actual building of a database is described by Spee & Visser (1999).

The following step in the GIS project is digitising the different gathered spatial data (i.e. the hand-drawn (field-)maps and topographic map). After digitisation, several coverages were created. Besides a digital coverage of the geomorphological, vegetation and the lithological map, a slope coverage, derived from the digitised contour lines of the topographic base map, was also created.

All coverages were finally fashioned into presentation form with the aid of the program ArcView® (appendix B2-B5). Both the vegetation and lithological coverage have polygonal attributes. The slope coverage is in grid-format. These types are easily presentable in ArcView®. The geomorphological map, however, comprised several different attributes (polygon, arc and point attributes). Difficulties in presenting these different attributes on one sheet, made it necessary for several units of the legend to still be drawn manually.

### 3.3 Mapping debris flow and channel features

At different sites in the investigated area debris flows have occurred (see chapter 4). Part of the research tasks was to adapt the debris-flow routing and deposition model of Benda & Cundy (1990) (section 2.2.3). This model is based on two criteria: the minimum channel gradient at which debris flow deposition certainly occurs (1) and the critical channel junction angle at which debris flows also come to a halt (2). These criteria have to be determined for the Riou Bourdoux system.

### 3.3.1 Mapping old debris flow deposits

Old debris flows located in the study area give much insight into the process of initiation, routing and deposition as well as information on possible size and frequency of occurrence. In order to gather the specific criteria of the model, several aspects of debris flow deposits found in the study area had to be determined. The following aspects were measured:

#### Depositional features

Old debris flows were identified in the field by their deposits. Again, the absence of useable aerial photographs impeded the identification process. Each deposit was measured with (standard) surveying techniques in order to determine its length, width and thickness (Benda & Cundy, 1990). For this purpose a measuring ribbon of 30 meters length was used. From these measurements an estimation of its volume was made.

The gradient of the channel where the debris flow has stopped (deposition angle  $\theta$ : figure 2.12) was subsequently measured. If the deposit was located at a junction between two different channels (junction-angle  $\beta$ : figure 2.13), the angle between these channels was also determined.

Finally, the sedimentological characteristics of the deposit were noted following the field-observation-form (appendix A2).

#### Flow path

Backtracking of the old debris flows revealed their flow path and initiation sites. Most deposits were easily tracked towards their triggering sites either due to a short distance



Figure 3.2 Section of the Riou de la Pare flowing through debris flow deposits and levees. The levees are (roughly) bounded by the marked red lines and the vegetation on the outer edges in the photo.

between triggering and deposition or, when the flow-path was long, by following the levees upstream (figure 3.2).

Along the path of the debris flow, only two characteristics were measured. If clear signs of debris-flow scouring were present, the channel gradient was measured. If the debris-flow path encountered a junction (and the path came from the contributing channel), the angle ( $\beta$ ) was measured and only noted if it was smaller than the (possible) junction-angle at the deposition site.

### Initiation site

At each determined source zone, the slope gradient was measured. This gradient is regarded as the angle at which the debris flow was triggered. The slopes at these zones were also inspected for their vegetation, lithology and overall active erosional processes, again following the field-observation form (appendix A2). These features have provided helpful hints for the construction of a landscape-unit map, in which units of debris flow source zones may be indicated (see chapter 5). They also give insight into the general triggering process of debris flows in the study area.

To test the assumption that Blijenberg's (1998) trigger-model is valid for the investigated catchment, the observed characteristics will be checked with those described in section 2.2.3.

Not all debris flow deposits and initiation sites were accessible in the study area. At some instances binoculars had to be used. In these cases, the triggering angle and angle of deposition (and if appropriate; the junction-angle) were estimated with the aid of the topographic map and the produced slope map (appendix B4).

The results of these measurements combined with those of Spee & Visser (1999) are presented in chapter 4.

### 3.3.2 *Identification of debris flow sources zones and colluvial storages*

Besides the recognition and mapping of debris flow deposits and their initiation sites, it is also important to determine *possible* debris-flow source ones and sources of *readily movable sediment* (Reid & Dunne, 1996). Although such sites may not have produced debris flows, they may contribute to the debris flow risk in the future.

Possible debris-flow source zones are identified based on the results of the characteristics described in section 3.3.1. A map can then be made to visualize all (possible) debris flow source zones.

Another important source of possible debris flows in the study area are sediment sinks. Sediment sinks are either hollows on slopes, where *eroded* sediment from the hillslopes are temporarily stored, or they are gullies or avalanche tracks (see figure 4.2), where hillslope produced sediment can also be retained (Reid & Dunne, 1996). Sediment sinks also include the large moraine deposits stored in the more stable hillslope areas and the colluvium stored in channel sections like figure 3.2. However, as will be shown in section 4.1 and 4.3, the latter do not contribute to the *present* debris flow risk.

These 'hazardous sinks' are identified by a number of characteristics. Again, the most important of these are surface lithology, local topography and vegetation (Reid & Dunne, 1996).

The most important aspects to be considered when identifying these sinks are:

- The stored sediment must be readily moveable by a local erosion process.

- Once in transport, the sediment must be able to reach a channel capable of further transporting it.
- The volume of the stored sediment must be large enough to consider it a 'hazardous' deposit, capable of producing a medium-scale debris flow.

Based on the above-mentioned aspects, only a few sediment sources were identified in the field, which are described in section 4.3.1. The identification occurred during the mapping procedure of the study area.

### 3.3.3 Channel process measurements

Two separate methods were adopted to determine channel process-activity of the main channel (3<sup>rd</sup> order) of the Riou Bourdoux.

#### Channel-change survey

As evident from chapter 2, no appropriate transport equations are available for this study of the Riou Bourdoux system. In order to get an idea about general process activity of the Main Channel, an analysis was adopted based on measurable changes in channel bed morphology during the period of investigation (Reid & Dunne, 1996).

The analysis was done on a selected stretch of the Main Channel, as well as on a 2<sup>nd</sup> order channel reach, which are described further on. This was done in order to compare the activity of (fluvial) transport during the research period between 2<sup>nd</sup> and 3<sup>rd</sup> order channels. Detailed survey of the deposits along and in channel reaches can also reveal the dominant type of transport process (fluvial / debris-flow) (Reid & Dunne, 1996), which may be used to estimate the relative influence of the Ubaye-reaching laves torrentielles on the Main Channel and to determine their transport conditions.

The survey is based on the analysis of the characteristics of bank deposits, alluvial (gravel) bar migration and the vegetation state. These characteristics give information on the nature of sediment production to stream channels, and the rate of remobilisation of deposits from floodplains, alluvial bars, and channel beds. Following Sutherland (1990) channel cross-sectional area is also monitored in order to determine storage change (see section 2.3.2).

Evidence of channel stability can mostly be recognized by the following features (Reid & Dunne, 1996): In-channel gravel bars are vegetated; large clasts are angular; large clasts are densely packed; bed is covered by large clasts; moss grows on bed sediment.

Following Reid & Dunne (1996), the representative channel-reach for observation qualified to the following features:

1. The reach is straight and contains no obstacles to flow.
2. The channel is bounded by alluvial sediments and is self-formed (thus undisturbed).
3. The channel has a uniform gradient and a homogeneous bed surface.
4. Flow is in a single thread.
5. The reach is not near a tributary confluence.

Since no undisturbed section (in the Main Channel) was found for measurements (see section 2.3.2), present-day ‘repair works’ are part regarded as a normal stable state of the Main Channel.

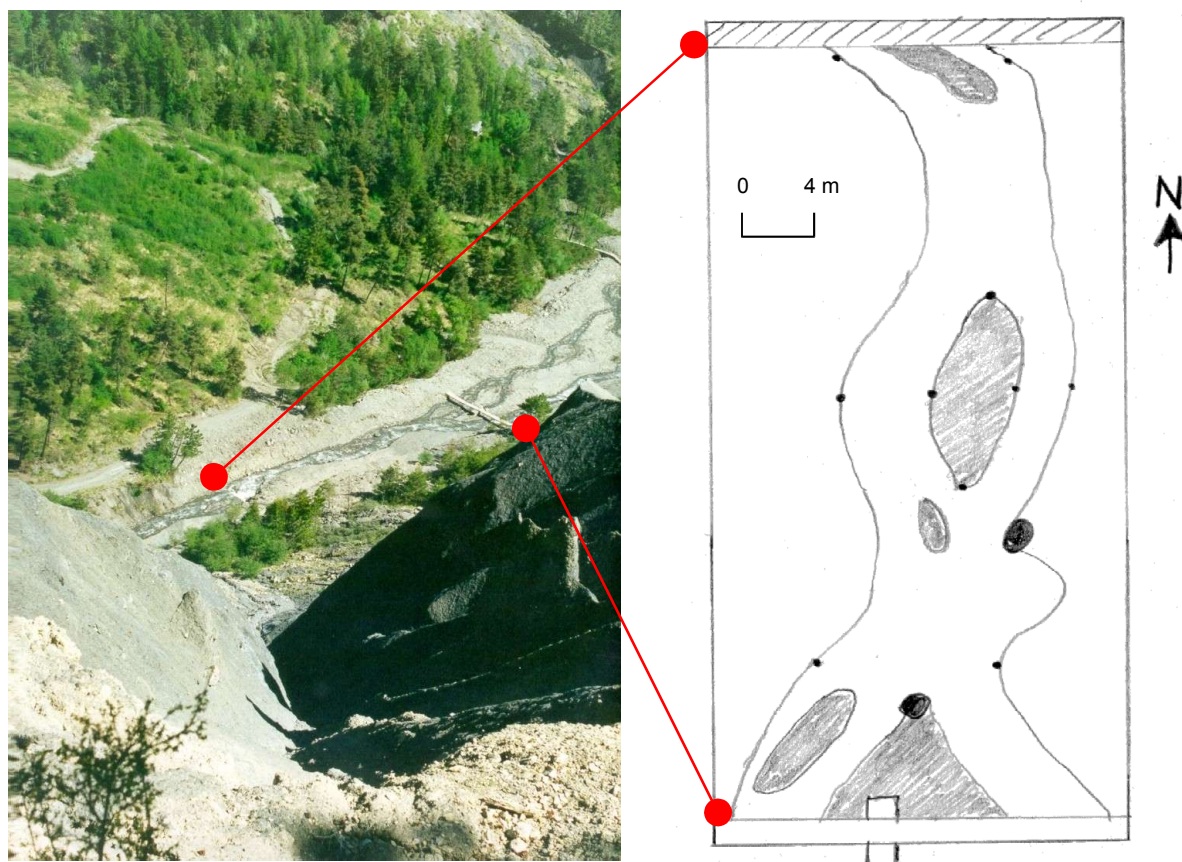


Figure 3.3 Photograph and sketch of the investigated channel-midsection of the Riou Bourdoux. Note that the sketch is orientated north, but the photograph is taken in an east-south-easterly direction

The selected stretch of the Main Channel (3<sup>rd</sup> order) is located at the site of the discharge measurements (appendix A1): a few hundred meters downstream of the location where the streams of the three investigated subcatchments confluence. It is a large section between two sediment-retaining dams (figure 3.3). The channel here is relatively straight and along the entire reach no tributaries join the Main Channel. The reach is 62 meters in length and has an average gradient of 5°. The ‘artificial’ shallow floodplain is on average 20 meters in width. Beyond the floodplain the enlarged banks, mostly more than 3 meters in height, retain much influx of sediment from adjacent slopes. Due to the yearly *repair works* in spring, the channel has no distinctly developed streamline and the character of flow can be defined as braided. No patterns are discernable (both laterally and in height) in the deposits of the (alluvial) plain, although the character of the riverbanks seems to point to a debris-flow origin (levees).

Approximately in the middle of the selected reach one large alluvial bar is present. The surface of this bar is unvegetated, consisting of gravels (diameters ranging from 0.5 to 30 cm) mixed with a matrix of clay particles (5% of surface), which is presumably derived from Terres Noires badlands. All along the edge of this bar large stones (up to 15 cm) are found.

This bar is monitored for changes in width and length during the research. The bar is shown in figure 3.3 and appendix F1 as a shaded area in grey.

Appendix F1 gives a detailed sketch of the entire channel-reach. At three points the width of the stream is measured. These points are indicated in appendix F1. It also shows the exact location of the alluvial bar. During the entire investigation, the channel cross-section and the alluvial bar were measured at about a weekly interval. Also, at one location an attempt was made to monitor streamside erosion of the slightly elevated floodplain (see appendix F1).

The 2<sup>nd</sup> order channel-reach under observation is a stretch of the Riou de la Pare near observation point 28 (appendix A2 & A3). A detailed sketch of this channel-section is shown in appendix F4. The section is relatively straight, is 14 meters in length and has an average gradient of 14°. It flows through colluvial deposits and is mostly confined by the surrounding hillslopes. Much streamside vegetation and mosses on stones are present, indicating surface stability in recent years. Corresponding to the measurements of the Main Channel, along this section three cross-sections were selected, where the average width of the stream and total bed width is measured. For all measurements the measuring ribbon of 30 meters length was used.

The descriptions of channels are based on the first day of observation. The monitoring of the Main Channel started on May the 27<sup>th</sup>, while observations at the Riou de la Pare section commenced on June the 2<sup>nd</sup>.

Besides measuring features at three transects, for each section a photographic time-series analysis was attempted. This was done because four different observers monitored the Main Channel, making it necessary to obtain additional objective visual data. In each monitored channel several (easily transportable) marker stones were selected, which could be recognized in the photographs. All photographs were manually taken from a predefined location (height and angle were kept as constant as possible). Results are given in chapter 4 and appendix F3 and F4.

#### Sedimentation-rate estimation

The other selected method for determining channel sediment transport and storage is the (empirical) estimation of rates of accumulation behind (artificial) barriers (Reid & Dunne, 1996). In the Main Channel, sediment-trapping dams have been built to counteract the *laves torrentielles* risk. Sediment, which has accumulated behind these barriers, is often provided by both fluvial processes and *laves torrentielles*, making this method indiscriminate between the two. It may provide, however, an order-of-magnitude of total channel sediment transport.

With this method, one determines the volume of debris stored in the reservoir between two dams and the duration of infilling. Although every reservoir volume can be estimated from measurements in the field, it is very time-consuming. Therefore, the reservoir volume was estimated from the topographic map.

There are 33 major dams built in the middle reach over a time-span of 100 years (pers. com. RTM, 2001). This means that on average 1 dam has been built every 3 years. It is assumed, since all reservoirs behind the dams are now practically full, that in 3 years time

one reservoir is completely filled. However, 24 of these dams have been built since 1950, indicating that the maximum time at which a reservoir is filled is 2 years ( $\approx 50 / 24$ ).

The dams vary in individual size and in distance to each other, resulting in varying reservoir volumes. For calculation purposes however, a fixed distance between neighbouring dams was assumed. The height of all dams was also assumed to be equal, resulting in an equal reservoir volume behind each dam. The amount of sediment stored behind one such assumed dam is calculated as follows (figure 3.4):

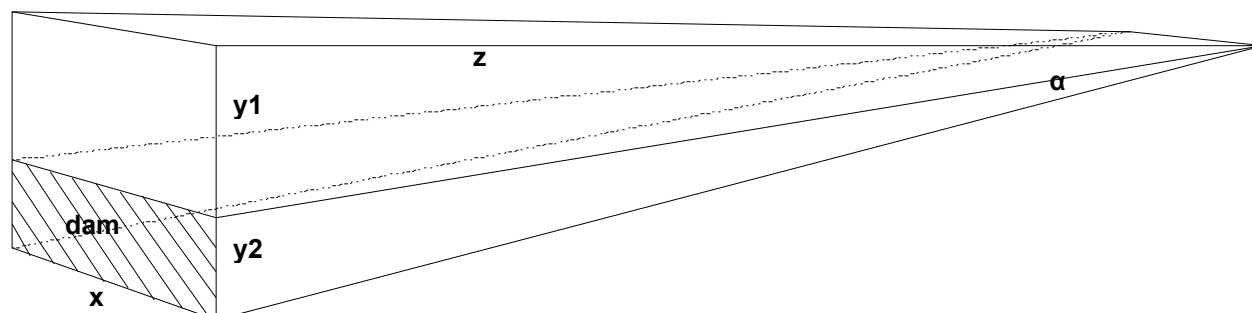


Figure 3.4 Schematic representation of the main channel of the Riou Bourdoux between 2 dams.

The total distance ( $D$ ) between the upper and lowermost dam built in the Main Channel is estimated from the topographic map. The average height and width of the dams will be assessed in the field ( $y_2$  &  $x$ ). The average reservoir-volume between two dams can now be calculated by the following equation.

$$V = (y_2 \cdot z \cdot \frac{1}{2}) \cdot x \quad (3.1)$$

where:

- $V$  = the amount of debris stored in the main channel per 3 (or 2) years ( $m^3$ )
- $y_2$  = the average height of the 33 dams located in the main channel
- $x$  = the average width of the 33 dams
- $z$  = the average distance between two neighbouring dams ( $= D / 33$ )

The minimum estimated sedimentation-rate in the Main Channel might now be determined by dividing the reservoir volume ( $V$ ) by 3 years. The maximum rate is defined as the volume ( $V$ ) divided by 2 (years). Although the use of averages provides a rough estimate of reservoir volume, it is usually accurate enough in order-of-magnitude (Reid & Dunne, 1996).

One disadvantage of this method is the assumption of a rectangular channel cross-section. The reservoir behind a dam is more likely to follow the original channel profile (presumably V-shaped). However, this original profile could not be observed anywhere along the Main Channel, therefore the (rectangular) base of each dam was chosen as reservoir base. Moreover, preliminary volume calculations using both rectangular and v-shaped profiles showed that changes herein do not greatly influence the total reservoir volume.

Another disadvantage is that the method assumes a reservoir sediment-trap efficiency of 100%. The actual efficiency, however, is usually less than 100%, especially concerning the finest material (having the lowest settling velocity), which is likely to be removed (Cooke & Doornkamp, 1990). The sedimentation-rate is therefore considered as a minimum value.

### 3.4 Hydrological measurements

#### 3.4.1 Rainfall measurements

During the entire investigation rainfall was measured within the Riou Bourdoux catchment. This was done in order to correlate several hydrological processes (including simulation of runoff) as well as doing predictions about the circumstances of debris flow initiation (see chapter 2) and also other mass wasting processes. If debris flows would have been triggered during the investigation, the antecedent rainfall conditions would have been known, giving better insight into the triggering process.

Rainfall is measured daily at the weather station Barcelonnette / St. Pons (1140 m a.s.l.). However, the three subcatchments are located at altitudes several hundred meters higher. Because it is well known that rainfall increases with altitude in mountainous regions (Singh and Kumar, 1997), several rain gauges were placed at different altitudes within the Riou Bourdoux catchment (see appendix A1 for location). Rainfall in mountain environments also depends upon several other factors, of which longitude (horizontal distance between two points) and aspect are found to be most influencing (Johnson *et al*, 1990). This was taken into consideration when choosing the locations for the rain gauges. The rain gauges were installed just above ground level with similar aspect (south-east) and horizontally as closely together as possible, in order to get a clear picture of the rainfall-altitude relationship.

The rain gauges were placed respectively at the following altitudes: 1400, 1800, 1950, 2260 m (a.s.l.). The data collected from the several rain gauges, in combination with the data provided from the weather station, will be used to calculate a possible rainfall-altitude relationship for the Riou Bourdoux catchment. This relationship may provide information on future rainfall amounts at any desired altitude, using measurements made at the weather station.

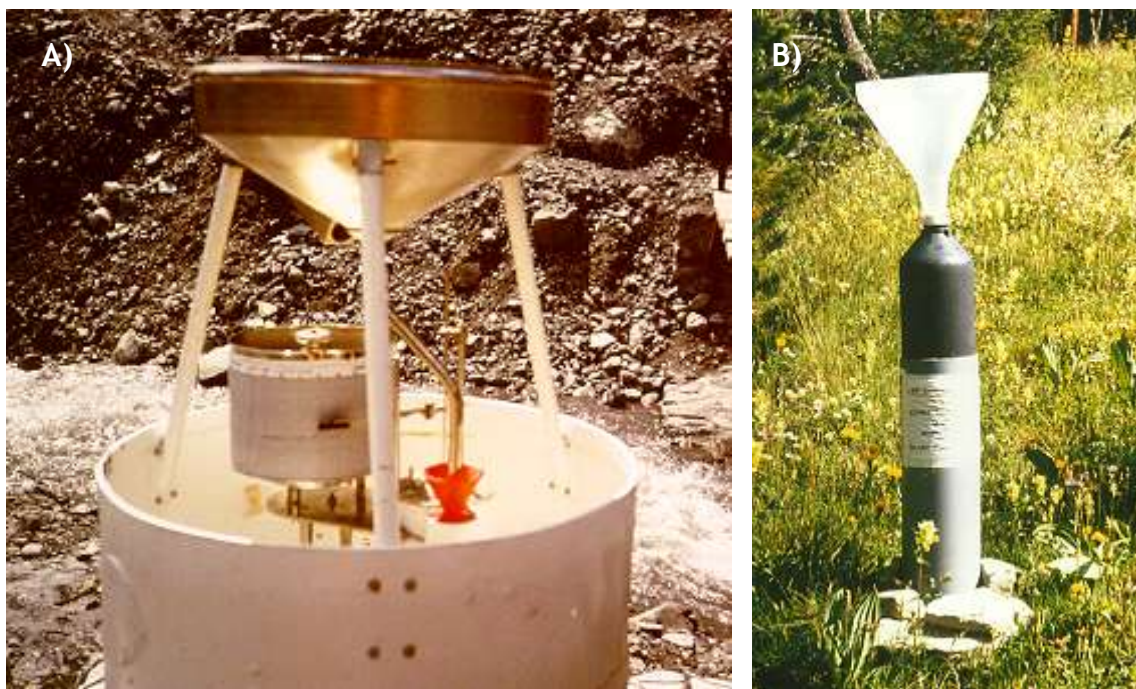


Figure 3.5 Rain gauges used during the fieldwork. A) showing the pluviograph located along the middle reach of the Riou Bourdoux, B) is one of the other type of pluviometers, showing the PVC-bottle and cylinder and the funnel on top of it.

To do predictions about several hydrological processes, it is not only necessary to register the total amount of precipitation, but also to have an indication about its duration and intensity. This, however, is not measured at the weather station. The instrument chosen to measure the intensity and duration of rainfall during the research period is a *pluviograph* based on a tipping bucket principle (figure 3.5: A).

This pluviograph was placed on the pedestrian bridge over the main channel of the Riou Bourdoux, near the channel measurement and discharge location (appendix A1), at the altitude of 1400 m a.s.l. The device has a reservoir, which drains itself when it is full. The reservoir is connected to a large funnel collecting any precipitation that falls herein. A floater is connected both to the contents of the reservoir and to a writing-pen, which registers on a chart recorder the amount of water present in the reservoir at any time. When the reservoir empties, the pen also goes back to its standard position (i.e. the bottom of the paper). The paper chart itself is attached to a cylinder turning slowly round, making a full 360 degrees in approximately one week. The constant rotation of the chart combined with the vertical movement of the pen over the paper, results in a detailed picture of every rainfall event (including time and duration, and hence intensity) over the entire period (appendix C2).

The calibration of this device and the times at which the paper charts were replaced is given in appendix C1 (respectively table 1 & 3). From the calibration it can be seen that every draining of the reservoir corresponds to 10.2 mm of unit depth of rainfall.

The other types of rain gauges used (French: *pluviometres*) are of a much smaller and simpler kind (figure 3.5: B). These were used in order to measure the total amount of rainfall for a given period. The rain gauges consist of a small PVC reservoir connected to a plastic funnel. The reservoir itself was encapsulated by another thick PVC cylinder in order to minimize evaporation. They were placed at the three remaining successively higher altitudes (1800, 1950 & 2260 m). Their location was chosen in such a way, that there was minimal influence from surrounding vegetation, which might cause interception loss. The influence of topography (and also the influence of the rain gauge itself), effecting local wind patterns and hence rainfall distribution, could not be averted. An ideal rain gauge for mountain environments, suggested by Johnson *et al* (1990) and De Villiers (1990), is a ground-level gauge with its rim placed parallel to the slope surface (surrounded by an anti-splash grid). Such a device was not available in this research.

A measurement scheme was developed in order to register all precipitation within small time-periods, so that the data gathered could be correlated with the rainfall-data of the weather station. Ideally, this would mean the recording of data every day. Due to the time-consuming labour of checking the standard rain gauges, a more practical 3-day interval was chosen. All rain gauges were installed on May the 27<sup>th</sup> and were removed from the study area on July the 15<sup>th</sup>.

During each observation all reservoirs were emptied. The measured volume of precipitation can be divided by the surface area of the funnel, resulting in a unit depth rainfall for each particular site.

The paper charts of the pluviograph were changed weekly (appendix C1: table 3) and were subsequently analysed in order to obtain rainfall amounts for the same period intervals (i.e. 3 days) as the other rain gauges (appendix C1: table 2).

The resulting rainfall amounts over all 3-day period intervals are used to determine the rainfall-altitude relationship. Since increasing rainfall amount at higher altitudes is in most cases caused by an increase in intensity and not in duration (Singh & Kumar, 1997), it is assumed that this relationship can also be used to determine rainfall intensities at higher altitudes. A problem may arise in determining this relationship, since practically all studies involved in rainfall-altitude correlations are based on month or year-average data (Singh & Kumar, 1997), while the research period only spans two months.

### 3.4.2 Infiltration capacity measurements on crucial landscape units

The infiltration properties of soils play an important role in the hydrological processes on the surface of a landscape. The most important aspect of determining the infiltration capacity in this study lies in the prediction of possible overland flow when the infiltration capacity is compared with known (or predicted) rainfall duration and intensities.

Following the assumption of the validity of Blijenberg's (1998) model, most debris flows are triggered by overland flow during high-intensity low-frequency rainstorms (section 2.2.3). During these low-frequency, high-intensity rainstorms the infiltration capacity of the ground surface can, after a short period, become less than the intensity at which the precipitation is falling. This will give rise to ponding of excess rainfall on the surface, which will continue as overland flow (Ward & Robinson, 1990). In order to calculate the time necessary for ponding to occur for each rainfall event, an infiltration envelope can be constructed (Kutilek & Nielson, 1994). An infiltration envelope describes the relationship between rainfall intensity and time-to-ponding (figure 3.6).

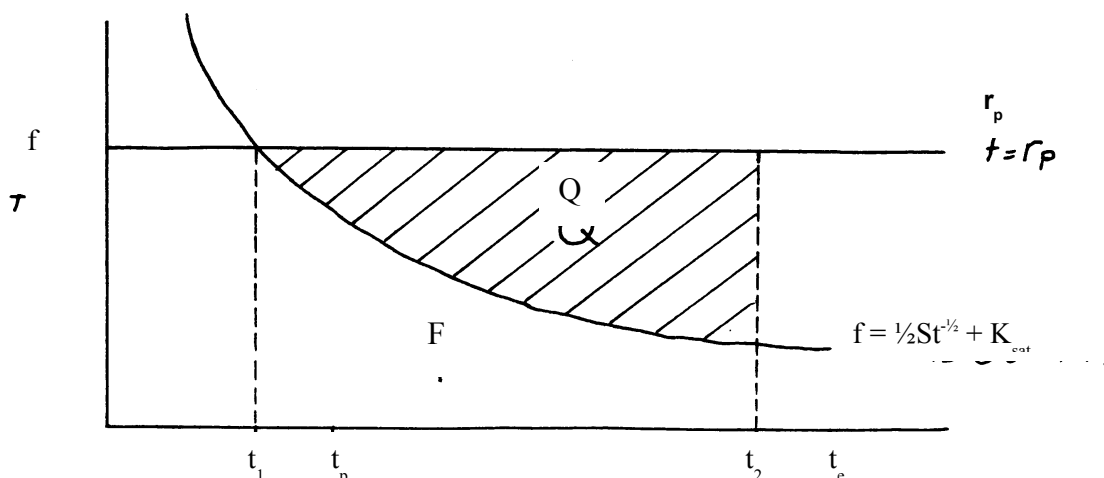


Figure 3.6 Infiltration envelope.  $r_p$  represents the rainfall intensity.  $f$  represents the course of the infiltration capacity with time.

This relation is described by Philip's infiltration equation:

$$f = \frac{1}{2} St^{-1/2} + K_{\text{sat}} \quad (3.2)$$

where:

$f$  = the infiltration capacity (in units of length/time; L/T)

$S$  = 'sorptivity' ( $L/\sqrt{T}$ )

$t$  = time (T)

$K_{\text{sat}}$  = saturated hydraulic conductivity of the soil (L/T)



Figure 3.7 A researcher handling the auger ( $K_{\text{sat}}$  measurements at site 1)

This equation shows that eventually (when  $t \rightarrow \infty$ ), the infiltration capacity assumes the value of  $K_{\text{sat}}$ . This is when infiltration takes place under saturated conditions (and hence under influence of gravity). During the first phase of infiltration, when the matrix suction of the soil is greatest, the first term of the equation dominates (i.e. sorptivity).

Determining the  $K_{\text{sat}}$  and sorptivity of the soil under field conditions was done using the inverse auger hole method described by Kessler & Oosterbaan (1974). The method consists of boring a hole to a given depth, filling it with water, and measuring the rate of fall of the water level.

First several landscape units were selected which were found to be important in triggering debris flows (see section 3.3.1, 3.3.2 and 4.3). The locations of the selected sites are shown in appendix A1. Site 1 consisted of

steep slopes (up to  $31^\circ$ ) in heterogeneous slope material (Riou de la Pare catchment). Site 2 was a slide in Terres Noires (Riou Chamous catchment). Site 3 consisted of moraine deposits on Terres Noires (Riou Guerin catchment). Site 4 was a mudflow in weathered flysch (Riou Chamous catchment).

At each site a representative area was chosen, and on each area 30 holes were drilled with a standard auger (see figure 3.7). Each hole is drilled to a depth of approximately 30 cm with a diameter of 4 cm. The holes are filled with water to the rim and are continuously wetted (i.e. again filled to the rim) during 20 to 30 minutes, after which time a quasi-steady flow has developed.

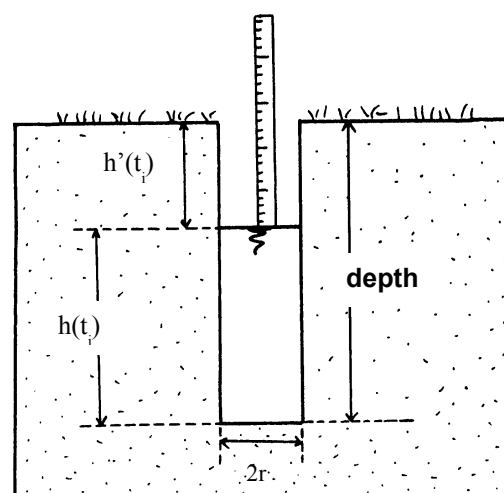


Figure 3.8 Inverse augerhole method (Kessler & Oosterbaan, 1974).

Finally the holes are filled one last time, at which point a stopwatch and a simple ruler are used to time the rate of fall of the water level in each hole (figure 3.8). Because all measurements with the ruler were made relative to the ground surface, the depth of each hole was measured and the draw-down of the water in the hole was converted to the height of the water-column ( $h(t_i)$ ). Using the rates measured on each area, the  $K_{sat}$ -value of the upper part of the soil can be calculated. The following explanation is reproduced after Kessler & Oosterbaan (1974):

The surface area over which the water is draining is described by:

$$A(t_i) = 2 \cdot \pi \cdot r \cdot h(t_i) + \pi \cdot r^2 \quad (3.3)$$

Where:

$A(t_i)$  = surface over which water infiltrates into the soil at time  $t_i$  ( $m^2$ )

$r$  = radius of the auger hole (m)

$h(t_i)$  = water level in the hole at time  $t_i$  (m)

Supposing that the hydraulic gradient is approximately 1, Darcy's Law can be written as:

$$Q(t_i) = K_{sat} \cdot A(t_i) = 2 \cdot K_{sat} \cdot \pi \cdot r \cdot (h(t_i) + r/2) \quad (3.4)$$

This assumption neglects the effect of the pressure head of the water column in the auger hole and also the negative pressure head in the surrounding soil on infiltration capacity (Messing & Jarvis, 1990). Because the depth of the auger holes is small (0.30 m) and the time of pre-wetting of the holes large, this problem is largely overcome.

The quantity of water infiltrated into the soil ( $Q(t_i)$ ) during the time interval  $dt$  over a water level fall of  $dh$  equals:

$$Q(t_i) = -\pi \cdot r^2 \cdot \frac{dh}{dt} \quad (3.5)$$

Substitution of equation 3.4 into 3.5 gives:

$$2 \cdot K_{sat} \cdot \pi \cdot r \cdot (h(t_i) + r/2) = -\pi \cdot r^2 \cdot \frac{dh}{dt} \quad (3.6)$$

Integration between the limits  $t_i = t_1$  and  $t_i = t_n$  gives:

$$K_{sat} = 0.5r \frac{\ln(h(t_1) + r/2) - \ln(h(t_n) + r/2)}{t_n - t_1}$$

(3.7)

The sorptivity in each hole was determined by measuring the rate at which water is absorbed by the soil during this very first “filling of the hole”. In a similar way like the  $K_{sat}$ , it can be calculated with the following equation (pers. com. Van Asch, 1998):

$$S = 0.5r \frac{\ln(h(t_1) + r/2) - \ln(h(t_n) + r/2)}{\sqrt{t_n} - \sqrt{t_1}} \quad (3.8)$$

The calculations were automated using a spreadsheet program. Because  $K_{sat}$  and sorptivity values may vary widely for each observation and the distribution of these values is mostly log-normal (Blijenberg, 1998), a logarithmic mean was chosen to calculate the average  $K_{sat}$  and sorptivity value for each area. Subsequently, all measured values that were found to be 2 orders-of-magnitude larger or smaller than the average were omitted in the calculations, and a new logarithmic mean was calculated. Appendix G1 and G2 give an example of, respectively, the sorptivity and  $K_{sat}$  calculations at site 1. Table 1 (appendix G1) shows the measured water level fall for each augerhole. Table 2 sets out the square root of time to the natural logarithmic ( $\ln$ ) of the measured height plus half the borehole radius. At the bottom of table 2 the calculated sorptivity values are displayed including the (logarithmic) average sorptivity for the investigated site. Appendix G2 shows a few of the  $K_{sat}$  calculations including an overview list (bottom) of all determined  $K_{sat}$  values for each borehole at site 1 (all terms used are from equation 3.7). The results of these calculations are given in chapter 4.

Using an infiltration envelope (figure 3.6) (or equation 3.2), the time-to-ponding for each landscape unit can be calculated for any rainfall event (with known intensity and duration). Smith & Parlange (1978) found the following equation to determine the “time-to-ponding” for each rain event:

$$t_p = \frac{S^2}{2 \cdot K_{sat} \cdot r_p} \ln \left( \frac{r_p}{r_p - K_{sat}} \right) \quad (3.9)$$

where:

$t_p$  = time-to-ponding (T)

$r_p$  = rainfall intensity (L/T)

Since the analysed sites have steep slopes, which offer little opportunity for surface storage, overland flow starts quickly. Hence, equation 3.9 will be used in this study to determine the frequency of overland flow (though actually surface ponding) based on characteristics of measured rain events and rain events recorded by Blijenberg (1998) in the Bachelard valley<sup>6</sup>. The equation, however, is based on constant rainfall intensities. Non-constant rain intensities pose a major calculation problem:  $t_p$  is obtained only by estimation because all calculations remain based upon the infiltration formula of Philip (Kutilek & Nielson, 1994), which works with steady intensities. For calculation purposes, a recorded

<sup>6</sup> Because of the vicinity of the Bachelard valley to the Riou Bourdoux catchment, their rainfall characteristics are regarded as similar.

rain event is divided into periods ranging from a few minutes to several hours, and average intensities (of the single rain event) are calculated for each of these periods. The intensity per period is assumed to be constant, and calculations are then carried out with each of these intensity/duration combinations (Blijenberg, 1998). The results are given in chapter 4.

Following equation 3.9 even the amount of overland flow may be calculated. In this report no overland flow amounts are calculated, due to the many uncertainties involved in this calculation. These uncertainties will be discussed in chapter 6. An attempt to make some preliminary calculations were done, however, and the reader is referred to De Joode (2000) for these results.

### 3.4.3 Discharge measurements

The discharge of a river at a certain moment is usually defined as the amount of water ( $\text{m}^3$ ) passing a certain point in one second. The discharge of a river depends upon a great number of factors, including the intensity and duration of rainfall within the catchment-area, properties of the catchment (like lithology and vegetation), storage and the hydraulic characteristics of the river-channel upstream of the measurement site.

The discharge of the Riou Bourdoux is measured and subsequently compared with rainfall and possible sediment transport values, which may reveal certain correlations, which can be useful for predicting flood risk and sediment transport. In general, it will be used to determine the rainfall runoff response of the Riou Bourdoux system.

There are several methods for determining the discharge of a river section. The most suitable method for steep mountain channels (with turbulent flow and an irregular bed), like the Riou Bourdoux, is the *salt tracer method* (Newson, 1994). The tracer method involves the use of a non-pollutant chemical substance with a high solubility, in this study commercial salt (NaCl), which is diluted by the water of the stream or river. The method is also called dilution gauging. There are two different approaches, namely the *constant input* and the *sudden input* method. Due to its relative ease of use with limited material demands, the sudden input method was adopted in this research. The method is applied to a section of the main channel of the Riou Bourdoux, slightly upstream of the channel measurement site (see appendix A1 and section 3.3.3).

The procedure, described by Benischke & Harum (1990) and Elder & Kattelmann (1990), is as follows: a known volume of salt solution ( $V$ ) with a known concentration ( $c_1$ ) is added to the stream. The amount of salt required is largely dependent on the background conductivity and the discharge of the river. The background conductivity of the river water was about  $500 \mu\text{S}/\text{cm}$ , while visual estimation proved the average discharge to be no more than half a cubic meter per second. As suggested by Gees (1990), about 5 kg of salt per cubic meter of discharge is required in this situation, so 3 kg of salt were selected. For every discharge measurement the chosen amount of salt was dissolved in 20 litres ( $V$ ) of river water. This salt solution will eventually mix completely with the river water, having an initial concentration  $c_0$ . Downstream a concentration-time curve (the pulse with variable concentration  $c_2$ ) will develop by dispersion (figure 3.9: A & B).

The variable concentration ( $c_2$ ) of the mixed water can be determined by measuring the electric conductivity (EC) of the water, with a conductivity probe. This is done at a certain minimum distance downstream of the “injection point” allowing for complete mixing of the tracer with the water. Usually this distance is found by multiplying the width of the river by 15 to 25 (Elder & Kattelmann, 1990). Since the Riou Bourdoux was about 3 to 4 meters wide, a minimum distance of about 60 meters was calculated. The first measurement, however, was done at the more conservative distance of 115 meters. This measurement produced a concentration pulse that was sufficiently acceptable (ie. exhibiting a rapid increase, a high maximum and a slowly falling recession limb lasting no more than five minutes in total: Elder & Kattelmann, 1990). Hence, all other measurements used this distance as well.

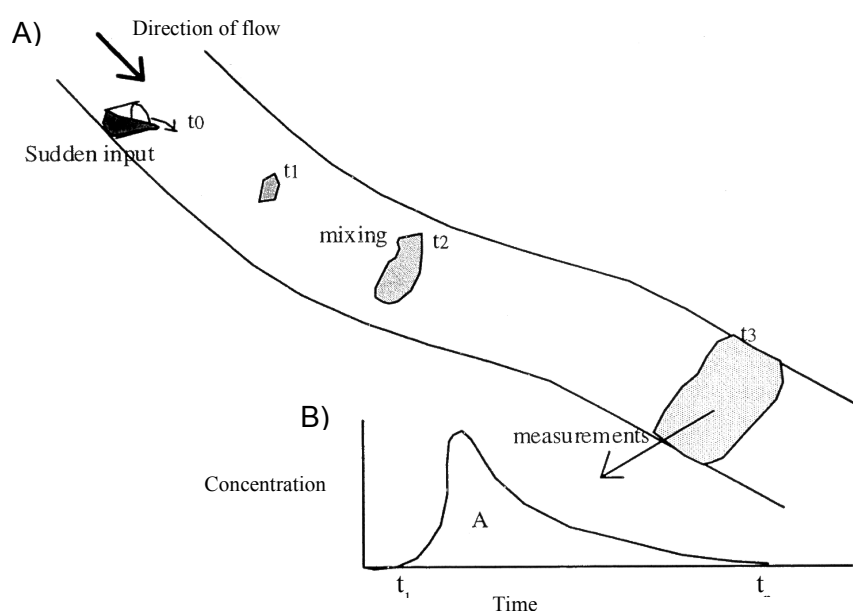


Figure 3.9 A) Drawing of the sudden input tracer method. B) Concentration-time curve constructed from the EC measurements.

At the measurement-point, the probe of the digital conductivity meter was placed, submerged, in the middle of the Riou Bourdoux, at a point where the stream was narrow. The placing of the probe was obviously done before injection.

Along the entire stretch between the injection and the measurement point the Riou Bourdoux was confined to a single watercourse, with no tributaries adding extra water from surrounding slopes. This section, with the above-mentioned characteristics, was selected in order to assure that the discharge and initial concentration ( $c_0$ ) would remain practically identical at both the injection and the measurement point.

After injection of the salt solution, measurements of the river EC-value were taken every 5 seconds (with the aid of a timing device) during approximately 5 minutes, following the salt dissolution measuring form (appendix D1).

To reconstruct the concentration corresponding with the measured EC-values, a calibration measurement is made before the salt solution is injected. An example of this calibration for one discharge measurement is shown in appendix D2 (left column). 5 ml of the injected solution is taken and is diluted with 250 ml of river water. The corresponding EC-

value is now measured. This whole process of adding 250 ml of water and measuring the EC-value is continued till the solution has a volume of 3000 ml. Next; from this volume (of 3000 ml) 250 ml of solution is extracted and again step-wise diluted to 3000 ml. The resulting pairs of EC-values and concentrations show a near perfect correlation ( $R^2 \approx 1$ ). The resulting regression formula can thus be used to convert all measured EC-values back to concentration-values. Because the background conductivity of the river water is different during each measurement, an individual calibration had to be made for each of the measurements.

The resulting concentration-values ( $c_2$ ) are related to time. The area (A) under the concentration-time curve (figure 3.9: B) is equal to the integral of the concentration over time. The initial volume (V) times the initial concentration of the tracer divided by the area under the curve gives the discharge of the river (Elder & Kattelmann, 1990)

$$(c_1 - c_0) \cdot V = Q \cdot \int_{t_1}^{t_n} (c_2 - c_0) dt \quad (3.10)$$

If  $c_1 \gg c_2$  the relation can be simplified to:

$$Q = \frac{V \cdot c_1}{\int_{t_1}^{t_n} (c_2 - c_0) dt} \quad (3.11)$$

Because we worked with a relative concentration  $c_r$  ( $= c_1$  diluted by  $x$  amount of river water) and correlated this to the measured EC-values (with the base EC-value of the river (circa  $500 \mu\text{S/cm}$ ) set as  $c_r = 0$ ), we get in equation 3.11 both in the numerator and the denominator an expression of  $c_1$ , and  $c_0$  becomes 0. Hence, the equation further simplifies to:

$$Q = \frac{V}{\int_{t_1}^{t_n} (c_r) dt} \quad (3.12)$$

This calculation was “automated” in a spreadsheet. An example of this calculation is given in appendix D2 (right column).

The resulting discharge values are discrete data. In order to correlate these values with the rainfall recorded by the tipping bucket rain gauge, the values had to be interpolated to a continuous data series. This conversion can be done by measuring the river stage. A stage-discharge relation can be used to convert the measured stages into discharge data (Shaw, 1994). The idea of the correlation between river stage and discharge is that in an ideal situation (triangular cross-sectional area and uniform flow) a difference in discharge is a direct function of a change in river height. Even though the Riou Bourdoux exhibits turbulent

flow and has an erratic cross-sectional profile, this correlation can still be evident. This relation is in almost all cases logarithmic (Shaw, 1994).

In order to make a statistical sound correlation, there is a minimum of 7 pairs of data required (Chapman McGrew & Monroe, 1993). So, the discharge was measured 7 times during the 8-week period of research. The river stage, however, was measured on a daily basis.

In order to measure the stage an iron rod was placed in the middle of the Riou Bourdoux, at the measurement point. The rod, approximately 120 cm in length, was driven into the bed in the centre of the stream. Its absolute length from the bed upwards was measured. The height of the rod above the water was measured with a ribbon ruler. The height of the rod above the riverbed minus the measured value gives the water stage.

The discharge and river stage values are plotted in a graph (see chapter 4), and a relation will be extracted from the trend-line through these values. The "trend"-formula can then be used to convert all measured river stages into discharge-values, resulting in discharge-data for every day of the research-period.

Problems arose, however, when the iron rod was displaced, presumably by tourists. A new iron rod was placed, but the resulting inconsistencies between the measured stages before and after this event, made the calculation of the stage-discharge relation impossible.

#### 3.4.4 *Suspended sediment load measurements*

Suspended load measurements were taken in order to determine the response of suspended load to rainfall and discharge. Reid and Dunne (1996) suggest that the result of these measurements can also be used to determine the percentage of bedload transport of a river. Due to the many uncertainties, the last method was not adopted.

During each of the seven discharge measurements, a water sample was manually taken at the same location where the conductivity probe was installed. All conditions during sampling were identical, except for discharge (and sediment load). A bottle with a large neck-cross-section was used in order to take the sample. A large neck was chosen, because a small opening may lower the amount of suspended load trapped with a sample, making it unrepresentative for the suspended load of the river. Through determining the amount of sediment in the water sample, it is possible to estimate for each discharge the amount of sediment that is transported.

In the laboratory each water sample was weighed and its volume determined. The contents of the bottles were then emptied into small reservoirs (of known weight), which were subsequently oven-dried (105°C), until all water had completely evaporated. Each empty bottle was weighed, and by subtracting the weight of the full bottles by the weight of the empty ones, the total weight of the water with suspended load was calculated. By measuring the weight of the dried sediment, finally, the proportion of sediment per litre of water (in ppm) can be calculated (see appendix D4).

### 3.5 Methods to determine the strength of Terres Noires<sup>7</sup>

Since small slides were observed in unweathered Terres Noires in the lower parts of the catchment, the strength of unweathered Terres Noires was determined. This strength is used in a stability analysis to estimate the contribution of the landsliding process to the sediment budget. Since in this report only the results of this stability analysis are used, the description of these methods and results are summarized.

Two tests were performed in order to determine this strength: an unconfined compression test and a direct shear test. Because the unconfined compression test failed, its results are not used in this stability analysis, hence this method is not described here.

#### 3.5.1 Direct shear test

The shear strength of Terres Noires is determined with a direct shear test. Test samples are split, and a direct shear test is exerted along the splitted surface. This is done in a direct shear box. This box consists of two sections. After a normal load (perpendicular to the shear plane) is applied, a piston moves one sample horizontally relative to the other. The horizontal force (or shear stress) acting on the specimen is measured.

For every sample the shear stress is measured over time for a constant applied normal load (normal stress). This is expressed in a so-called strength envelope (figure 2.9 A). The peak and residual shear strengths of the Terres Noires sample can now be derived from this curve. For different samples the values found for the shear strength and the corresponding normal stress are plotted in a diagram like figures 2.9 B and 3.10. Since the contact plane

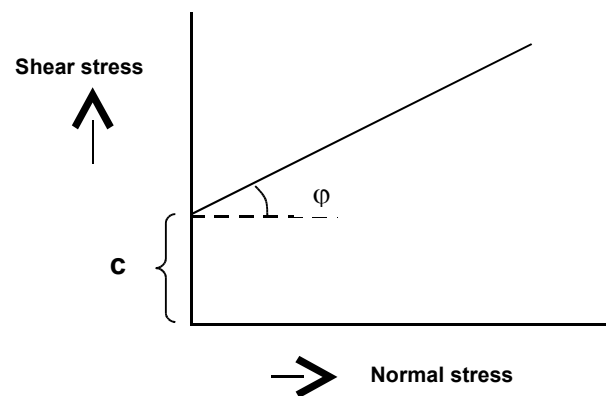


Figure 3.10 Shear strength versus normal stress for a specimen with cohesion.

between two slices of Terres Noires is used as a shear-plane, the cohesion is 0. The regression-line intersects the origin ( $c=0$ ) (figure 3.10) and the angle of internal friction ( $\phi$ ) can be determined from the diagram or computed from the regression equation. The cohesion and angle of internal friction based on the regression line of peak strength is used for failures that occur in material that has never failed before, the values based on residual strength describe slides in sediment that already has failed.

<sup>7</sup> This section is taken in short from De Joode (2000).

The following equation has been used to determine the peak strength along the joint surfaces, taking account of surface roughness (Hingston & Jermy, 1998):

$$\tau = \sigma \cdot \tan(JRC \cdot^{10} \log(JCS / \sigma) + \varphi_b) \quad (3.13)$$

where:

- $\tau$  = peak shear strength (kPa)
- $\sigma$  = effective normal stress (kPa)
- JRC = joint roughness coefficient (-)
- JCS = joint wall compressive strength (MPa)
- $\varphi_b$  = basic friction angle (°)

For an explanation of these terms, the reader is referred to De Joode (2000).

Apart from the strength of Terres Noires, the strength of coarse debris is an important factor for debris flow initiation (Blijenberg, 1998). In the upper part of the Riou Bourdoux catchment where debris flows have shown to initiate, the strength of the coarse flysch debris has to be determined. Blijenberg (1998) determined the strength for flysch deposits in the Bachelard valley, and those results will be used here.

### 3.5.2 Stability analysis

For stability analysis the factor of safety (F) is introduced and defined by:

$$F = \frac{\textit{Shear strength of the material}}{\textit{Shear stress along potential shear plane}} \quad (3.14)$$

A stable slope exists where the safety factor exceeds 1 (van Asch, 1992).

In this study the infinite slope analysis method is applied to the broken Terres Noires. The expression for the factor of safety (F), in case of cohesionless material (c=0) is given by:

$$F = [(1 - \gamma_w / \gamma) \cdot (\tan \varphi' / \tan \beta)] \quad (3.15)$$

In which:

- $\gamma_w$  = water unit weight (kNm<sup>-3</sup>)
- $\gamma$  = unit weight of the soil or rock (kNm<sup>-3</sup>)
- $\varphi'$  = angle of internal friction (°)
- $\beta$  = slope angle (°)

A stability analysis is carried out for the results of the direct shear test.

Benda and Cundy (1990) used this model to determine the critical slope angle for initiation of debris flows (based on the assumption of landslide triggering of debris flows). If debris flows initiate in Terres Noires the resulting critical slope angle (chapter 4) will be used to predict locations of initiation. For debris flows that initiate at locations with coarse debris, the values found by Blijenberg (1998) for shear strength will be used for stability analysis.

### 3.6 Dating techniques<sup>8</sup>

Two methods have been used for the estimation of debris flow and landslide frequency: dendrochronology and lichenometry.

#### 3.6.1 Dendrochronology



Figure 3.11 Example of curved trees found in the Riou Bourdoux catchment.

Curved trees (figure 3.11) can be found on slopes with mass movement activity, since the movement of soil will affect trees in their growing process. After inclination of the trees, reaction wood develops which causes the inclined trees to curve gradually upward to restore vertical growth. A consequence of reaction wood development is the change in eccentricity of the annual rings. As a result of one or more tilting events, changes of forms of the trunk are visible. Analysis of the form of the trunk can reveal the (minimum) number of tilting occurrences, their direction of tilt and their relative age. The precise number and date of tilts can be revealed by analysing the

course of eccentricity as measured along at least two radii, taken at right angles to each other, or from a cross-section of the trunk (Braam *et al*, 1987). The application of dendrochronology requires cores to be taken for each inclination direction (and at right angle with the inclination angle).

At 6 locations (within the Riou Bourdoux catchment area investigated in 1997, see appendix A1), showing visible signs of (old) landslides, samples were taken of at least 7 (for statistical reliability) trees with a deviated stem form. The locations are described by Spee & Visser (1999). For collecting the cores an incremental bore of 5 mm diameter and 300 mm long is used. The collected cores have to be prepared for analysis. During analysis the ring widths are counted using a microscope and a pulse generator. The measurements are

<sup>8</sup> This section is summarized from Spee & Visser (1999).

verified after which the data is checked for missing rings, dating errors and other measurement errors. The eccentricity is calculated, and a statistical T-test is performed on the data. An inclination occurrence is now defined as a significant change of the relative eccentricity level with duration of several years (Braam *et al*, 1987). For more details and the results of this method, the reader is referred to the report of Spee and Visser (1999).

### 3.6.2 Lichenometric dating

Lichenometric dating is based on the growth of lichens, which is assumed to be constant over longer time periods. This means that the older the lichen is, the larger its thallus will be. The age of a deposit covered with certain lichens will correspond to the age of the lichen with the largest thallus. By using a growth curve (figure 3.12), lichen age can be determined. A growth curve is a diagram showing the relation between lichen age and thallus diameter. In the studied area the growth curve of Orombelli & Porter (1983) is applied to debris flow deposits and deposits of avalanches.

In the investigated area lichens of the *Rhizocarpon Geographicum* family are used to date a number of deposits (predominantly debris flows in the upper regions of the subcatchments). This lichen prefers to grow on acid substrates, for example on sandstones and does not grow on limestones. Some sandstone is found in the Flysch à Helminthoïdes. Since these sandstones are not abundantly present just a few lichens are found in the Riou Bourdoux catchment. Details are described by Spee and Visser (1999).

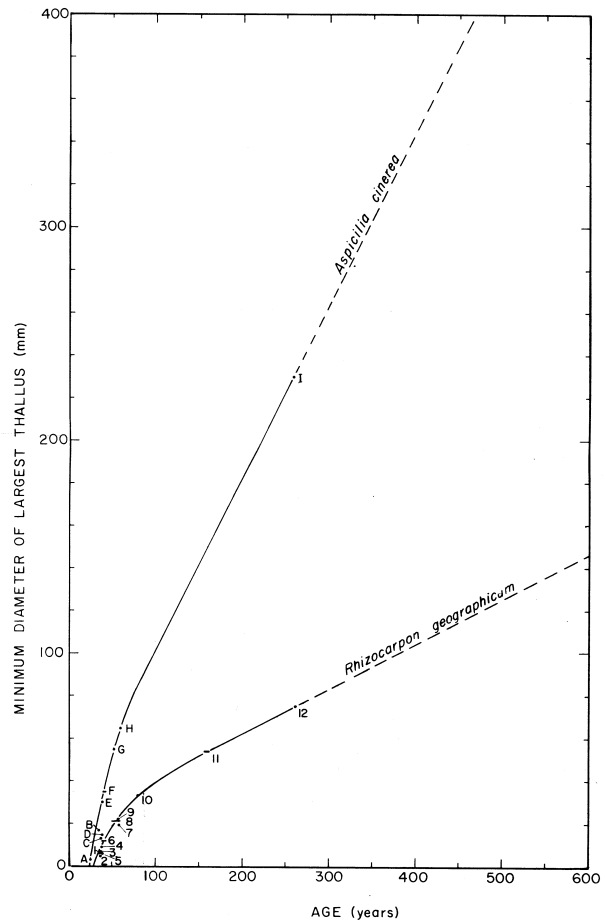


Figure 3.12 Relation between the age of the lichen and the diameter of the largest thallus, valid for *Rhizocarpon Geographicum* (Orombelli & Porter, 1983).

## 4 Results

### 4.1 Detailed description of the study area

In the introduction some aspects of the (Southern) French Alps, like geology, geomorphology and vegetation are described, including a topographic description of the study area. In this section a detailed description of the investigated area (appendix A1) is given on the basis of geomorphology and process activity. The maps in appendix B are based on the field observations (appendix A3) and are used to illustrate the description.

The study area can be divided into four parts:

- 1) upper debris slopes,
- 2) morainic 'threshold',
- 3) old landslide,
- 4) Terres Noires slopes.

These sub-areas are indicated in figure 4.1. These parts will be described in the following sections.

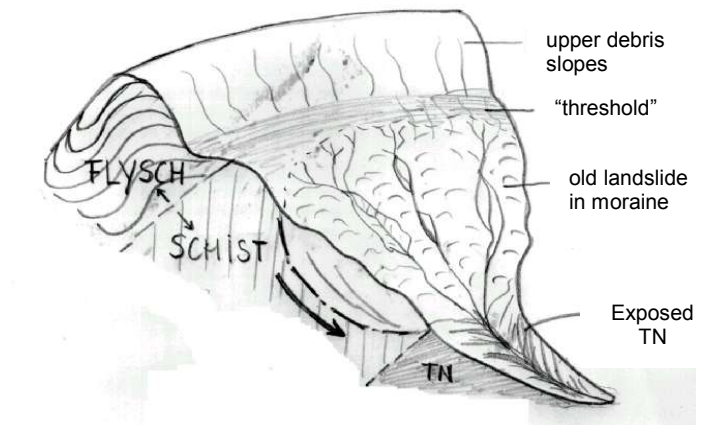


Figure 4.1 Block diagram of the investigated area. The 4 parts are indicated and the movement of the old landslide is marked (De Joode, 2000).

#### 4.1.1 Upper debris slopes

The upper region of the Riou de la Pare subcatchment consists of solid bedrock (appendix B1 & B2). It is mostly limestone and sandstone from the Flysch à Helminthoïdes. Outcrops of bedrock are only visible around the summits. The rest of the upper region is largely covered with debris slopes (figure 4.2). These debris slopes have developed by weathering processes, especially frost weathering. The slopes have a concave profile with slope angles mostly above 30° just underneath the outcrops, while towards the 'threshold' they decrease to a minimum of 10°. The slopes consist of coarse debris (observation point (o.p.) 15, appendix A2) with an average diameter of 30 cm (o.p. 51 & 52), and lacking any fine matrix. At many places on these slopes the debris-thickness is small and bedrock can be seen as small outcrops. Towards the 'threshold' the thickness of the deposits increases, with deposits taking the shape of debris fans. Vegetation on the slopes was practically absent at the end of May, while towards mid-July grass was growing abundantly, indicating the in-activity of debris transport under present conditions. Still, a few of these debris slopes are still active. Because no clear sorting effects can be distinguished, several transport

processes may be active. Rockfall is one option, although the action of flowing water is also important.



Figure 4.2 Photograph of two gullies in the upper debris slopes (taken in mid July). In the top exposed bedrock (flysch) can be identified.

Dissecting the debris slopes at many places are several bedrock channels or gullies (o.p. 60: figure 4.2). These channels are filled with coarse colluvial deposits. The gullies terminate into small fans, indicating an origin of flowing water. For the transport of the coarse sediment much water has to be available, which can be provided by rapid snowmelt in spring or extreme rainstorms. In some of these channels debris flows have occurred

(appendix B5), most of which have come to a halt on the flatter slopes of the 'threshold'. The typical source, transport and deposition zone of a debris flow (see section 2.2.3, figure 4.2) are also present, indicating that at least some of the gullies may have been formed due to erosion by debris flows. The absence of *recent* debris flows (o.p. 51), however, seems to indicate that this process is not very active. Snow avalanches, which are abundantly present (appendix B5), may also form such channels (Luckman, 1992) and transfer a lot of sediment downslope.

#### 4.1.2 Morainic 'threshold'

The debris slopes terminate on a marked flattening of the relief around 2300 m (figure 4.3). This flattening of the relief is caused by the bulk of the morainic material from the Pleistocene. The particular (bowl) shape of the upper catchments of the Riou Bourdoux system (appendix A1) indicate that during the glaciation of the Ubaye valley, the upper part of the Riou Bourdoux may have been a cirque. The thickness of the moraine deposits is uncertain. The deposits form a narrow zone with an average width of about 150 m and are largely covered by dense grass (appendix B3), with a few patches of pine trees reaching to the end of the debris slopes.

Most gullies from the upper debris slopes are discontinuous, losing their character on this *threshold*, presumably due to the loss of transport velocity (of flows or avalanches) by decreasing slope angles or the loss of competence of flow by infiltration of water into the morainic subsoil. The increasing vegetation also has a negative influence on transport processes, hence the chosen name of morainic *threshold*.

Only at a few places (appendix B5) small gullies from the upper debris slopes are able to traverse the threshold and continue across the edge to the steeper zone downslope.

These gullies act as snow avalanche tracks (o.p. 44), transporting little to no material across this zone. The most active slope process in this zone is creep, manifested as small lobes and terracettes.

#### 4.1.3 Old landslide

Downslope of the threshold, the slope angles increase again (appendix B4). After the Ubaye valley glacier retreated, the morainic deposits formed part of a large oversteepened terrain (chapter 1). Moreover, the

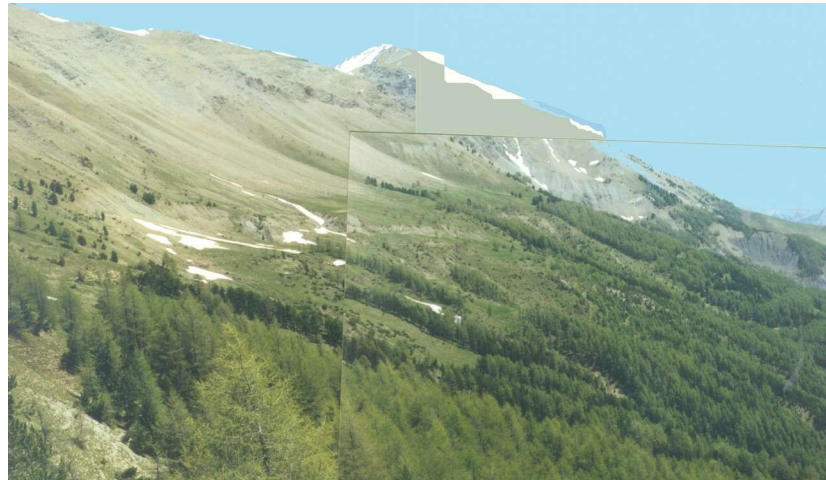


Figure 4.3 Photograph showing the debris slopes and morainic 'threshold' of the study area. Quickly decreasing slope angles and increasing vegetation mark the border between the two sections.

weight of the glacier caused compression of the underlying schist (Flysch à Helminthoïdes), and after the glacier had retreated joints may have developed in the schist due to pressure release. The oversteepened terrain and the possible process of pressure release caused a large section of the slope to become unstable, with subsequent failure resulting in a large mass movement complex. Evidence of the mass movement are the weakly stepped slopes across this entire section (appendix B4). The slope angles vary between  $11^{\circ}$  and  $30^{\circ}$  (o.p. 21, 22 and 23). Other indications are the presence of old, now very densely vegetated, scarps (o.p. 9 and 10) and the absence of a distinct surface lithology along the scarps or ravines.

The surface of this mass movement complex is at some places deeply incised by gullies and streams. In-between, large areas are covered by dense forests of pines (*pinus sylvestris*) and larches (*larix decidua*) (appendix B3). These areas are now largely inactive except for some creep.

In the higher regions many snow avalanche tracks are distinguished (appendix B5). They start from or continue across the threshold. The presence of broken tree-trunks and their distribution on the slopes seems to suggest that most snow avalanches start when large patches of snow fail. Downslope, these avalanches quickly concentrate into gullies or debris flow tracks, indicating that most of the avalanches are slush avalanches and probably result due to rapid melting of snow in spring (the slopes being adrets). Appendix B3 shows that the tree-line, which is located in this zone, is very irregular. When compared to the location of avalanches (appendix B5), it is clear that the tree-line recedes downslope exactly at locations where snow avalanches have occurred. At the barren locations many broken tree stumps are found, so the avalanches destroy trees along their path (figure 4.4). The length of these snow avalanches rarely exceeds 750 m and in their tracks little transported colluvium can be found.

On the higher regions of this section (just below the threshold) many headwater channels have formed. They occur both as *gully type 1* (o.p. 14, 31, 32 & 42) as well as *gully*

*type 2* (o.p. 26 & 55), which are fed by sources. Incision by the former is erratic: at some points they are deeply incised, forming badlands or active debris slopes on their adjacent slopes (appendix B5), while further downstream the incision may temporarily halt. Where the streams are perennial (*gully type 2*), incision increases and becomes constant. Vegetation along sections of incision is either absent or is dominated by grass cover (appendix B3). One perennial stream, the Riou des Primas (lower left most stream, appendix B5) shows no signs of fluvial incision.



Figure 4.4 Debris flow / avalanche track at observation point 37. A small dam is visible in the foreground. The old levees of a debris flow are distinctly visible due to the trees growing on the fine matrix.

Along stream incisions, slopes are very steep (up to 40°: o.p. 30). On these barely vegetated slopes, the nature of the subsoil is exposed. This consists of mixed morainic deposits and broken up 'Terres Noires' (Van Asch & Mulder, 1988), most of which is poorly sorted. Due to the mass movement, no distinct regolith horizon or thickness can be identified. This so-called *heterogeneous material* is very erodible, which may also explain the pattern of stream incision in the subject area. Most un-vegetated streamside slopes in this material were typified as badlands (appendix B5),

because wash erosion (including rill and gully erosion) showed to be the dominant process. A few locations however, were dominated by dry ravel and rockfall, and these are indicated as debris slopes. In both cases large debris accumulations were present on the foot of the slopes. Higher up these slopes only a very thin layer of debris was present. Most of the hillslope gullies do not reach to the top of the slopes, in part explaining the fact that the edge between these slopes and the more stable (morainic) areas is very abrupt (appendix B5). On some of the slopes small debris flows are found (o.p. 54 and 47) and here the initiation mechanism of Blijenberg (1998) is recognized.

The various perennial streams confluence in the lower region of this section. Here the mass movement complex is reactivated and several active slides including one slump have developed (appendix B5). The reactivation is probably due to undercutting (and subsequent failure) of the slopes by the joint fluvial erosion of the streams.

Along the 1<sup>st</sup> and 2<sup>nd</sup> order streams not many fresh debris flow tracks (appendix B5) were identified. Medium-scale debris flows do not seem to be triggered often within the Riou de la Pare catchment. Only two were identified: one was initiated in heterogeneous slope material near o.p. 48 and the other in Terres Noires near o.p. 3. The latter, however, can also be regarded as the coulee (mudflow: figure 2.7) of the landslide around o.p. 64. Still,

several small check dams have been built in gullies in the entire study area to counteract the activity of debris flows (figure 4.4, appendix B5) and fluvial incision.

#### 4.1.4 *Terres Noires slopes*

The Terres Noires (marls) reach to an altitude of approximately 1850 m (appendix B1 & B2). The Riou Bourdoux and its tributaries have deeply incised in the Terres Noires and have exposed large, unvegetated slopes. These slopes are dominated by rill and gully erosion (o.p. 3). The lowest section of the subcatchment consists of these slopes.

A lot of fine sediment is transported down these slopes, especially during extreme precipitation (Oostwoud Wijdenes & Ergenzinger, 1998, Antoine *et al*, 1995). These slopes are indicated as badlands. On top of the Terres Noires a layer of moraine is found except for the recently incised parts. This combination is highly unstable. Water infiltrating in the moraine will stagnate on the impermeable Terres Noires. The water will flow on this regolith barrier, creating a slip face on which the moraine will fail (o.p. 3 and 64). The moraine may move downslope to the stream or be stored in a gully, where it can be transported by micro-scale debris flows. The finer particles of the moraine and Terres Noires are flushed out by flowing water.

This area is not only highly erodable due to the presence of the Terres Noires, but also due to the fact that some of the material in this area is the weathered and crushed mixture of moraine, schist (flysch noir) and Terres Noires, being part of the coulee (toe) of the earlier mentioned old landslide (heterogeneous material). This material can easily be reactivated. Spee & Visser (1999) even observed small slides in *unweathered* Terres Noires, which had developed where the Riou Chamous undermined the steep slopes.

In this section no check dams can be built (pers. com. RTM, 1997) because the Terres Noires are very unsuitable as a substrate for dam-construction.

#### 4.1.5 *Linkages*

For a sediment budget it is important to know how much sediment is transferred to the basin outlet and how much material is stored. So far, the processes active within the four sub-areas have been described. The processes that can transport sediment from one sub-area to another and finally to the outlet are also investigated. Three processes were found; snow avalanches, debris flows and the transport by running water.

Snow avalanche deposits are especially found in the upper parts of the investigated area (o.p. 31, 32, 33, 34, 35 and 43). Because these avalanches only transfer broken tree trunks and almost no sediment, they are of no importance to the sediment budget. Spee & Visser (1999) on the contrary found large block fields deposited by snow avalanches.

Debris flow deposits are found in the lower part of the area. Small-scale debris flows can be found on the slopes of the Riou de la Pare (o.p. 29, 30). These debris flows, however, do not transfer large quantities of sediment to the main course of the Riou

Bourdoux, due to their short travel distance. Hence, medium-scale (channelled) debris flows have to be initiated to transport the sediment stored in the 1<sup>st</sup> and 2<sup>nd</sup> order channels to the Main Channel of the Riou Bourdoux (o.p. 1, 2, 3, 47, and 48). From o.p. 1, 2 and 3 it is clear that these medium-scale debris flows can bring a lot of debris from lower order to higher order channels. One debris flow deposit is also identified in the upper part (o.p. 36 and 37), but this one is not large enough to cover the long distance to reach the outlet of the basin and pose a risk. The stagnated debris flow deposits may be transferred further downstream during a new debris flow event or a portion of it may be transported as bed load during high discharges (see section 4.3).

Several observation points (o.p. 6, 9, 10 and 28) and indications on channel stability described in section 4.3.2, show that medium-scale debris-flow activity has been very low in the past few decades (figure 4.5), and streamside colluvium is being vegetated. Many of the 2<sup>nd</sup> order channels within the subcatchment are aggrading.



Figure 4.5 Photograph of the 2<sup>nd</sup> order channel near observation point 6, showing increasing surface stability in recent years.

Finally, some remarks must be made about the last mechanism: transport by running water. During several (dry) months most channels in the study area (1<sup>st</sup> and 2<sup>nd</sup> order) do not carry any water. Only the perennial streams will then have water (o.p. 5 and 61). Only if snowmelt is high or during extreme rainfall, water will flow through most gullies and channels. If stream power is large enough, the water can erode sediment.

So, especially sheet wash, gully erosion and small-scale debris flows bring sediment to the channels of the subcatchment. In these channels some fluvial activity is present, but the absence of debris-flow activity combined with general channel aggradation seems to indicate that medium-scale debris flows are the most important erosion and transport process. This means that the hypothesis of Benda & Dunne (1987), where 1<sup>st</sup> and 2<sup>nd</sup> order channels are predominately cleared by debris flows, is valid for the Riou de la Pare subcatchment.

## 4.2 Hydrological results

### 4.2.1 Rainfall characteristics

The measured amount of precipitation at each raingauge and the data from the St. Pons weather station are presented in table 4.1. During the investigation only two rainfall

events were observed having snowfall in the upper reaches of the Riou Bourdoux system (above 2000 m). The amount of precipitation in these events was small enough to discard possible recording difficulties.

Date / raingauge	St.Pons	1400 m	1800 m	1950 m	2260 m
<b>30-5-1997</b>	0.0*	0.0	0.0	0.0	0.0
<b>2-6-1997</b>	12.5	18.7	18.9	17.7	19.0
<b>6-6-1997</b>	1.2	8.6	9.1	11.5	12.1
<b>9-6-1997</b>	0.0	0.0	0.0	0.0	0.0
<b>12-6-1997</b>	0.0	0.0	0.0	0.0	0.0
<b>17-6-1997</b>	2.7	8.6	10.9	11.4	12.9
<b>20-6-1997</b>	6.4	6.7	7.5	9.3	9.5
<b>23-6-1997</b>	16.3	17.7	18.8	20.3	23.3
<b>26-6-1997</b>	2.0	4.7	8.9	10.8	10.3
<b>30-6-1997</b>	41.0	44.2	48.7	50.2	50.9
<b>3-7-1997</b>	4.8	5.6	10.7	11.1	13.4
<b>7-7-1997</b>	16.7	15.6	21.0	23.5	28.2
<b>10-7-1997</b>	0.0	0.4	0.8	1.0	1.4
<b>14-7-1997</b>	21.8	23.2	30.5	25.7	26.6
<b>Total rainfall</b>	125.4	154.0	185.8	192.5	207.6

Table 4.1 Rainfall-amounts at various altitudes in the Riou Bourdoux catchment (summarized from table 4, appendix C1). \*All data are in mm of unit depth rainfall.

As can be seen from table 4.1, there is a definite increase in rainfall with altitude. To obtain this relation the total amount of rainfall at each location is plotted against altitude (appendix C3). This relation is shown in figure 4.6.

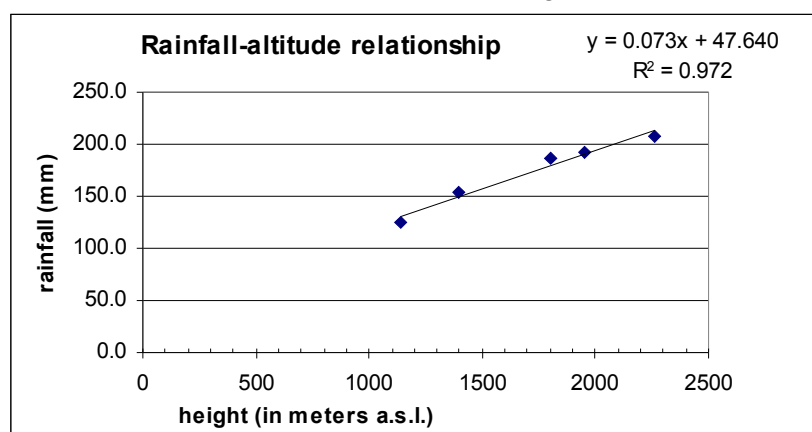


Figure 4.6 Graph showing the relationship between rainfall and altitude for the Riou Bourdoux catchment.

The graph shows that the relationship is clearly linear and that total precipitation amounts typically increase 7.3 mm per 100 m of altitude (based on the regression formula, figure 4.6). However, caution should be used with the application of this relationship. Table 2 in appendix C3 gives the

calculated rainfall-altitude regression formulas for each 3-day-interval (table 4.1). It shows that rainfall not only increases with altitude, but likewise with the amount of precipitation. This relationship can therefore not be used for predicting rainfall-amounts at various altitudes for individual rainstorms and is only valid for a similar period (May – July) with corresponding precipitation amounts.

From appendix C2 the duration and intensity of several rain-events during the period of investigation can be extracted. Only a few rainstorms were observed, and their duration and intensity are given in table 4.2. This table also gives an overview of the characteristics of

rainstorms that have occurred in the Bachelard valley during the period 1991-1994 (Blijenberg, 1998).

Rainfall-event	Duration (h)	Amount (mm)	Average intensity (mm/h)
<b>1-6-1997</b>	2.5	10.2	4.1
<b>22-6-1997</b>	2	10.2	5.1
<b>28-6-1997</b>	5.5	14.3	2.6
<b>5-7-1997</b>	3.5	9.5	2.7
<i>once a year*</i>	<i>5 min</i>	-	<i>75</i>
<i>&gt;5 times a year</i>	<i>5 min</i>	-	<i>40</i>
<i>once a year</i>	<i>30 min</i>	-	<i>30</i>
<i>twice a year</i>	<i>10 min</i>	-	<i>50</i>

Table 4.2 The duration and amount of a few rain-events registered by the tipping-bucket raingauge. The intensity is averaged for the observed time-interval. \*Data in italics are from Blijenberg (1998). These characteristic storms have triggered debris flows in the Bachelard valley.

The rain-events recorded by Blijenberg (1998) have triggered debris flows in the Bachelard valley. During the period of investigation no debris flows occurred in the study area (section 4.3.1), which is not surprising since all measured rainfall intensities are an order-of-magnitude smaller than those recorded by Blijenberg (1998). This probably indicates that the observed rain-events did not produce critical overland-flow conditions for debris-flow triggering.

The period of investigation was a relatively wet period, with little to no high-intensity, low-frequency rainstorms. Especially the month of June showed to be wetter (100 mm) than normal (70 mm). The rainfall during this period resulted primarily from low-pressure frontal systems, creating rain of low intensity. No conditions arose during the research period for unstable air masses to rise (convection) rapidly resulting in local (but intense) thunderstorms. This has consequences for the estimated process activity of debris flows and fluvial processes during the research. The resulting estimates are thus regarded to be in the lower range of values.

#### 4.2.2 Saturated conductivity and sorptivity

At four sites (appendix A1), described in section 3.4.2, the infiltration capacity measurements have been determined. The calculated saturated conductivity ( $K_{sat}$ ) and sorptivity values for each borehole (at every site) are given in appendix G3 (table 2 and 3) and are summarized in table 4.3 (table 1, appendix G3).

At site 2 and 4 several surface cracks were observed. It is clear from table 4.3 that this greatly increases the infiltration capacity of the soil.

Site	Slope material	Sorptivity (mm/ $\sqrt{h}$ )	$K_{sat}$ (mm/h)
<b>1</b>	heterogeneous	-5.45	-1.06
<b>2</b>	weath. Terres Noires (slide)	-50.22	-37.38
<b>3</b>	moraine	-77.82	-37.28
<b>4</b>	weathered schist (mudflow)	-26.08	-12.72

Table 4.3 Sorptivity and  $K_{sat}$  of the 4 different sites in the upper Riou Bourdoux catchment.

Using the  $K_{sat}$  and sorptivity values in combination with equation 3.9 (Smith & Parlange, 1978), the time-to-ponding is determined at each site for the rain-events given in table 4.2. Equation 2.4 (Caine, 1980) is also used in order to assess the possibility of debris flow initiation in the study area (section 2.2.3). The results are given in table 4.4.

Rain-event	Caine	Site 1		Site 2		Site 3		Site 4	
		t.t.p.*	o.f.*	t.t.p.*	o.f.*	t.t.p.*	o.f.*	t.t.p.*	o.f.*
<b>22-6-1997</b>	-	0.64 h	+	>>		>>		>>	
<b>28-6-1997</b>	-	2.82 h	+	>>		>>		>>	
<b>once / year</b>	+	10 s	++	18 min	-	44 min	-	4 min	+
<b>5x / year</b>	+/-	34 s	++	2.30 h	-	5.46 h	-	15 min	-
<b>once / year</b>	+	60 s	++	>>		>>		29 min	+
<b>twice / year</b>	+	22 s	++	56 min	-	2.22 h	-	9.5 min	+

Table 4.4 Qualitative indications of overland flow based on the Smith & Parlange (1978) equation. The second column represents the difference between the critical and observed rainfall intensity (Caine, 1980). If the observed intensities are higher than the calculated (+), debris flows are assumed to be triggered. If they are less (-), no triggering will occur. Note that the equation of Caine (1980) is solely based on rainfall characteristics. **t.t.p.\***: This column indicates the calculated time-to-ponding (>> = no t.t.p.). **o.f.\***: This column shows whether the duration of the rain-event is more (+, thus overland flow) or less (-) than the calculated time-to-ponding. Double symbols indicate a large difference.

As table 4.4 shows, the (in this study) recorded rain events do not trigger debris flows according to Caine (1980), which concurs with the observations (section 4.2.1). Only site 1 and 4 seem to be locations that may trigger debris flows due to overland flow. Assuming that the rain events in the Bachelard valley are also representative for the Riou Bourdoux catchment, critical conditions for debris flow triggering will arise at these locations a few times each year. The other locations (site 2 and 3) may point to the activity of other slope processes than overland flow, presumably mass wasting. This is evident from the landslides found in moraines (appendix B5) and in unweathered Terres Noires (Spee & Visser, 1999).

The badlands developed in unweathered Terres Noires produce overland flow very quickly (section 4.1.4). They were therefore not tested in the procedure above.

#### 4.2.3 Discharge and suspended load of the Riou Bourdoux

During the period of research the discharge was measured 7 times in the middle reach of the Riou Bourdoux (appendix A1). As stated in section 3.4.3, the river water was first calibrated for the injected salt-solution, resulting in a formula for converting the measured EC-values to relative salt concentrations (appendix D2, left column, 2<sup>nd</sup> page). Every calibration showed a near perfect correlation between EC-values and concentrations, and was thus successful; the resulting formulas were used to convert the measured time-series of EC-values to concentration-time data. Appendix D3 shows the concentration-time data of each measurement plotted in graphs. It is clear that their form corresponds well to the ideal of figure 3.9 B. Using expression 3.12, the discharge was determined; The results are given in table 4.5.

Date	Main Channel		
	Discharge (l/s)	Suspended load (g/l)	Suspended discharge (g/s)
2-6-1997	234.2	0.202	47.4
10-6-1997	99.3	0.092	9.1
17-6-1997	183.4	0.159	29.2
24-6-1997	187.9	0.097	18.2
30-6-1997	355.3	0.145	51.4
7-7-1997	256.7	-	-
10-7-1997	357.0	0.085	30.4

Table 4.5 Calculated discharges and sediment load for every measurement.

During each measurement, a suspended load sample was taken (section 3.4.4). The calculation of the suspended load concentration and - discharge is given in appendix D4 (table 1 and 2). The results are summarized in table 4.5. The relation between sediment load and discharge will be discussed in section 6.1.

An attempt was made to convert the 7 discharge data to a continuous data series for the period of investigation. The river stage (flow depth) was measured (almost) daily. The measured results are given in appendix D5. Following table 2 in this appendix a correlation

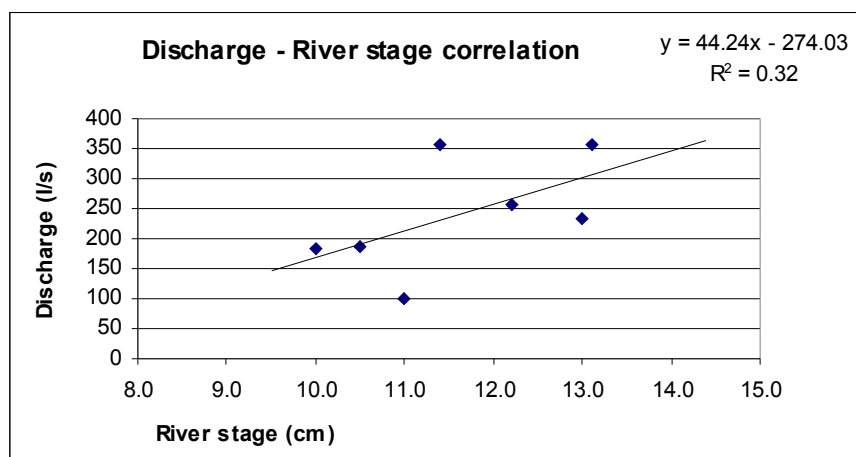


Figure 4.7 Graph showing the relation between the measured discharge and river stage. With a  $R^2$  of 0.32, the correlation is very poor.

between river stage and discharge was made. The result is given in figure 4.7. The graph clearly shows that no correlation can be made with the gathered data. The presumable reasons for this were already mentioned in section 3.4.3. So, no discharge could be determined for other

days than the 7 observed. This lack of a discharge-time series for the period of investigation has made a detailed analysis of a possible rainfall-runoff relationship impossible.

## 4.3 Debris-flow and channel process results

### 4.3.1 Debris flow characteristics

#### Observed debris flows

During the fieldwork, a small-scale debris flow was initiated during a rainstorm of moderate intensity (28-6-1997, table 4.2). The initiation site of the debris flow was situated in a gully on a Terres Noires slope along the main channel of the Riou Bourdoux. In the gully morainic material was present. Based on observations on the same slope during a rain event on June the 30<sup>th</sup>, which only generated overland flow, the follow debris-flow triggering

mechanism for the debris flow (on this slope) is proposed: Overland flow, which developed on the Terres Noires, quickly turned into a hyper-concentrated flow and saturated the morainic deposit. The deposit failed and moved downslope as a slurry. The velocity of the debris flow decreased when it reached the enlarged riverbanks. Part of the flow managed to cross this bank and plunge unto the floodplain several meters below. The flow-path is shown in figure 4.8. The characteristics of this event are described in appendix H (deposit 1). Besides this event, no other debris flows have been initiated during the research period.

Furthermore, in total only 5 deposits of recent (less than several years old) debris flows have been found. They are described in appendix H, of which table 4.6 gives a summary.

Several other, presumably much older, debris-flow tracks were identified (o.p. 37, 46, 47, 48, 52, 60, appendix A2 & B5). However, the surfaces of these deposits (located in channels and gullies) were so degraded (overgrown or partly eroded) that no volume or other characteristics could be assessed in the field. This in part indicates that on a longer time-scale fluvial transport may be important in transporting sediment in 2<sup>nd</sup> order channels of the subcatchment, if debris-flow activity is low.

Based on the evidence provided in table 4.6 and appendix B2 and B5, it can be concluded that debris flows, which are able to reach the Main Channel, do not initiate in source areas of a single rock-type, but mostly at locations consisting of a mixture of two or more rock-types. Further analysis shows that all debris-flow source areas are unvegetated, most of which are subject to overland flow, and all have slope angles of 30° or more. From these observations it may be concluded that, in part, Blijenberg's (1998) initiation model is valid for the Riou de la Pare subcatchment. It also suggests that, based on the source areas, three types of debris flows occur in this catchment and along the main course of the Riou Bourdoux:

- 1) debris flows triggered along the Main Channel, originating on the streamside Terres Noires slopes partly covered with morainic colluvium. They are either small-scale,



Figure 4.8 Flow-path of the observed small-scale debris flow during the research period. The steep dark blue-grey slopes in the background are Terres Noires slopes. On top of these slopes a thin veneer of moraine can be seen. In the foreground (light grey) a small debris-flow fan has developed. The slightly darker grey track in the middle is the fresh flow-path.

when they are triggered by overland flow ( $10^1 \text{ m}^3$ , table 4.6) or they can be up to medium-scale, when their origin is from a mass movement (deposit 5, table 4.6). The former type builds small debris fans along the Main Channel.

- 2) debris flows in flysch deposits. These are triggered on the upper slopes, but rarely traverse the morainic threshold (if this threshold is present).
- 3) debris flows, originating from unvegetated slopes in heterogeneous (mixture of Terres Noires, schist and moraine) material. This type of debris flow is the only one observed, that travelled a large distance through a 2<sup>nd</sup> order channel within the study area. Estimation showed that this debris flow type (o.p. 46-48) is medium-scale.

Deposit	Location	Source area		Depositional area		
		characteristics	angle	$\beta$	angle	estimated volume
1	Main Channel	moraine – T.N.	36°	90°	18°	7.5 m <sup>3</sup>
2	Main Channel	moraine – T.N.	36°	50°	9°	15 m <sup>3</sup>
3	Main Channel	moraine – T.N.	36°	35°	11°	16.5 m <sup>3</sup>
4	<i>confluence point</i>	-	-	75°	10°	6525 m <sup>3</sup>
5	confluence point	moraine – T.N.	32°	10°	12.5°	6930 m <sup>3</sup>

Table 4.6 Summary of the characteristics of the analyzed debris flow deposits. The slope-angle of the source area represents the initiation angle of the debris flow.  $\beta$  is the angle between the contributing and receiving channel (figure 2.13). The deposit marked in italics most probably belongs to the august-1996 lave torrentielle. The 'confluence point' is the location where the Riou Chamous, Riou de la Pare and the Riou Guérin confluence (o.p. 1, appendix A2).

This evidence is confirmed by the characteristics of debris flow deposits found in the Riou Chamous and Riou Guerin subcatchments (Spee & Visser, 1999). Due to the fact that so few distinct deposits were found, the above-mentioned division is not conclusive, although it is clear that the diverse surface lithology in the Riou Bourdoux system produces several different types of debris flows.

Finally, the risk of a medium-scale debris flow from the Riou de la Pare catchment should be assessed. The only debris flow of this scale, which reached the Main Channel, is deposit 5 (appendix H: table 4.6). However, this debris flow is part of the coulee of the mass movement at observation point 3 (appendix A2). This particular debris flow is assumed to have been rigid, being unable to move further than the confluence point. Since this deposit is now largely vegetated, and is not covered by fresh debris flows from the study area, no medium-scale debris flow has passed this point in many years. Furthermore, the absence of fresh medium-scale debris flow deposits throughout the entire subcatchment (especially at o.p. 61 where the channel gradient is low enough for debris flows to be deposited) strengthens the indication that debris flow activity in the Riou de la Pare subcatchment has been very low in recent years (see also section 4.1.5). Unfortunately, no year-ring data were gathered from vegetation growing along stabilised debris flow tracks, so no exact time-span of inactivity can be given. Since laves torrentielles do still occur (in the Main Channel), the present risk is discussed in section 6.3.

### Size estimation

Sediment sinks of *readily transportable colluvium* were identified and, where possible, their volume estimated (section 3.3.2). Again, only a few clear hazardous sinks were recognized. The sediment storages were all largely unvegetated, connected to the drainage

network, and located on steep slopes ( $> 30^\circ$ ) on the typical source areas defined above. The deposits are described in appendix A3 (o.p. 33, 34, 41, 60).

All of the deposits described at observation point 60 are located in gullies on the upper slopes. The average estimated deposit-size (order-of-magnitude) in each gully is  $10^2 \text{ m}^3$ . At observation point 33, 34 and 41, the size of each deposit is respectively  $10^2$ ,  $10^1$  and  $10^3 \text{ m}^3$ . Only these deposits are regarded as transportable by debris flows to the confluence point. Spee & Visser (1999) found typical volumes of storages of  $10^1$ - $10^2 \text{ m}^3$ . They also found that, at least in the Riou Chamous, debris flows could be triggered by small landslides of comparable volume.

The other sediment storages (sinks) in the subcatchment, already mentioned in section 3.3.2, are the morainic slope deposits and the colluvial storage of sediment in 1<sup>st</sup> and 2<sup>nd</sup> order channels. Most morainic deposits are for now largely stabilised under a dense forest cover (section 4.1.3, appendix B3 & B5). The sediment stored in the channels has also largely been stabilised by vegetation (figure 3.2, 4.5, appendix F4). The gradient of these channels (mostly  $15 - 20^\circ$ ) may be too low for the sediment to be incorporated by a passing debris flow (see next paragraph).

Debris flows that travel through channels are known to scour sediment from the bed (section 2.2.3). Unfortunately, the volume of colluvium stored in 1<sup>st</sup> and 2<sup>nd</sup> order channels in the study area could not be assessed. Figure 4.5 is a typical example of a 2<sup>nd</sup> order channel. In this photograph it can be clearly seen that the stream flows over the stored colluvium (flat bed contrary to v-shaped) and that a lot of colluvium is stored on the stream banks. This picture was seen in many of the 2<sup>nd</sup> order channels in the study area (see also figure 3.2). So, the volume of colluvium stored in these channels must be considerable.

Due to the lack of (fresh) debris flow tracks the critical channel-gradient, at which a debris flow may scour the channel-bed or deposit material, could not be determined.

All deposits of medium-scale debris flows are around  $10^3 \text{ m}^3$  (deposit 4 & 5, table 4.6 and o.p. 46-48). These deposits show that most debris flows from the three investigated subcatchments are unable to travel far beyond the confluence point, because this point is marked by a sudden decrease in channel-slope (to about  $5^\circ$ ) and a sudden increase in width, making flows loose their competence. A wide plain is present here, which is primarily composed of debris flow deposits (most of which is reworked by bulldozers).

As mentioned in chapter 1, a large lave torrentielle reached the Ubaye in August 1996. The small pedestrian bridge, where the tipping-bucket raingauge was installed, showed signs that during this event it was almost submerged. Based on the average speed and duration of medium-scale debris flows (section 2.2.3) and the geometry of the channel-bed (cross-sectional area) at this point, the size of this event was estimated (see appendix H, deposit 4). This size is  $6 \cdot 10^3 - 6 \cdot 10^4 \text{ m}^3$ . No indications were found along the Main Channel that debris flows are likely to exceed this volume, indicating that the largest possible laves torrentielles are of this estimated size.

The origin of this event (triggering site and mechanism) is undeterminable, although it most likely came from the Riou Chamous subcatchment. This is because the mouths of the Riou Guérin and the Riou de la Pare were found to be relatively stable (presence of

vegetation; absence of fresh deposits). At the mouth of the Riou Chamous, however, a large, fresh deposit was found (deposit 4, appendix H). This deposit is assumed to be part of this event, probably indicating a separate surge of a more rigid type. It is important to note that only the more fluid surge was able to travel through the Main Channel, passing all 33 barriers. Another important observation is that this event did not destroy the pillar of brick on which the pedestrian bridge is suspended. These observations indicate the mobility and fluidity of this lave torrentielle. Based on this evidence, it may be concluded that events such as these are unable to block the Ubaye (and cause flooding in Barcelonnette).

Summarising: the volume of most storages at initiation sites are only up to  $10^2 \text{ m}^3$ , indicating that the bulk of the volume of medium-scale debris flows ( $10^3$ - $10^4 \text{ m}^3$ ) must be eroded from colluvium stored in the 1<sup>st</sup> and 2<sup>nd</sup> order channels. This shows that these debris flows typically increase (more than) ten-fold in size by incorporating sediment from channels.

#### Routing model

Based on the characteristics presented in this report and by Spee & Visser (1999), an attempt was made to adapt the debris-flow routing model of Benda & Cundy (1990) (figure 2.12) for the upper-catchments of the Riou Bourdoux. A summary of the observed angles is given in table 4.7.

Only at two locations initiation angles have been lower than  $30^\circ$ . The debris flows at these locations have been triggered by landslides. The slope angle at which most debris flows come to a halt lies between  $10$ - $13^\circ$  ( $\theta$ ). Most debris flows have come to a halt at channel-junctions, where the minimum junction angle is about  $45^\circ$  ( $\beta$ ).

With these data the model of Benda & Cundy (1990) could be modified. Possible rheological differences between the various types of observed debris flows does not seem to have a great influence on the values presented in table 4.7, although the modified model should be applied with caution since only few data are available.

Moreover, these data are only applicable to the debris flows along the Main Channel and within the subcatchments. The behaviour of the more fluid laves torrentielles, capable of reaching the Ubaye, cannot be described with this model.

Initiation angle	Deposition angle	Junction angle ( $\beta$ )
36	9	50
36	11	35
36	18	75
36	13	45
37	16	43
32	10	90
21	10	73
40	13	118
33	20	102
40	-	64
25	-	54
35	-	68

Table 4.7 Summary of all observed initiation, deposition and junction angles. Data in italics are from Spee & Visser (1999). The data sequence is no particular order. All junction angles are derived from locations where deposits came to a halt.

### 4.3.2 Channel process activity

The results of the surveys of the monitored sections of the Main Channel and the Riou de la Pare are given in appendix F2 and F4 respectively. The data in appendix F2 suggest that the three cross-sections of the Main Channel continually vary in size, although only the cross-section at the junction point (appendix F1) is definitely decreasing in width. The alluvial bar also seems neither to enlarge nor be reduced in size.

Date	Discharge (l/s)	3 <sup>rd</sup> order	2 <sup>nd</sup> order
2-6-1997	234.2	*	
10-6-1997	99.3	-	*
17-6-1997	183.4	+/-	-
24-6-1997	187.9	+/-	
30-6-1997	355.3	+	+
7-7-1997	256.7	+/-	
10-7-1997	357.0	+/-	

Table 4.8 Qualitative comparison between discharge and cross-section of the monitored channel-reaches. A + indicates general increase in width compared to the previous measurement; - a general decrease. \* indicates the first measurement and empty fields, no data.

Likewise, in appendix F4, the data show variation in the width of the cross-sections of the 2<sup>nd</sup> order channel, but neither a definite increase nor decrease. Table 4.8 shows a qualitative analysis of the results compared with the measured discharge data.

This table shows that part of the measured differences can be

ascribed to differences in discharge. At a higher discharge, more of the alluvial bar and banks are flooded, resulting in an increased channel width (but not effecting channel storage). At a lower discharge, the opposite occurs.

To check these results, photographs were taken of the two channel reaches during the different observation-days. This resulted in two photographic time-series, which are analysed in appendix F3 and F4 (3<sup>rd</sup> and 2<sup>nd</sup> order respectively). Careful examination of these photographs show that visually no differences can be distinguished. Even the marker stones have all remained in place. This evidence indicates that fluvial bedload transport in both channel-sections was very low during the research period.

Further evidence of channel surface stability are the streamside vegetation and mosses on stones found along the Riou de la Pare. Along the Main Channel this evidence could not be found, but this might be contributed to the reworking of the riverbed by the RTM.

In order to estimate general transport rates, the average rate of sediment accumulation behind the 33 dams in the Main Channel was calculated (equation 3.1, section 3.3.3).

The total channel length between the lowest and highest located dam is 2250 m (appendix A1). This yields an average distance of 68 m between two dams (z). Field investigation showed that each dam was on average 2.5 m in height (y<sub>2</sub>) and 20 m in width (x). The average volume of each reservoir then becomes  $1.7 \cdot 10^3 \text{ m}^3$ . The sedimentation-rate in the Main Channel then becomes  $5.7 - 8.5 \cdot 10^2 \text{ m}^3$  a year (section 3.3.3).

The estimated volume of the reservoirs may be larger, due to the unrealistically chosen channel form (i.e. horizontal subsurface). The sedimentation rate is therefore presumably larger, especially when the sediment-trap efficiency is less than 100%, which is very likely. Still, assuming only medium-scale debris flows ( $10^3 - 10^4 \text{ m}^3$ ) are able to deposit large amounts of sediment in the Main Channel, the estimated rate indicates a return-period of

these flows of 2-10 years (= debris flow volume divided by sedimentation rate). This value corresponds to the return-period determined by Van Asch and Van Steijn (1991) (section 2.2.3).

#### 4.4 Other results<sup>9</sup>

##### 4.4.1 Shear strength of Terres Noires

The measured shear strength (section 3.5.1) is plotted versus time for each sample (see appendix E). Peak and residual strength are indicated. Failure takes place at the point where peak strength occurs. The value of residual strength is at a point where the strength becomes constant with displacement. This residual strength can be used as shear strength for material that already has failed but moves periodically.

The shear strength (either peak or residual) was plotted versus the corresponding normal stress for all samples, which resulted in a graph, in which a regression-line was constructed. The arctangent of the slope of this line is equal to the angle of internal friction. The resulting angle of internal friction of broken Terres Noires is:

Peak strength: 30.5°

Residual strength: 24.5°

Using the empirical expression of Hingston and Jermy (1998), the basic angle of internal friction ( $\varphi_b$ : equation 3.13) is also calculated. In short the result is:  $\varphi_b = 44.29 \pm 4.25^\circ$ .

Using expression 3.15, De Joode (2000) determined the critical angles at which Terres Noires slopes would remain stable. Using the angle of internal friction of peak strength ( $\varphi = 30.5^\circ$ ), a stable slope may not be more than 20.3°, otherwise failure will occur. Using the basic angle of internal friction ( $\varphi_b$ ), no failure occurs at a slope angle of 31.4° or less. In both cases pore-water pressure is not taken into account.

The internal friction angle for Flysch clasts is used for stability analysis of the upper debris slopes ( $\varphi = 38.3^\circ \pm 0.5$ ; Blijenberg, 1998). Failure of loose Flysch colluvium (resulting in a possible debris flow) can occur at slope-angles of 51.4° (De Joode, 2000). Such slope angles, however, are not present in the subcatchment, indicating that the triggering of debris flows in these areas is aided by other processes, presumably overland flow.

##### 4.4.2 Landslide and debris-flow frequencies

Two locations in the Riou de la Pare catchment proved useful for dendrochronology: location RB3 (south of o.p. 16) and RB4 (o.p. 31, appendix A2). Analysis of the sampled tree-rings showed that at location RB3 12 mass movements have occurred in a 90-year timespan, indicating a landslide frequency of once in every 7.5 years. At location RB4 8 landslides occurred during a 93 year period, resulting in a recurrence interval of 11.5 years. It was assumed that creep would dominate this location (due to the presence of continuously

<sup>9</sup> Results taken in short from De Joode (2000) and Spee & Visser (1999) (respectively).

curved trees and a hummocky surface, and the absence of scarps), but analysis of the tree-rings could not show this satisfactory. Spee & Visser (1999) determined an average volume for these landslides of  $10^2 \text{ m}^3$ .

At just one location (o.p. 52) in the investigated subcatchment some lichens were found on a small-scale debris flow deposit. The presence of mosses and grass on the deposit indicate a high age. The thalli of lichens measured are:

Lichen thalli (cm)			
3.8	2.4	2.2	2.8
3.4	2.5	1.9	-

Table 4.9 Measured diameter (thalli) of the lichens found at observation point 52 (length measured in cm).

Using the growth curve of Orombelli and Porter (1983), Spee & Visser (1999) determined the age of the deposit on 69 years. This corresponds to the range of data from the other investigated subcatchments, where Spee & Visser (1999) found ages between 50 – 70 years for debris flow deposits on the upper debris slopes.

## 5 Debris-flow model of the Riou de la Pare catchment

### 5.1 A partial sediment budget for the Riou de la Pare catchment<sup>10</sup>

A lot of variables influence the form of a sediment budget, increasing its complexity. In figure 5.1 the flow-chart of the sediment budget recommended for the Riou de la Pare catchment (including the Main Channel) is given. The catchment is divided into a hillslope part (including channels up to 2<sup>nd</sup> order) and a channel part (3<sup>rd</sup> order channels or higher).

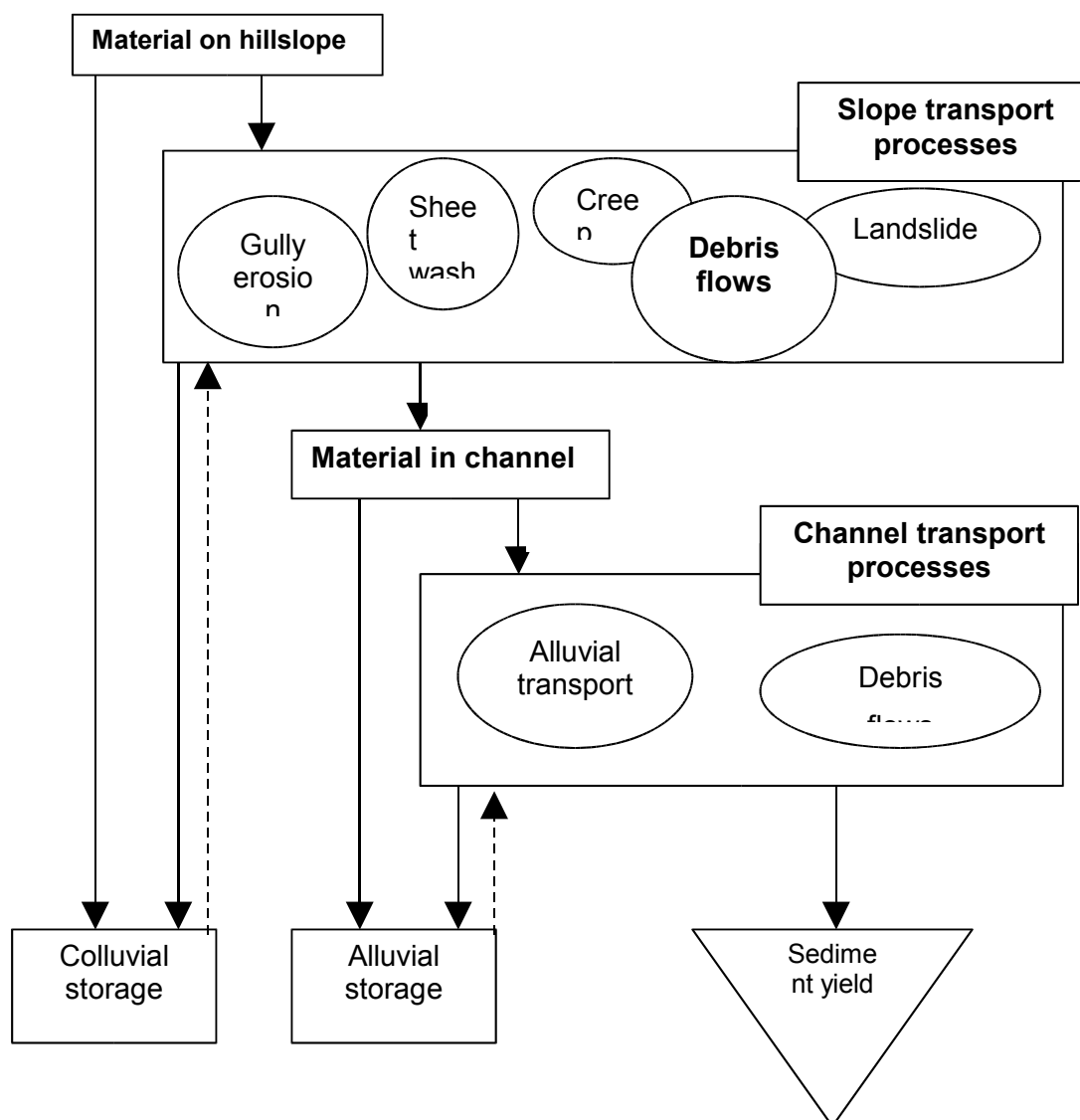


Figure 5.1 Flow-chart of the sediment budget recommended for the Riou de la Pare subcatchment (adapted from De Joode, 2000).

The sediment on the hillslopes will be transported by hillslope transport processes to the channels or will be (re)stored on the hillslopes as colluvium. When stored in the channel,

<sup>10</sup> First paragraph adapted from De Joode (2000)

the sediment can be discharged out of the catchment by channel transport processes or be (re)stored further downward in the channel network. As was seen in the results, 2<sup>nd</sup> order channels do exhibit fluvial processes, and, when debris-flow activity is very low, they may dominate transport. This means that grouping 2<sup>nd</sup> order channels to areas dominated by hillslope processes may not be entirely appropriate.

From the results (chapter 4) and figure 5.1, it can be seen that gully erosion, sheet wash, creep, landslides and debris flows are the main hillslope transport processes. As was shown in chapter 2, the contribution of creep, gully erosion and sheet wash to the sediment budget is difficult to determine. The lack of debris-flow deposits made it also difficult to quantitatively assess the influence of debris flows. And as was seen in section 4.3.2, no definite change in storage along the monitored 2<sup>nd</sup> and 3<sup>rd</sup> order channel reach was observed, inhibiting predictions of fluvial transport. The results also show that few storage sites on hillslopes were found and estimations of storage in the 1<sup>st</sup> and 2<sup>nd</sup> order channels could not be made.

This lack of quantitative data impedes the completion of the recommended sediment budget. Because of this, it is better to speak about a partial sediment budget. Reid & Dunne (1996) suggest that in such a case, comparative data from similar (neighbouring) catchments can be used to complement the sediment budget. However, no data are available, since this is a pilot-study on sediment-budgeting in the area. With the partial sediment budget, no quantitative GIS model could be constructed.

De Joode (2000) has attempted to construct a sediment budget model on a rainfall-based approach, in order to get insight into the relative importance of the active processes in the Riou de la Pare catchment. The catchment was divided into an active and an inactive area. The active area comprised mostly Terres Noires and heterogeneous material. She used the infiltration characteristics of these slope materials in order to determine the process activity (small-scale debris flows, overland flow and landsliding) on the active slopes during different rain-events. The discharge and suspended load data were used to make estimates of channel transport.

The model showed that during an extreme rain event (100 mm/h, 1 min of duration), small-scale debris flows are the main transport processes on hillslopes. During less intense rainstorms (but of longer duration), overland flow is the main (and only) erosion process. The model also showed that landslides in Terres Noires are not initiated solely due to internal failure. Presumably, the landslides observed in the Terres Noires are triggered when slopes are undercut by the streams. When landslides occur, they are the main contributor to the sediment budget, because the predicted values of production (both size and frequency) are large in comparison to the other processes.

Spee and Visser (1999), on the contrary, were able to construct a quantitative sediment budget (GIS) model for the Riou Chamous subcatchment. This catchment has only one large central stream, the Riou Chamous, which has incised deeply into its catchment, has a very steep gradient and is v-shaped. All slopes in this catchment are directly connected to the stream-channel, greatly simplifying estimations of storage and sediment

delivery to the channel. Since there is only one channel, no debris-flow routing had to be considered.

They divided the subcatchment into six areas of assumed uniform process-activity based on the developed geomorphological map. The process are: denudation of flysch slopes (limestone), rockfall, soil detachment (overland flow), landslides, denudation of Terres Noires and debris flows. In order to calculate sediment production in these areas, they used formulas and values from literature, the measured infiltration capacity, characteristic rain-events recorded by Blijenberg (1998), the dendrochronological results, and assessments of volumes from field observations.

Their model was run over a period of 100 years, with time-steps of one year. All of the simulated processes delivered material for debris flows to the central channel. Debris flows were initiated randomly, based on slope angle. The model resulted in an overestimation of the expected volume of debris flows of at least one order-of-magnitude. This was mostly due to the fact that the model was very sensitive to changes in the parameters describing debris production.

The model of Spee & Visser (1999) is thus primarily a hillslope debris production model, with a simple channel routing of debris flows. They assumed that when a debris flow is triggered it travels the entire length of the channel to the outlet point of the subcatchment. As was shown in the results (section 4.3.1), this is often not the case in the Riou de la Pare catchment. In order to complement the model of Spee & Visser (1999), a model was created with special emphasis on the triggering and flowing mechanism of debris flows through the stream network. The model is qualitative, simply designed in an attempt to simulate debris-flow routing according to the model proposed by Benda and Cundy (1990) (section 2.2.3).

A pre-emptive note should be made about the triggering mechanism of debris-flows. As Blijenberg (1998) showed, it is exceedingly difficult to model this triggering. An ideal triggering-mechanism would have to trigger many small- and only occasionally medium-scale debris flows, based on rain events. The present model, however, is run over 100 years. On such a time-scale it is difficult to model individual rain events due to their variable character, not only within each year, but also between years. This poses a problem in their use for debris-flow triggering. Therefore, it was only attempted to simulate triggering based on alternate (random) wet and dry years on a trial-and-error base.

## 5.2 PCRaster modelling

The model has been created using the PCRaster<sup>®</sup> environmental software package. This is a grid-based GIS package. A grid database is build up of a number of (grid-)cells, organized in rows and columns. For modelling, PCRaster needs digital (grid) input maps. As already described in section 3.2.3, the maps (appendix B2-B5) were created with ARC/INFO and ArcView. For this model, several maps were needed: a vegetation map, a lithological map, a map showing all water courses, a map showing the outline of the subcatchment and finally, a digital elevation model of the subcatchment (DEM).

Exporting GRID-maps from ARC/INFO requires the conversion of all maps into a GRID database. With the help of the "GRID-ASCII" command in ARC/INFO, the maps were transformed into ASCII-tables. In PCRaster, the relevant maps were then imported and converted to PCRaster's own database files (maps). The exact procedure is described by Spee & Visser (1999). An overview of the converted maps is given in figure 5.2.

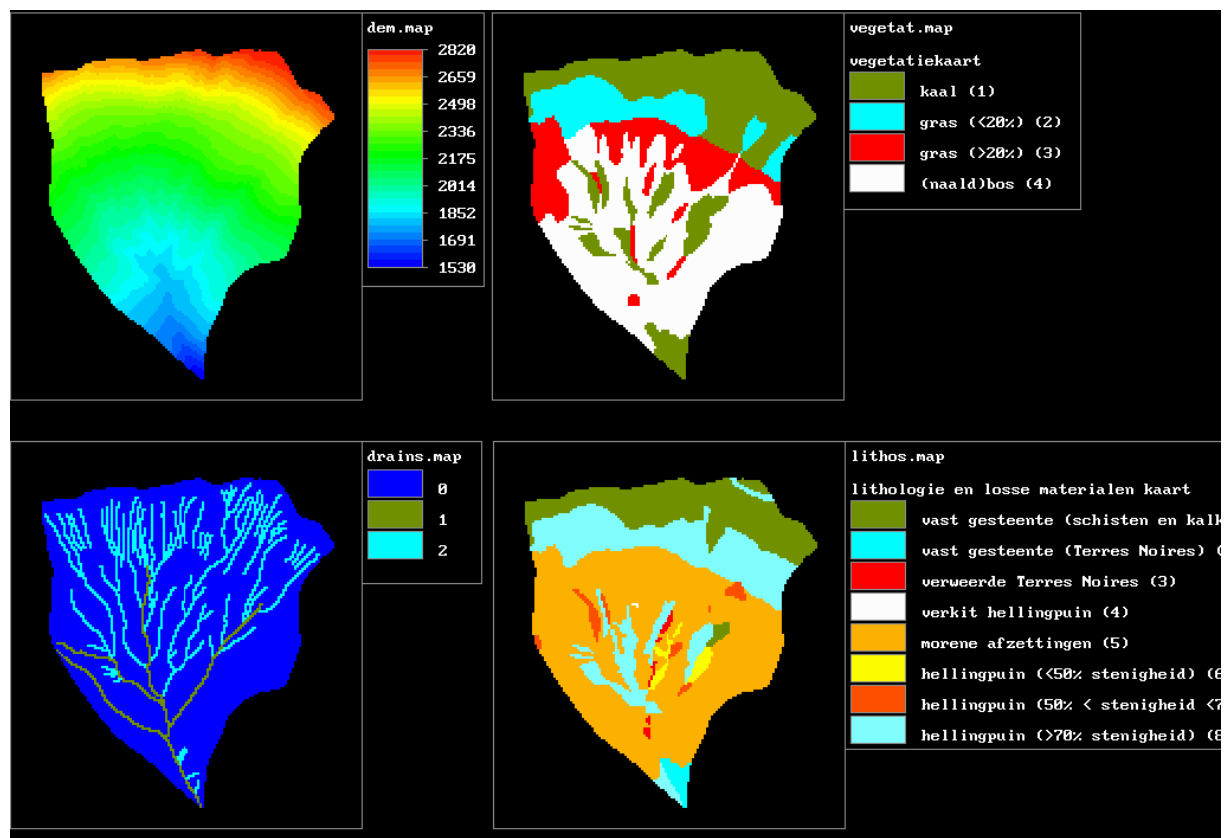


Figure 5.2 Overview of the imported PCRaster maps. Lithos.map and vegetat.map correspond respectively to appendix B2 and B3.

Since the model must simulate flow behaviour in both time and space, the model is dynamic. Dynamic models in PCRaster are made using a so-called *script-file*. This is an ASCII-file in which processes can be simulated using logical (Boolean) and mathematical algorithms. The calculations are done with different databases.

The dynamic script-file consists of the following sections (Karssenbergh, 1998): *binding*, *areamap*, *timer*, *initial* and *dynamic*. The script of the created model is shown in appendix I1.

The first section is the *binding* section. This section defines the links between the names of variables used in the script and the MSDOS-filenames of in- and output maps.

The *areamap* section defines the size, geographical location, GRID resolution and coordinate system. This is done, so that all produced maps overlap exactly making analysis possible. The information is provided by a base map, here called "Catchment" (appendix I1). This map consists of 165 rows and 150 columns, with a cell size of 20 by 20 meters. The large surface area for each cell was chosen in order to reduce the database size, making it more manageable, but still have enough detail for modelling. The coordinate system used is identical to that of the topographic map (1:10.000, I.G.N., 1982/83), with map dimensions in meters.

The third section is the *timer* and gives the time domain of the model. It contains three statements: the first gives the time at the start of the model, the second the time at the end of the model, and the last defines the time-step. The model is run over 100 years (following Spee & Visser, 1999), but here with a time-step of 2 years (due to calculation restrictions) (appendix I1).

The last two sections (*initial* and *dynamic*) contain statements and algorithms defined in PCRaster operations. These sections comprise the actual model. The *initial* section describes the state of the model (framework) at the beginning of the first time-step. The operations in the *dynamic* section change the variables or calculate new ones according to the PCRaster operations. These calculations are made from top to bottom (of the script-file). This section is rerun every time-step. At the end of each time-step, the calculated variables (maps), defined in the *binding* section, are written to the database. The model thus produces a time-series of the spatial database of any desired variable.

For a more detailed general description of dynamic modelling, the reader is referred to Spee & Visser (1999).

### 5.3 Model construction

This model, which is a simplified representation of the subcatchment predicting debris-flow behaviour in the drainage network, must answer the following questions: Where are debris flows initiated? Once initiated, what is the predicted path of a debris flow? Where will the debris flows deposit the bulk of their material? So, this GIS model must be able to simulate transport and deposition of material (gathered in gullies). In this model, it is assumed that transport is due to debris flows only (section 4.3.1). Even though the adapted debris-flow routing model of Benda & Cundy (1990) may not be very accurate due to a lack of data (section 4.3.1), the observed values for the critical angles are used nevertheless. Future research may yield more accurate values for the model.

The assumptions of what happens with material in the streams (in this model), after it has come from the hillslopes, are given below.

When debris enters the channels, the following will happen: The debris is stored, waiting to be scoured by a debris flow. Debris flows are triggered within the drainage network only (in this model: not on hillslopes). Once in motion, the debris flow can grow in volume downstream by incorporating debris from the channels. This may happen when a debris flow passes cells in which debris is stored above a certain critical angle. The debris flows come to a halt when the channel gradient is lower than the critical gradient for deposition, or when they encounter a critical junction angle.

The model will be described per simulated process.

### 5.3.1 Initial assumptions and values

The original drainage pattern proved to be too difficult to work with. The original pattern (figure 5.3: drains.map) shows both perennial and intermittent streams. Many of the intermittent streams are discontinuous, and trial runs with the model showed that this discontinuity posed a problem. Therefore, a simplification was chosen, which was calculated following box 5.1.

```

initial
  dem1=dem;
  report ldd1=lddrepair(lddcreate(BurnedDem,1e20,1e20,1e20,1e20));
  report slope1=scalar(atan(slope(dem1)));
  upl=accuflux(ldd1,1);          # create new simpler stream network
  report Drains = boolean(if(upl ge strdim,1,0));
  StreamOrder = scalar(streamorder(if(Drains,ldd1)));
  Aspect=aspect(dem1);
  AspectGullybottom = scalar(if(Drains,Aspect));
  FlowPoints = if(Drains and (downstream(ldd1,StreamOrder) ne StreamOrder),boolean(1),0);
  report BetaAngle = if(Catchment,if(FlowPoints,(AspectGullybottom-downstream(ldd1,AspectGullybottom))));
  report CriticalBeta = if(Catchment,cover(if(BetaAngle gt 45 or BetaAngle lt -45,boolean(1),0),0));
  DebrisInGully=scalar(Catchment)*0;
  TotFluxOut=scalar(Catchment)*0;
  DebrisProduced=0;

```

Box 5.1 Script-section (initial) for calculating the starting conditions in the model (appendix I1).

An imprint of the original drainage pattern on the DEM (*BurnedDem*: box 5.1), in which the perennial streams were accentuated, was used to determine a new pattern. If the amount of upstream cells for a cell was greater or equal than 150, a stream would begin (*Drains*). The new drainage pattern is visible in figure 5.3 (*newdrain.map*). It can be seen that two *extra* streams are created this way (lower right). Since these produce no debris flows in the model, their presence need not be corrected.

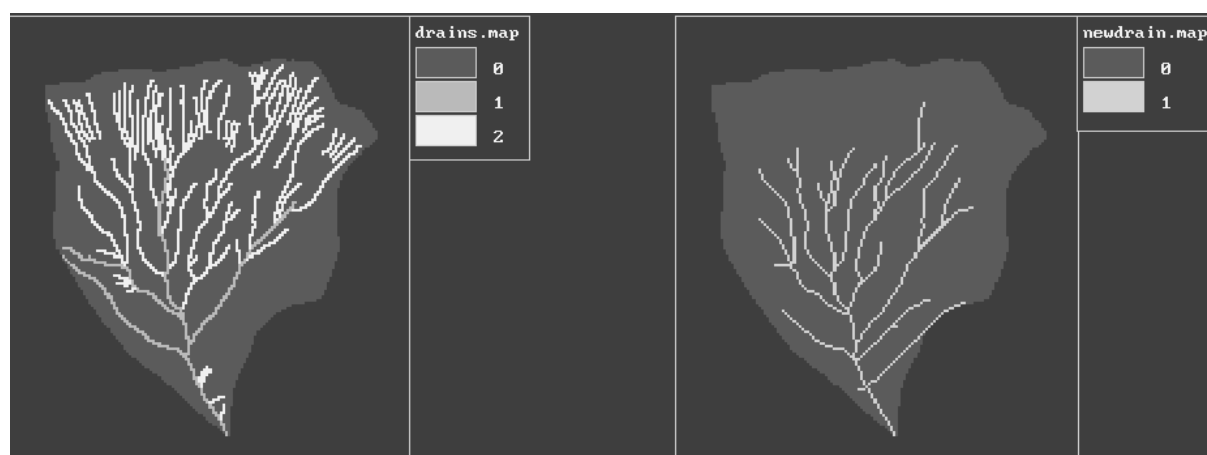


Figure 5.3 New simplified river-pattern.

The new drainage pattern is analysed in this section, in order to locate stream junction-points which exceed the critical angle determined in section 4.3.1 ( $\beta = 45^\circ$ ). Debris flows will not travel beyond these cells. The aspect in the channels is first calculated (*AspectGullyBottom*). Secondly, using a difference in stream-order between two adjacent cells, junction points can be determined. The angle ( $\beta$ ) between the contributing and

receiving channel is calculated by determining the difference in aspect between these channels (*BetaAngle*). Junction points having an angle above 45° are critical and will be used to determine deposition points of debris flows in the model (*CriticalBeta*).

Other initial assumptions at the start of time-step 1 are that in the beginning no debris for debris flows is available in the streams (*DebrisInGully*), no debris has yet come out of the catchment (*TotFluxOut*) and the total amount of produced debris of the entire model run is still 0 (*DebrisProduced*: section 5.4). A slope map (*slope1*) is also created, based of the digital elevation model (figure 5.2).

### 5.3.2 Sediment production

In order to model transport of entrainable debris through the channels, an estimate had to be made of the amount of material gathering in these channels. As indicated in section 5.1, this is a qualitative model. Therefore it was decided to simply appoint a value of 'debris production' to the several landscape-units. Thus, during every time-step each landscape-unit will produce a specific (and fixed) amount of material.

The landscape-units were created out of the combination of the lithology and vegetation maps (appendix B2 & B3). 14 different units are distinguished (table 5.1 and figure 5.4), of which 13 are debris producing.

Lithology	Vegetation	"Erosion-value" (m / 2 years)
Flysch	Bare	0.006
Terres Noires	Bare	0.030
Weathered Terres Noires	Bare	0.040
Weathered Terres Noires	Forest	0.015
Moraine	Bare	0.015
Moraine	Gras	0.004
Moraine	Forest	0.001
Debris: < 50 %stones	Bare	0.015
Debris: < 50 %stones	Grass	0.003
Debris: < 50 %stones	Forest	0.001
Debris: > 50 %stones	Bare	0.007
Debris: > 50 %stones	Grass	0.003
Debris: > 50 %stones	Forest	0.001

Table 5.1 The different landscape-units with the corresponding "erosion"-values that have been used in order to determine sediment production on the hillslopes (*eenheidstabel*: Box 5.2, appendix I2).

The 'erosion-values' are expressed in meters of sediment production. Their purpose is merely to provide material for debris flows and to distinguish landscape-units producing much material (active) from those producing little (inactive). The values have been estimated based on the debris production calculations of Spee & Visser (1999), in order to produce a realistic order-of-magnitude for debris flows.

All produced material on the slopes is transported within a time-step to the channels (i.e. no storage on slopes), and remains here. This is indicated in figure 5.5.

Because it is assumed that hillslope processes will transport more sediment to the channels when the slope-gradients are higher, slope-angles are considered in the calculations. For this purpose, the slope-angles are grouped into classes. Every class has its own value, indicating its relative influence on erosion (table 5.2). The class comprising the steepest slopes has a value of 1, indicating maximum erosion.



Figure 5.4 Location of the different landscape-units (*eenheid*: Box 5.2).

Slope-angle class	Erosion-fraction
[0, 5>	0.1
[5, 10>	0.2
[10, 15>	0.5
[15, 20>	0.7
[20, 25>	0.8
[25, 30>	0.9
[30, >	1

Table 5.2 Slope-angle classes (*slopefraction*: Box 5.2, appendix I2).

In the script the amount of sediment production is calculated according to box 5.2.

```
# sediment delivery of each 'eenheid' to the drainage network in meters / 2 years
NewEenheid=if(Drains,99,eenheid); # No sediment production in gullies
SedimentProduction=lookupscalar(slopefraction,slope1)*lookupscalar(eenheidstabel,scalar(NewEenheid));
SedSlopeToGully=if(Drains,upstream(1dd1,accuthresholdflux(1dd1,SedimentProduction,(500*scalar(Drains))))),0);
report dem1=dem1-SedimentProduction;
slope1=scalar(atan(slope(dem1)));
DebrisInGully = SedSlopeToGully + DebrisInGully;
```

Box 5.2 Script-section (dynamic) describing the calculation of the availability of material for debris flows (appendix I1).

The landscape-unit map is combined with the slope-fraction and an 'erosion-value' (figure 5.5; *SedimentProduction*, Box 5.2). No sediment will be produced in the channels (*NewEenheid*). All material is now transported to the nearest downstream channel (*SedSlopeToGully*), where it is stored (*DebrisInGully*). This is done with the operation 'accuthresholdflux'. This operation routes all material downstream over the local drain direction map, until it reaches a predefined threshold (a variable). If the value of the threshold is larger than the amount of transported material, all material will be deposited. If

the threshold is lower, all material will be further transported to a downslope cell. In this case, only the channels (*Drains*) have a high threshold (value: 500), while all the slopes have no threshold, assuring the routing of all material to the channel network. If there is still material present in the channels from the previous time-step, the new material is added. A correction for the erosion of the slopes is also made to the DEM.

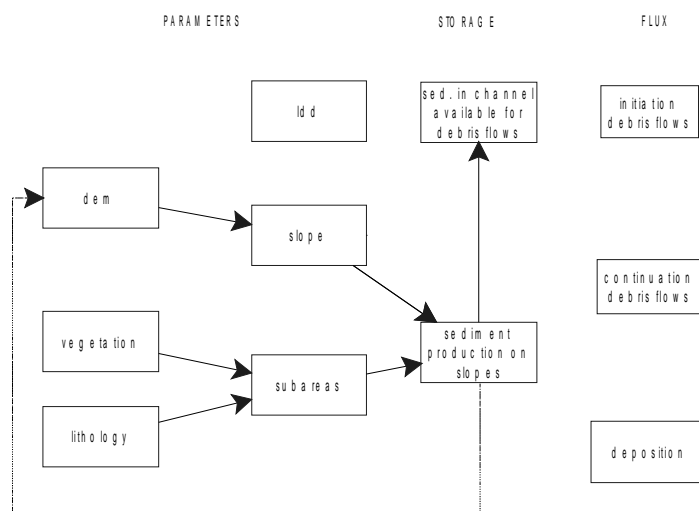


Figure 5.5 Flow-chart depicting the sediment production of the model.

### 5.3.3 The debris-flow 'trigger'

After producing sediment to the channels, the model checks whether the available debris can be transported as a debris flow. A set of specific conditions is calculated ('trigger'), to which the material will be compared. The operations are shown in Box 5.3.

```
# generate rainfall map as a random map per 2 years
report rf = 0.01*mapnormal() + ppt + 0.0002*(dem1-base);

# generate sites of possible debris flows based on amount of debris, slope and rainfall
Trigger=(16 + (3/rf))*if(slope1 gt 30,(30/slope1),500);
triggerflux,triggerstate=accutriggerflux,accutriggerstate(ldd1,DebrisInGully,Trigger);
```

Box 5.3 Script-section (dynamic) calculating the triggering of debris flows (appendix I1).

The trigger consists of a combination of rainfall ( $rf$ ), critical slope-angle ( $>30^\circ$ , in the cell where debris is present) and the amount of material (*Trigger*). 'Accutriggerflux' is used as the triggering operation. If the amount of material in the cell (*DebrisInGully*) exceeds the trigger, all material in the cell will be initiated into a debris flow. If no triggering occurs, all material will remain stored in the cell.

The trigger is inversely correlated to rainfall, since increasing rainfall results in an increase in debris-flow triggering, and thus a lower trigger. Rainfall ( $rf$ ) itself was based on a year-average rainfall amount of 750 mm (ppt) and was varied each time-step with a random factor (*mapnormal*) and showed an increase with altitude (not based on section 4.2.1). Finally, a high slope-angle means quicker debris-flow triggering, and thus likewise an inverse correlation with the trigger. No debris flows are triggered if the slope-angle is less than  $30^\circ$  (section 4.3.1).

As was stated in section 5.1, this trigger was fully developed on a trial-and-error base, in order to produce a balance between size and frequency of the simulated debris flows.

#### 4.3.4 Debris-flow initiation

Box 5.4 shows the PCRaster formulas for calculating the locations (cells) of initiation of debris flows, and the possible resulting flow-paths. The first calculation in box 5.4 creates a map showing only cells, which have triggered debris flows (*InitiatedDebris*).

```
# calculate start amounts of debris flow material
report InitiatedDebris=if(Drains and triggerflux ne 0 and upstream(Idd1,triggerflux) eq 0,triggerflux,0);
report DebrisPath=boolean(accuflux(Idd1,InitiatedDebris));
DebrisInGully=DebrisInGully-InitiatedDebris;
SlopePath=if(DebrisPath,slope1);
SlopeClass=scalar(if(SlopePath ge 20,1,if(SlopePath lt 20 and SlopePath gt 10,2,3)));
```

Box 5.4 Script-section (dynamic) calculating the possible flow-path of transported debris (appendix I1)

This map shows the locations of initiation (cells) and the amount of triggered material. This is necessary, because the trigger (*triggerflux*: box 5.3) merely determines whether triggering occurs, and results in a map showing a flow path. The initiated debris is then transported through the drainage network (Idd1) to a possible location of deposition. This is schematically represented in figure 5.6.

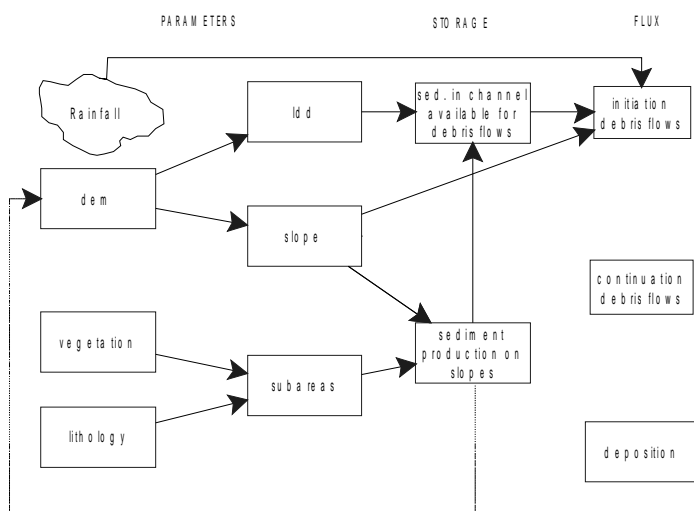


Figure 5.6 Flow-chart of the initiation of debris flows in the PCRaster model.

Once in motion, the material will travel a certain path. The longest travel path (*DebrisPath*) is determined by the operation 'accuflux'. This operation creates maps showing the flow path if the debris flows would reach the outlet point of the subcatchment without hindrance. The routing of a debris flow will, among others, depend upon the gradient of the channel along its flow path. To determine the slope angles in the flow paths, the algorithms for 'SlopePath' and 'SlopeClass' have been used. The gradient along the possible flow path is subdivided into three classes. The slope in the flow path is either greater than 20° (class 1), between 20 and 10° (class 2), or less than 10° (class 3).

### 5.3.5 Debris-flow propagation

The adapted values of the model of Benda and Cundy (1990) (section 4.3.1) are now applied to the maximum predicted flow path. If the slope-angle of the flow-path is lower than  $10^\circ$  ( $\theta$ ), all debris flows will come to a halt. Between  $10^\circ$  and  $20^\circ$  the debris flows will move through the channel, but do not incorporate sediment from the channel-bed. So, these sections (cells) are not eroded, but aggradation occurs due to continuing sediment input each time-step. Above  $20^\circ$  debris flows will “scrape” all available debris in the channel. Finally, if the critical junction angle exceeds  $45^\circ$  debris flows will be deposited. The modelling of this behaviour is shown in box 5.5.

```
# flux continuation?! and resulting state
Threshold=cover(if(upstream(Idd1,if(DebrisPath,scalar(CriticalBeta),0)) eq 1,1500,if(SlopeClass eq 1,0,if(SlopeClass
eq 2,DebrisInGully,1500))),1500);
DebrisInPath=if(DebrisPath,(DebrisInGully+upstream(Idd1,InitiatedDebris)),0);
report ContinueFlux,ContinueState=accuthresholdflux,accuthresholdstate(Idd1,DebrisInPath,Threshold);

# flux deposition
MatDeposition=cover(if(SlopeClass eq 3 and upstream(Idd1,ContinueFlux) gt 0,upstream(Idd1,ContinueFlux),0),0);
report MatDepoFlux,MatDepoState=accufractionflux,accufractionstate(Idd1,MatDeposition,0.2);
```

Box 5.5 Script-section (dynamic) involved in modelling the continuation of debris flows (appendix I1).

In order to model the above-described behaviour, the operation ‘accuthresholdflux’ was chosen again (section 5.3.2). The threshold (*Threshold*, box 5.5) is determined as follows:

At a channel-gradient greater than  $20^\circ$  (*SlopeClass* = 1) the threshold is 0, indicating that all debris, stored in cells along the flow-path within this class, is eroded. In section 4.3.1 it is shown that this value could not be determined for the subcatchment. In order to see whether scouring by debris flows could be modelled, this assumed slope angle was used.

At gradients between  $10^\circ$  and  $20^\circ$  (*SlopeClass* = 2) the threshold is equal to the amount of debris stored in the particular cells (*DebrisInGully*). This means that only the material, which has come from upstream of the cell is transported through the cell downstream. The amount of material that was already present remains stored.

At a gradient lower than  $10^\circ$  (*SlopeClass* = 3) the value for the threshold is set to an extremely high value (1500), assuring the deposition of all transported material from upstream. At locations where the junction angle is larger than  $45^\circ$ , the threshold will also have this value.

Before the ‘flow’ is calculated, the model first determines the available debris for transport (*DebrisInPath*). The initiated material is added to its first downstream cell, after which only the material present along the path of the debris flow is considered. The debris located in the possible flow-path (*DebrisInPath*) and the *Threshold* are now combined in the ‘accuthresholdflux’ formula, in which the actual path (according to the routing model) is determined (*ContinueFlux*). *ContinueState* gives the amount of material stored in each cell (along the flow-path) after the (possible) debris flows have occurred.

It is assumed that the debris flow does not come to an instant halt, when conditions for deposition arise. This assumption is modelled because debris flows have a certain fluidity. The last two lines in box 5.5 determine this depositional run-out. First the point of deposition

(cell) and the amount of deposited debris is calculated (*MatDeposition*). This is done by locating the lowest (most downstream) point of each debris flow path, where the next downstream cell has no value (from the *ContinueFlux*). Next, the corresponding amount of material in this point is routed further downstream, with every downstream cell receiving 20% of its neighbouring upstream cell (where 80% of the material is stored), creating the debris flow run-out (*MatDepoFlux*). The value of 20% was chosen arbitrarily.

### 5.3.6 Debris-flow routing

Box 5.6 describes the operation to produce the total debris flow track (*DebrisFlowFlux*). This track is calculated by adding the initially triggered debris, the *actual* flow path and the depositional run-out.

```
# Total flux and resulting states
report DebrisFlowFlux=InitiatedDebris+ContinueFlux+MatDepoFlux;

# calculate remaining debris in the gullies after possible df
DebrisInGully=if(boolean(ContinueFlux),ContinueState,(DebrisInGully+MatDepoState));
```

Box 5.6 Script-section (dynamic) for calculating the total debris flow track and remaining debris.

For the next time-step it is important to determine exactly the amount of debris that remains in all the channels. The remaining debris in the flow path (*ContinueState*) must be combined with the amount of sediment present in all the channels in the area (including those that did not produce a debris flow; *DebrisInGully*) and added to the material produced by the depositional flux (MatDepoState). This is calculated in the new *DebrisInGully*, which will be used as an input to the next time-step.

The completed model is shown in figure 5.7.

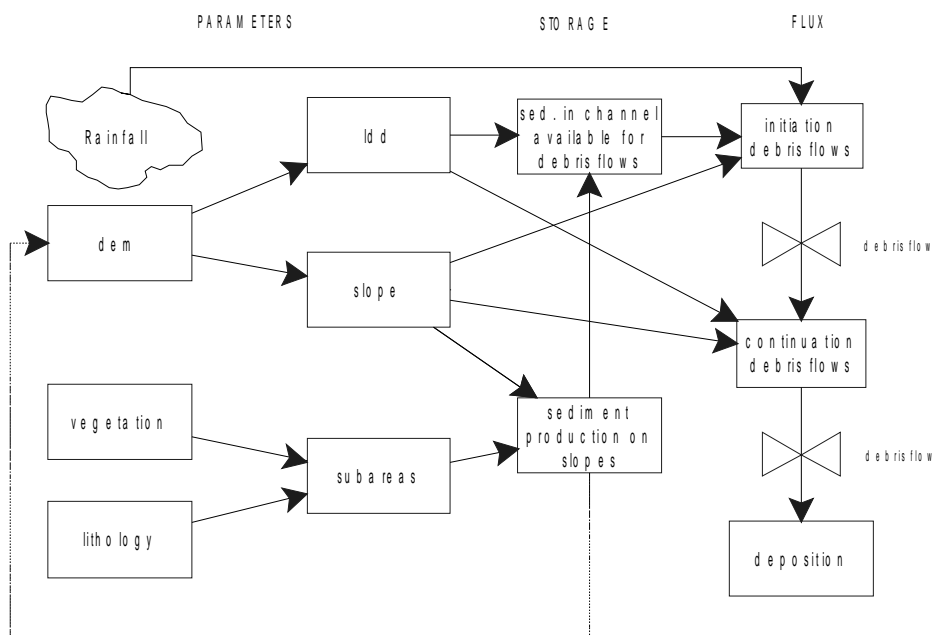


Figure 5.7 Flow-chart of the entire debris flow routing model.

## 5.4 Model results

The above-described model has several results for each calculated time step. One representative time step (50) has been selected, of which the results are shown here (figure 5.8).

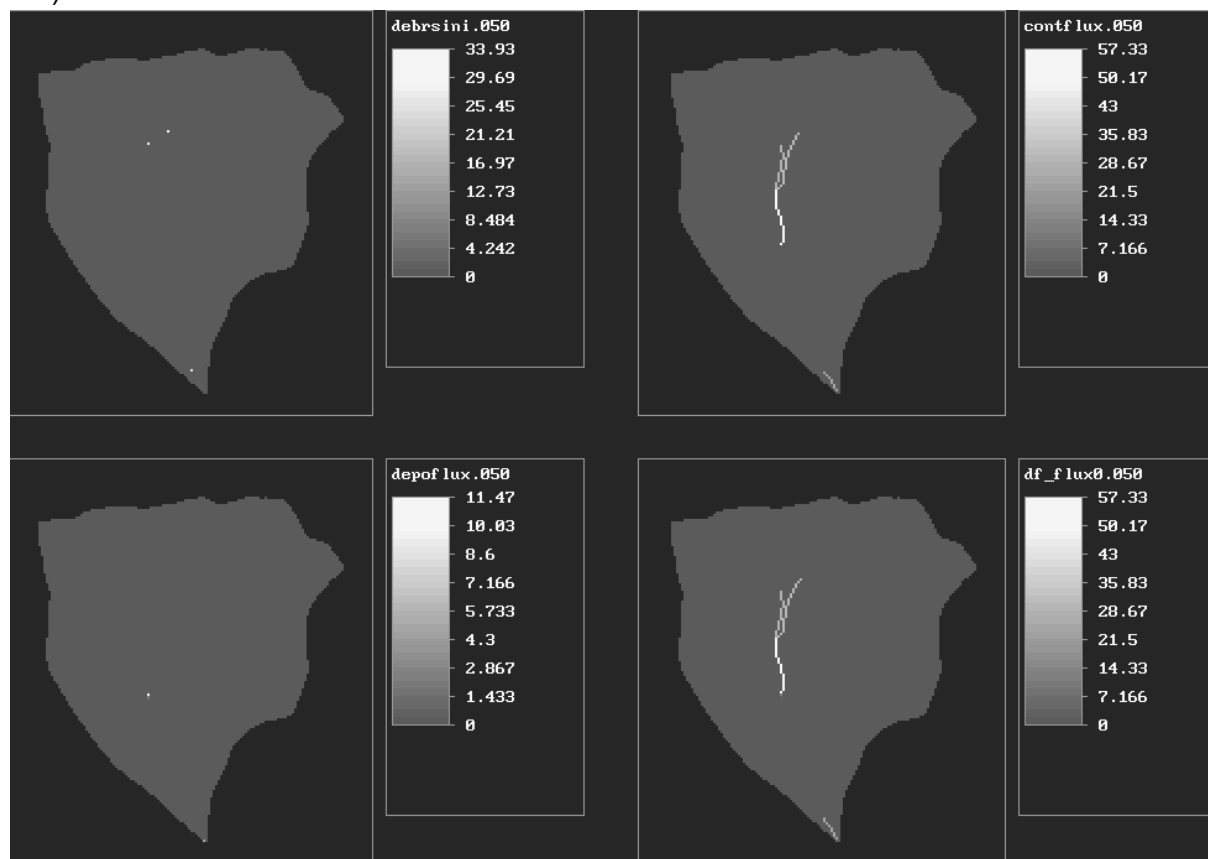


Figure 5.8 Results of time-step 50.

To get an impression of a whole 'run' over 100 years (50 time steps), the reader is advised to use the model included as appendix I4.

In the upper-left picture the locations of initiation of debris flows are shown (for time-step 50). The upper-right map shows the tracks of the resulting debris flows, till their point of deposition (lower-left). The last map in figure 5.8 gives the total debris flow track. The legends are all in unit depth (meters) per pixel-area.

A mass-balance was calculated in the model. The calculation is shown in box 5.7. The mass balance is described as the difference between the total produced debris (*Debris-Produced*) and the sum of all debris leaving the outflow point of the catchment (*TotFluxOut*) plus the amount of material remaining stored within the gullies (*DebrisInGully*). If this difference is 0, the mass-balance is fitting and all material is accounted for in the model.

The mass-balance is given in appendix I3, and is illustrated by figure 5.9. It shows clearly that this difference is very small and increases linearly with each time-step. The total difference after 50 time-steps is only about 0.24% of total sediment production, spread over the entire catchment. This suggests that the difference is caused by rounding effects during

the calculations. It also indicates that all material produced (in the model) is accounted for in the routing-algorithms.

```
# calculate mass balance
DebrisProduced=SedimentProduction+DebrisProduced;
report MassBalance1=maptotal(DebrisProduced);
OutFlowPoint=if(Iddmask(Idd1,Catchment) eq 5 and ycoordinate(Catchment) lt 245000,boolean(1),0);
TotFluxOut=if(OutFlowPoint,DebrisFlowFlux,0) + TotFluxOut;
report MassBalance2=maptotal(DebrisInGully+TotFluxOut);
```

Box 5.7 Script of the massbalance.

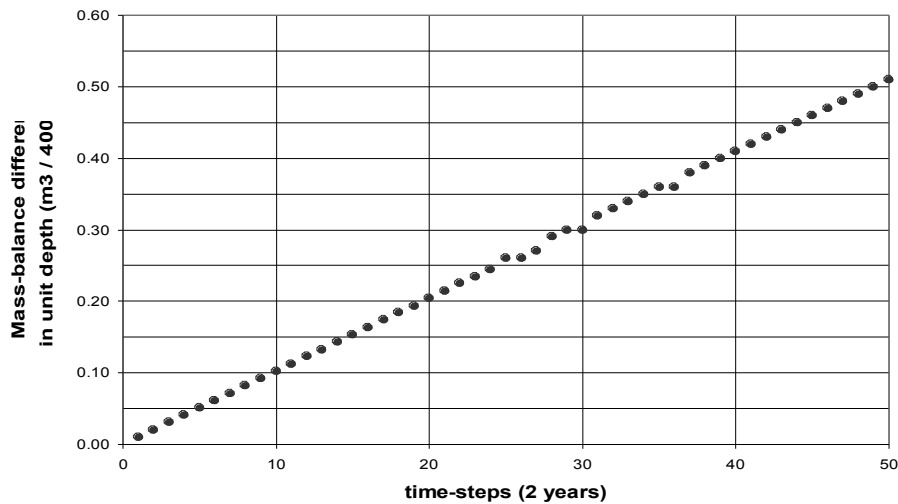


Figure 5.9 Graph showing the total mass-balance difference at each time-step.

A discussion of the model is given in section 6.2.

## 6 Discussion

### 6.1 Hydrological interpretations

#### 6.1 *Methodological discussion*

The several applied hydrological methods are prone to some well-documented errors, which are of influence on the interpretation of the results.

The major source of error in the rainfall measurements is the influence of wind. Wind turbulence around a raingauge usually results in underestimates (Ward & Robinson, 1990). All measurements were done with rain gauges of similar height and funnel-diameter, making it presumable that the underestimates are equal for all sites. De Villiers (1990) showed that a standard installed raingauge (as is used in this research) underestimates the amount of precipitation by at least 25%.

The tipping bucket raingauge does not perform well under conditions of extreme rainfall events. The reservoir may take too long to empty itself resulting in, again, an underestimate. In case of extreme events, which can be quite localized and may last only a few minutes (Ward & Robinson, 1990; Blijenberg, 1998), the raingauge network may not register it adequately. Monitoring such extreme events, known to trigger debris flows, may provide actual triggering intensities. Thus, it may be desirable in future research to monitor rainfall using a very dense raingauge network. Because this may be very impractical, a weather radar may be employed (Andrieu *et al*, 1997). When such a radar would be installed at Pra-Loup, it will have a wide angle view of the entire Riou Bourdoux catchment. The data gathered by this radar may be used in a early-warning system for debris flows (section 6.2).

The discharge-river stage correlation failed although the section that was chosen was ideal (chapter 3). This was mostly due to the loss of the stage measurement rod, and the installation of a new one. Other problems that may arise with this method are predominately controlled by channel-bed morphology and instability during the period of research (Shaw, 1994). Since there was an absence of large changes in discharges due to the precipitation pattern during the research (section 4.2.1), this factor has had little influence.

Since the depth of flow was very small and the channel was not constrained between high banks, an increase in discharge may well have led to an increasing width of flow, and not primarily an increase in height. The measurement rod can therefore best have been placed in a deeper and more v-shaped part of the stream channel. However, no such section along the entire middle reach was found. The discharge measurements themselves are regarded as reliable.

The measurement of the infiltration characteristics on slopes is subject to many difficulties. First of all, most infiltration-equations are only valid for infiltration through a plane horizontal surface (Kutilek & Nielson, 1994). Since some of the sites had steep slopes, lateral spread of water from the auger holes may have resulted in an overestimate of  $K_{sat}$ .

values. The overestimate caused by such lateral conductivities may be as much as 50% (Malik *et al*, 1994). Blijenberg (1998) also showed this overestimation of  $K_{\text{sat}}$  by comparing infiltration envelope calculations with calculations from rainfall infiltration simulations. The difference was circa 25%.

$K_{\text{sat}}$  values are also known to vary widely on slopes. Factors influencing this variability within the Riou Bourdoux catchment include surface cracks, macro pores (increasing  $K_{\text{sat}}$ ), and surface sealing and air entrapment during infiltration (decreasing  $K_{\text{sat}}$ ). Surface cracks were especially observed on and near mass movements, where they showed to increase  $K_{\text{sat}}$  considerably (site 2 and 4, section 4.2.2). On the other hand, the slaking of aggregates due to impact of raindrops or the washing in of fine particles by overland flow, can cause the slope-surface to seal rapidly. This seal can be very thin (less than 1 mm), but can reduce the  $K_{\text{sat}}$  of the surface by as much as 3 orders-of-magnitude (Kutilek & Nielson, 1994). Since the inverse-augerhole (IAH) method involves drilling through the topsoil, this factor is not taken into account, although the influence of cracks remains.

The drilling of the slope surface also influences the infiltration capacity in another way. Blijenberg (1998), using a rainfall infiltration simulation, observed that the saturated zone never extended more than a few centimetres into the regolith, rendering the measurements of the IAH-method (at 30 cm depth) inappropriate. Moreover, at a depth it was sometimes found that the texture of the soil changed, and thus the infiltration characteristics.

Other factors controlling infiltration are slope angle and vegetation. These factors were also seen to vary (sometimes considerably) at the investigated sites.

All of the above-mentioned factors illustrate the complex nature of infiltration into a sloped surface. This may explain the wide range in  $K_{\text{sat}}$  values observed at every measurement site (appendix G3).

The sorptivity, evaluated from the early stage of infiltration, depends on initial water content of the soil. Therefore it should be measured a few days after a rainfall event (Kutilek & Nielson, 1994). Since this criterion was met, the sorptivity is considered a reliable value.

Considering the errors produced in the rainfall and infiltration capacity measurements, the following can be stated on the time-to-ponding calculations (table 4.4). From the factors influencing infiltration capacity determined with the IAH-method, one may conclude that the observed values are overestimates, and are likely to be (much) less. The rainfall amounts and intensities recorded in the research period, however, are underestimates. The influence of wind turbulence has also not been considered by Blijenberg (1998), making the data from the Bachelard valley also minimum values of actual rainfall intensities. Therefore, the time-to-ponding, calculated in section 4.2.2, must be considered as a maximum value. Actual time-to-ponding is likely to be less. This corresponds to the field observations at the investigated plots, where signs of (extensive) overland flow were present (except on moraines). Such signs can only develop if overland flow occurs regularly.

A better technique for measuring the infiltration capacity can make a more accurate determination of overland flow. A preferred method for this is the rainfall infiltration simulation, since it measures the actual infiltration *at the soil surface*. In order to accurately assess the infiltration capacity of a slope, more than one plot should be examined, making comparison between plots of a single landscape unit possible.

### 6.2 Rainfall-runoff relationship<sup>11</sup>

Most processes in the subcatchment are driven by rainfall. It is expected that a relation exists between rainfall and discharge. Usually the discharge increases with rainfall after a time lag. This lag depends on catchment characteristics, like lithology (water storage), vegetation (interception and overland flow) and drainage network. To determine the relation between these two variables, they are compared in figure 6.1.

As can be seen, peaks in the rainfall data seem to coincide with higher discharge measurements. However, no information about the timelag between peaks in rainfall and discharge can be extracted, since no time-series of discharge data could be created.

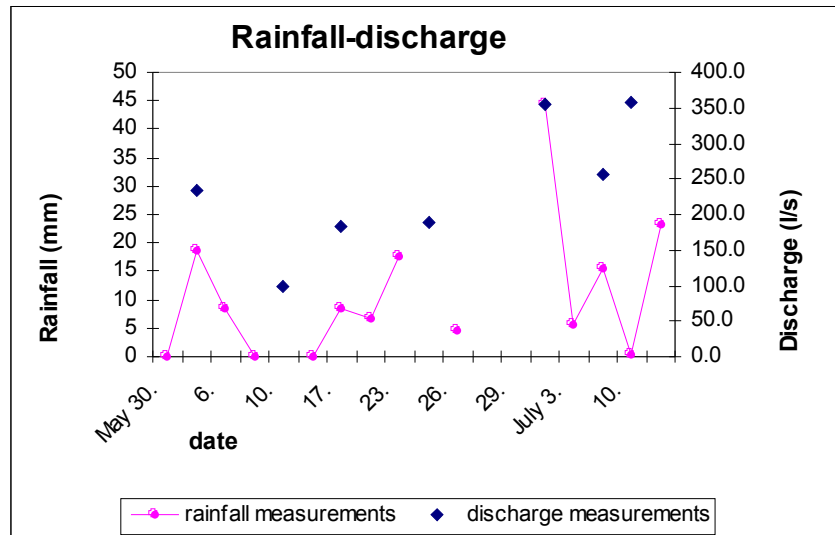


Figure 6.1 Graph showing the discharge and rainfall (tipping bucket: appendix C1) data against time.

It was observed during the research that after rainfall events the water in the main channel of the Riou Bourdoux turned very grey, indicating a large discharge of suspended load. This increased suspended load may be related to an increase in discharge (due to rainfall) resulting in fluvial erosion (of the channel bed). Or it may be directly related to rainfall, in which case it is probably derived from overland flow on badlands. A combination of both processes is also possible. From figure 6.2 it can be

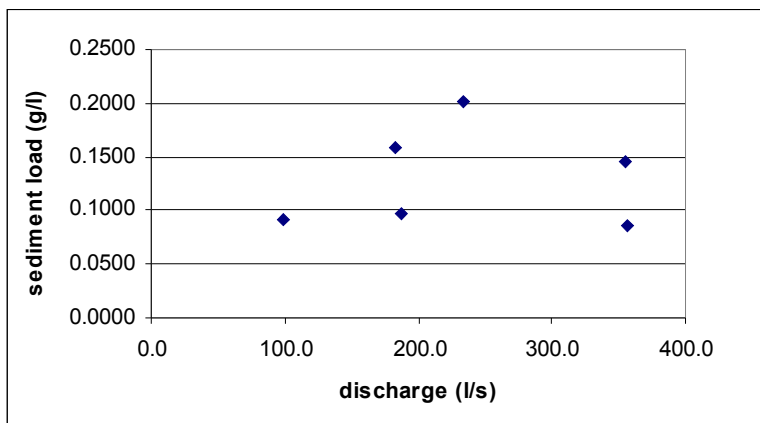


Figure 6.2 Graph showing the sediment load versus discharge (appendix D4).

concluded that no definite relation exists between suspended load and discharge. The absence of this relation may be explained. In the Riou Bourdoux system most channels are filled with coarse sediment. Only a small part consists of the fine sediment (< 2µm) as found in the suspended load samples. During higher discharges, bedload transport may increase, although this would not largely affect the suspended (wash) load in the channels. Moreover, the coarse sediment may act as surface layer, protecting the

<sup>11</sup> Partly taken from De Jooode (2000).

finer material (in between the gravels) from fluvial erosion. Another problem is that the observed high discharges within the period of research were probably too low (due to the absence of large rain storms) for the competence of the stream flow to increase significantly, and cause considerable fluvial erosion.

It is more likely (in the observed field situation) that during and directly after a rain-event (fine) sediment will be eroded from the badlands by wash processes and is immediately discharged by the river when entering the streams. Since turbulent conditions exist in most channels, the fine sediment will not be deposited at the channel bottom.

Table 6.1 checks this assumed rainfall-suspended load relation. The suspended load amounts are compared to the relative amount of rainfall (appendix C2) that has fallen in the 24 hours preceding the suspended load measurements. The sediment load after a 24-hour period of no precipitation is considered a *basic* sediment load.

date	Rainfall category*	Sediment load (ppm)
<b>2-6-97</b>	1	202
<b>10-6-97</b>	0	92
<b>17-6-97</b>	1	159
<b>24-6-97</b>	0	97
<b>27-6-97</b>	2	637
<b>29-6-97</b>	3	2941
<b>30-6-97</b>	1	145
<b>10-7-97</b>	0	85

Table 6.1 Measured amount of sediment load compared to the relative amount of rainfall fallen in the preceding 24h. \* *Rainfall category: 0= no precipitation, 1= some precipitation, 2= rainfall with total volume exceeding 10.2 mm (one tipping), 3= rainfall with total volume exceeding 20.4 mm (two tipplings).*

After a rainfall event with a total volume of 22.4 mm (two tipplings of the pluviograph, the largest rainfall event measured during the fieldwork period) the sediment load was very high. (Rainfall category 3, table 6.1). The results in table 6.1 show that a relation between antecedent rainfall and sediment load can be found (in order-of-magnitude). So, the volume of sediment load is strongly related to rainfall and thus overland flow wash erosion.

## 6.2 GIS-model discussion

Analysis of the different resulting maps shows that most debris flows (in the model) are initiated near the *threshold* (as defined in section 4.1.2). This is due to the fact that in the model much debris from the upper flysch slopes is available in these locations (in the model). However, in the field situation, not many triggering sites were found at this location (in the Riou de la Pare catchment). Since the modelled triggering process is partly based on the amount of debris present, this result is not surprising. Further analysis showed that only debris flows, triggered in the lower section of the catchment (Terres Noires), can reach the outflow point, which corresponds to the observed field situation. The routing model can thus be regarded as a successful simulation of actual debris-flow routing, although it does not predict behaviour of the laves torrentielles which can reach the Ubaye.

A major drawback of the model is the way in which a dynamic model is calculated in PCRaster. Each separate process has to be modelled one after another. In the present approach it was decided to calculate debris production first, then delivering all material to the channels, and finally determine whether debris flows are triggered or not. The actual field situation is more complex, with each debris-producing process working on different time-scales, sometimes episodic, and the possibility of debris-flow triggering during each rainstorm. Such complex interactions (both spatial and temporal) are impossible to model with PCRaster.

Debris-flow triggering in the model is now largely based on the amount of debris present in the gullies and the slope-angle. Actual debris-flow triggering in the area will produce many small-scale, and only occasionally medium-scale debris flows. The trigger should be more realistic towards this triggering behaviour. The trigger should also be realistic towards the return period of (medium-scale) debris flows (pers. com. Blijenberg, 1999).

When modelling a sediment budget over 100 years, several other drawbacks occur. At such a time-scale, the use of rain-event data in triggering debris flows is unfeasible. Still, every modelled situation only describes summer process-activity. One option is to use precipitation characteristics from a longer period (i.e. 30 years). Such characteristics may show wetter and drier years, which may be modelled as an influence on process activity. However, this means that a debris flow trigger will become more stochastic than parametric (Riezebos & de Roo, 1996).

This problem is also reflected upon the transport of material. In the case of event-based modelling, a direct link to rainfall amounts and intensities can make the transport of material more accurately defined. This link becomes increasingly obscure with the size of a catchment and the period of modelling (Riezebos & de Roo, 1996). Therefore, it is best to model event-based processes on small plots. For larger catchments, like the one used, debris production may be calculated in the form of fixed values for amount and frequency of sediment delivery to channels.

Both situations of debris production were not used in the present model. If the present model is combined with that of Spee & Visser (1999), it may result in a more realistic description of the sediment budget. Combining the models, however, may prove difficult since both models are quite elaborate. A combination may result in a very large model, containing many variables. This will reduce the clarity and simplicity of the model, which are always a prerequisite.

The above-described limitations of the model, lead to the following conclusions. For modelling the present study area (or other subcatchments of similar size) at the defined time-scale, the model should become more stochastic. Debris production and debris-flow triggering should be based on process-intensity (amount) and frequency. Such a stochastic model, combined with the present routing model, may result in a sediment budget model for any subcatchment within the area.

The parametric approach should be used on smaller spatial and temporal scales. A model may be developed to predict the behaviour of individual slopes or trigger sites. A monitoring program may provide parametric values, and modelling can be based on

individual rain events. Such a model may be incorporated in an early-warning system. Detailed rainfall measurements, the infiltration capacity, and slope angles are needed for such a model. Electronic rain gauges can be installed at these sites, combined with a small transmitting device or a weather radar may be used. The data could be combined in a real-time GIS model, predicting time-to-ponding and the amount of overland flow during rainstorms. If extensive overland-flow occurs on such crucial slopes (indicating possible debris flow triggering; Blijenberg, 1998), public warning may be issued.

### 6.3 Long-term catchment development

In general the relative importance of the different processes has been determined. Also some quantitative contributions have been calculated. These values give an indication about the order-of-magnitude of the amounts of sediment transported by the processes under the given conditions. These data may be used in future research in neighbouring catchments to provide the necessary additional data for a complete sediment budget. A discussion of the sediment budget is given in De Joode (2000).

In this section two important factors controlling the activity (both spatial and temporal) of the upper region of the Riou Bourdoux system, will be discussed.

When comparing the Riou Guérin, Riou de la Pare and the Riou Chamous catchments a distinct spatial pattern is discernable (for maps: see appendix B, and Spee & Visser, 1999). The Riou Guérin is heavily forested, has no large contributing areas for overland flow (only in the lower section), and is predominately influenced by mass wasting processes. The Riou Guérin itself is not very deeply incised. Evidence showed that not many debris flows are triggered in this subcatchment.

The Riou de la Pare catchment is also densely vegetated, although less than the Riou Guérin. It has more areas contributing to overland flow (even higher up in the catchment), and is influenced by mass wasting and wash processes. The several streams draining this subcatchment are moderately incised; at several locations very deeply. The more eastern streams are however more incised than the western ones. A few medium-scale debris flow deposits are present here, although none have come out of the catchment (section 4.3.1).

The Riou Chamous catchment is dissected by one stream only, the Riou Chamous. It has incised very deeply. Many of the slopes in this catchment are largely unvegetated, are prone to extensive overland flow, and are also susceptible to a wide range of mass wasting processes. The august-1996-event was triggered in this catchment (section 4.3.1), and many other debris flow deposits can be found on its slopes.

So in short: the entire upper region of the Riou Bourdoux system has slopes facing from southeast to southwest (figure 6.3). The south to southeast facing flank is more vegetated, more prone to mass wasting, and has shallow stream incision. The south to southwest facing flank is increasingly unvegetated, less prone to mass wasting (although increasing slope steepness promotes this process again), has deep stream incision (and

hence very steep and long stream-side slopes), and process-activity is largely dominated by overland flow (badlands), combined with debris flows and mud-flows.

Such a spatial pattern between slope-aspect and geomorphological processes was also found by Faulkner (1994). His study showed that process-activity in a (hypothetical) south-exposed semi-arid drainage basin is controlled by insolation-differences (figure 6.4).

The locations receiving the highest degree of solar radiation (south-west exposed) are usually driest, resulting in a decline of vegetation. Moreover, this high insolation also causes strong local convective rise of air masses, resulting in rainstorms, which will be most intense

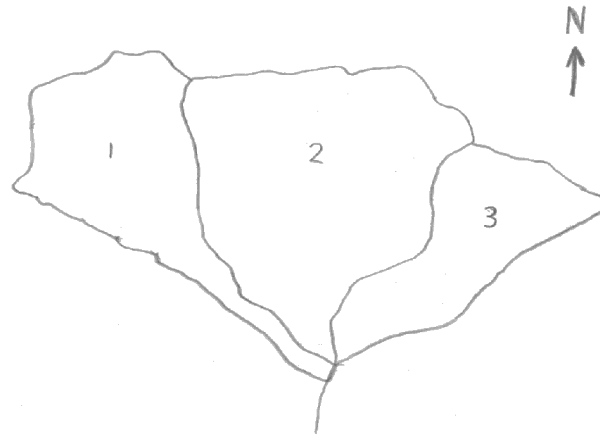


Figure 6.3 Orientation of the three subcatchments (appendix A1). 1= Riou Guérin, 2= Riou de la Pare, 3= Riou Chamous.

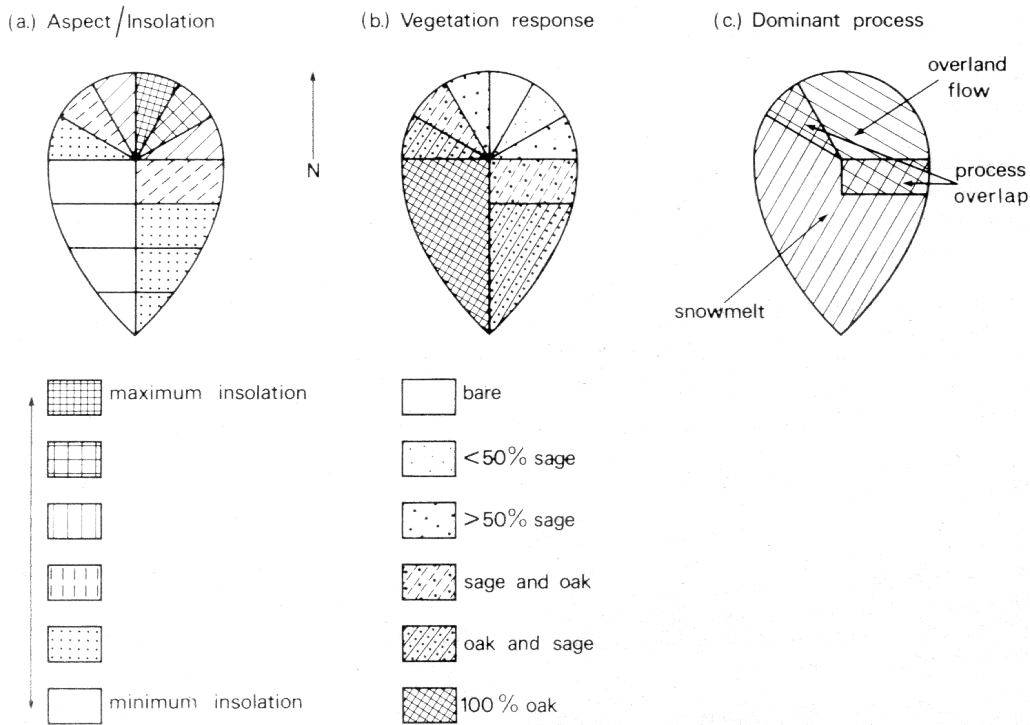


Figure 6.4 Insolation-controlled process response of a hypothetical south-exposed (semi-arid) drainage basin (Faulkner, 1994).

on exactly those locations. These are thus sites where overland flow is the dominant process. On the more south-west exposed slopes, decreasing insolation causes increasing soil moisture content, resulting in a more dense vegetation cover. Overland flow will be less dominant here. In spring, snow will remain longer at these locations (due to less rapid melting), producing a constant delivery of water to the slopes, which is a favourable factor for mass-wasting.

When analysing the spatial process pattern in the Riou Bourdoux, it is clear that this pattern follows closely the one suggested by Faulkner (1994). This is remarkable since the Riou Bourdoux system has a very complex geological (and hence lithological) composition and geomorphological development (chapter 1). Based on this evidence, future process patterns in the system will most probably continue to follow this spatial distribution.

Since it was shown that in the investigated subcatchments debris flows are predominantly triggered on slopes prone to extensive overland flow (section 3.3.1; Spee & Visser, 1999), one would suspect that the subcatchment posing the largest risk of producing debris flows is the Riou Chamous catchment. This is, however, not only due to the presence of the many badlands in the catchment.

In this report, only a few sediment sinks or readily transportable colluvium were found (section 4.3.1). Spee & Visser (1999) also found just a few of such sinks. The most important area within the catchments where there is an abundant supply of coarse debris for debris flows are the upper flysch slopes. Most debris flows, initiated on these slopes, cannot travel over the morainic threshold (section 4.1.2). In the Riou Chamous catchment, this threshold is not present (anymore). Debris flows initiated on these slopes, can travel easily to the Riou Chamous.



Figure 6.5 Outflow-point of the Riou Chamous at the confluence point. In the lower left and right of the photograph large debris flow deposits can be seen (deposit 4, appendix H).

This channel (as was seen earlier) is a steep, v-shaped, relatively straight channel to which all slopes within its catchment are connected. The channel itself has practically no sediment stored outside its channel-bed. Debris flows, reaching the headwater gullies of this channel, can thus travel far through the catchment, growing in size, and they may even reach to the outflow point (figure 6.5). This process is not likely to happen in the Riou de la Pare catchment, because many of its streams are not straight, many tributary points are present (making debris flow propagation difficult), and the threshold is still intact.

The debris flows from the Riou Chamous, which reach the outflow point, will not travel further. This is because the uppermost sediment-retaining dam has created a large plain here, with a low gradient ( $5^\circ$ ). Debris flows will be easily deposited due to the possibility of lateral spreading, resulting in a loss of competence. Moreover, the gradient will be too low for the debris flows to continue. However, the mobility of the triggered debris flows in this catchment can increase considerably due to the presence of large streamside badlands in the Terres Noires. During debris-flow triggering rain events, a lot of hyper-concentrated flow

may reach the central channel of these badlands (Antoine *et al*, 1995). When a debris flow passes these badlands, it may grow in size and fluidity, becoming a very mobile lave torrentielle capable of reaching the Ubaye. This process may continue further in the Main Channel, where there are also many large streamside badlands in the Terres Noires.

Another option is the possibility that debris flows, which reach the outflow point (i.e: confluence point appendix H), will temporarily come to a halt here. The Pra Bellon landslide (see sketch, appendix H) has made a very narrow passage in the Main Channel just downstream of the large plain. The debris of a debris flow may be retained here, in combination with much floodwater (mostly from the Riou de la Pare catchment due to its large surface area). When this mixture of water and debris has built up enough pressure, it may break through the narrow passage. However, because the plain is fairly large (some 40 by 200 meters) and has a low gradient, the debris in the mixture will easily settle on the floor of the plain. Another problem is that the rainfall-runoff response of Riou de la Pare catchment may be much lower than the debris-flow triggering response of the Riou Chamous catchment (for a debris-flow triggering rain storm). This is due to the presence of large sections of moraine covered by dense forests in the Riou de la Pare catchment (appendix B3), retarding the runoff response. This option is therefore not very likely, although the Riou de la Pare catchment can still contribute some water to a passing debris flow from the Riou Chamous catchment.

It can thus be concluded that the subcatchment of the Riou Chamous is the only catchment capable of producing large events, like the lave torrentielle of August 1996.

The other important factor greatly influencing the activity of the investigated subcatchments is their confluence point (see sketch, appendix H). The Riou de la Pare and the Riou Guérin catchments are largely stable now, in a sense that they do not pose a great risk to major mass wasting processes or debris-flow development. This situation, however, is not likely to remain.

The so-called confluence point is very sensitive to erosion. Many fresh landslides, active badlands and debris flow deposits are found here (appendix B5 and Spee & Visser, 1999). This activity may have several causes.

At the base of the catchments large sections of Terres Noires are exposed. The channels at these locations have their bed situated in the Terres Noires, resulting in rapid fluvial incision. The slopes at these locations are therefore very steep (appendix B4) and are continuously undercut resulting in streamside mass wasting (appendix B5). Moreover, the combined fluvial action of the three contributing channels also causes rapid erosion at the confluence point.

The area may become (more) unstable in the future due to the presence of the old landslide in the Riou de la Pare catchment (section 4.1.3). Because much of the surface material within this catchment has already failed, its residual strength is considerably less. If this old landslide will be eroded at its base (due to headward travelling erosion on the Terres Noires slopes), it may be reactivated. Since repeated erosion at its base is likely, it may develop into a progressive failure (Selby, 1993), greatly increasing the instability of the area.

Unfortunately, no dams can be built on a Terres Noires slope to reduce erosion, since these are simply washed away during rainstorms (pers. com. RTM, 1997). This is why the

Riou Chamous can hold no dams. In the other two catchments many dams are now being built upstream of the Terres Noires slopes in order to promote stabilisation and retain possible debris flows (pers. com. RTM, 2001). However, since erosion is travelling upward from the Terres Noires slopes, these dams will be undermined, and subsequently collapse.

Another factor promoting rapid incision by the streams in the Terres Noires slopes, is the presence of the sediment retaining dams in the Main Channel. As stated earlier, the uppermost dam has caused a large plain of debris flow deposits to develop around the confluence point. The slope angles of the streams in the Terres Noires drop sharply at the transition with this plain. In the *natural* state, this transition would be far more gradual. This plain can thus be seen as a (raised) local erosion base level. This situation promotes the development of gullies (gully type 3, section 2.2.1). In order to establish a new steady-state profile, a gully will cut backward within the existing channel. This process is depicted in figure 6.6.

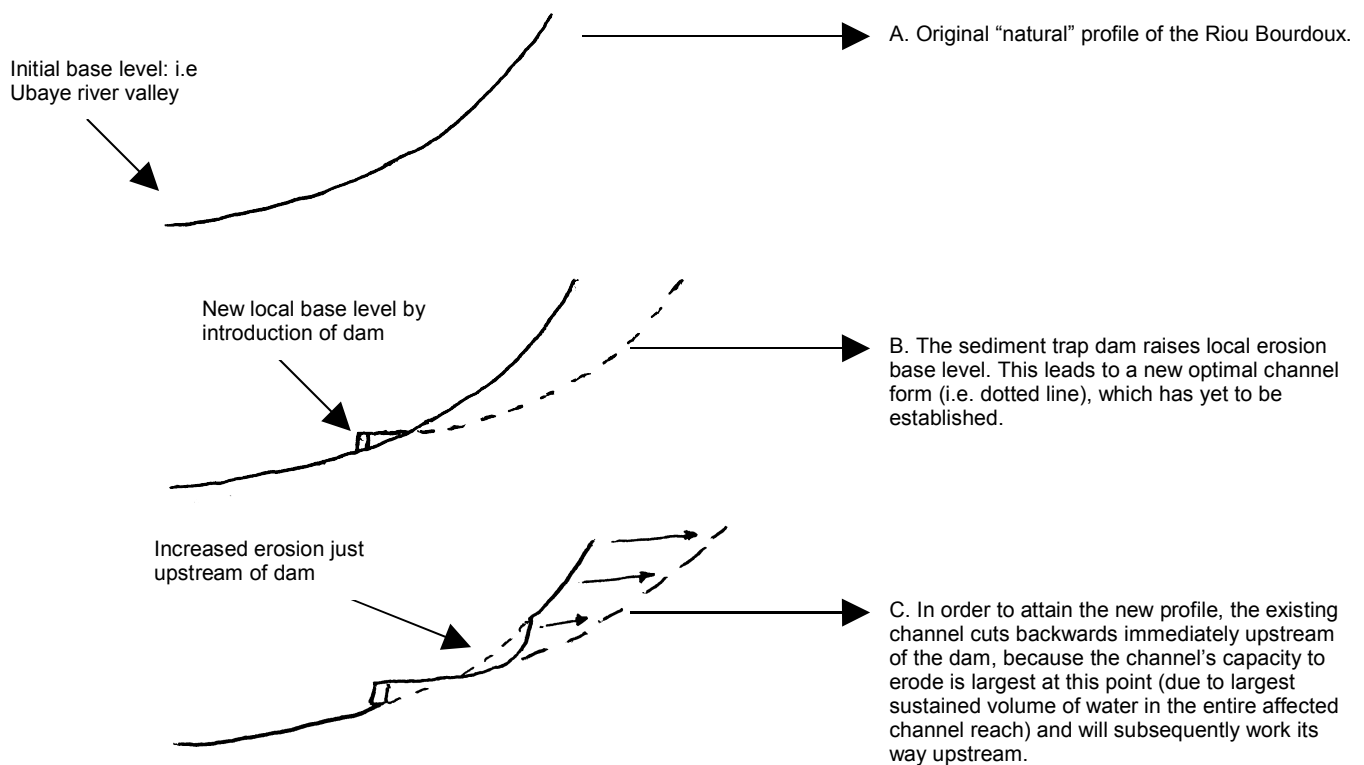


Figure 6.6 Schematic longitudinal profile of in-channel gullying at the confluence point.  
(Note: both horizontal and vertical scales are greatly exaggerated)

So, the building of the dams in the Main Channel to reduce the risk of a lave torrentielle reaching the Ubaye, has given rise to an increase in instability of the Riou Guérin and the Riou de la Pare catchments. The increasing instability, however, is not likely to promote the development of (Ubaye reaching) laves torrentielles from the Riou Guérin and Riou de la Pare catchments in the near future. Most of the Terres Noires slopes at the confluence point have insufficient access to coarse debris to create medium-scale debris flows (, because (moraine) deposits on the top of these slopes are very thin here). The debris flows that are triggered from these slopes usually turn into hyper-concentrated flows after a short travel-distance, due to the rapid disintegration of Terres Noires during movement

(Antoine *et al*, 1995). However, when the gullies have cut back to the location of observation point 61 (appendix A2), a lot of sediment will be available, although this may take many years to occur.

A final note on the Main Channel is now given. The low gradient and large width caused by the dams have reduced the fluvial and debris-flow activity to a minimum. Practically all debris flows come to a halt when reaching this channel. Due to its present characteristics practically no stored bed-material will be transported either by fluvial or debris-flow (scraping) action. So, debris flows in the Riou Bourdoux must have a large enough size and fluidity by the time they reach the Main Channel in order to reach the Ubaye. Without these dams, the Main Channel has probably been a very efficient debris flow transport zone. The channel was v-shaped, confined by steep Terres Noires slopes, offering little to no room for channel storage. The large alluvial fan along the Ubaye is proof of this activity in the past (chapter 1). The repair works of the RTM have successfully shifted the aggradation of the alluvial fan to within the confines of the Riou Bourdoux catchment. This storage, however, cannot be maintained indefinitely, which may pose a serious problem in the future. No prospect of an alternative long-term risk prevention plan can be given based on this study.

## 7 Conclusions

The final conclusions of the report are now given. First, the questions concerning the spatial and temporal distribution of hillslope and channel processes in the Riou de la Pare subcatchment, raised in section 1.2, will be addressed. Next, the conclusions on the activity of the three studied subcatchments (the Riou Guérin, Riou de la Pare and Riou Chamous) including the main channel of the Riou Bourdoux are presented. Finally, a conclusion about the use of sediment budget analysis in the study area is given.

On the hillslopes of the Riou de la Pare catchment, several active processes were found. The most important in delivering sediment to channels are rill, interrill and gully erosion (badlands), small-scale debris flows and landslides. These processes are active on the streamside slopes along the incised streams within the catchment. Typical volumes of debris created by these processes are  $10^1$ - $10^2$  m<sup>3</sup>. Few storage sites of readily transportable material (under present conditions) were found on the hillslopes; most of the material that could be triggered into debris flows was found on the upper slopes. The presence of the morainic threshold largely stops these flows from traveling far through the catchment.

Typical debris flow source zones in the Riou Bourdoux system consist of steep slopes (> 30°), with the presence of mixed slope-material (both coarse and fine). All of these zones are very sparsely vegetated (sometimes totally unvegetated). Debris flows in these zones are primarily triggered during low-frequency high-intensity rainstorms, when extensive overland flow occurs (section 4.2.2), which concurs with the model presented by Blijenberg (1998).

Generally, many channels in the subcatchment (especially 2<sup>nd</sup> order) are aggrading and have large quantities of colluvium stored (section 4.3.1). The amount of colluvium in the channels could not be estimated. The aggradation is the result of the low (medium-scale) debris-flow activity in recent years. Some indirect evidence of fluvial transport was found in 2<sup>nd</sup> order channels, which has become important in absence of these debris flows. Only two distinct medium-scale debris flow tracks were identified. The typical volumes of these debris flows are  $10^3$ - $10^4$  m<sup>3</sup>. These debris flows increase more than ten-fold in size by scraping sediment from the 1<sup>st</sup> and 2<sup>nd</sup> order channels in the subcatchment.

The few deposits of debris flows found in all investigated subcatchments show that they come to a halt at tributary junctions, where the angle between the contributing and receiving channel is greater than 45° ( $\beta$ ), or when the channel gradient drops below 10° ( $\theta$ ). The model of Benda & Cundy (1990) could thus be adapted for the Riou Bourdoux system, although future research may provide a more accurate model assessment. Only debris flows initiated on the Terres Noires slopes in the lower region of the subcatchment (Riou de la Pare) are able to reach the confluence point (i.e. the tributary point of the three investigated subcatchments). The presence of a large floodplain (caused by a large dam built a few hundred meters downstream of the confluence point), combined with a sudden decrease in slope gradient, results in the deposition of all debris flows coming out of the subcatchment. The depositional influence of the floodplain on debris flows is partly indicated by the lack of

deposits located beyond this point. The subcatchment appears unable to produce large Ubaye-reaching laves torrentielles.

The main channel of the Riou Bourdoux showed no fluvial bed load transport during the period of investigation. Suspended load measurements indicated that rain events produce much wash from badlands, but that the resulting increase in discharge does not promote an increase in bed load. Extensive repair and maintenance work by the RTM (dams and bulldozer-action) have reduced fluvial transport to a minimum, although occasionally laves torrentielles are still able to traverse this section, and reach the Ubaye. Still, general sedimentation has been successfully shifted from the alluvial fan to within the confines of the Riou Bourdoux catchment. A rough estimate of storage-change behind the dam-reservoirs shows a recurrence interval for Ubaye-reaching laves torrentielles ( $6 \cdot 10^3 - 6 \cdot 10^4 \text{ m}^3$ ) of 2-10 years. Comparison between the three investigated subcatchments show that only the Riou Chamous catchment is capable of producing such drastic events. Information on the size and mobility of these events, gathered along the main channel of the Riou Bourdoux, also shows that they will not be able to block the Ubaye.

General evidence shows that contrary to the Riou Chamous, the Riou Guérin and the Riou de la Pare subcatchments are now relatively stabilized. Increased fluvial erosion of the Terres Noires slopes in the lower sections of these catchments will, however, cause increasing instability, with a possible development of a large progressive failure. Still, this will not greatly increase the risk of medium-scale debris flows from these catchments in the near future.

Sediment budget analysis proved very useful to quickly determine the relative importance of all processes acting in the subcatchments, and to indicate crucial areas for debris flow initiation. Only a partial sediment budget could be constructed due to the fact that some processes could not be quantified (size or frequency), although the order-of-magnitude of debris flows was estimated. A more extensive monitoring plan may well yield all data required for a complete budget.

The partial sediment budget has been used to create a GIS (routing) model, which accurately simulates debris-flow propagation through the drainage network of the Riou de la Pare subcatchment. The adapted model of Benda & Cundy (1990) could successfully be converted into GIS-algorithms. A large disadvantage of the model is the fact that a realistic debris-flow trigger could not be modelled.

Due to the complexity of the subcatchments, a total sediment budget (both sediment production and routing) cannot be converted into a GIS model. At the scale of these catchments a stochastic approach is recommended, combined with the routing model of Benda & Cundy (1990). A solely parametric approach should only be applied to individual debris flow source areas.

## References

- ANDRIEU, H., CREUTIN, J.D., DELRIEU, G. & FAURE, D.**, 1997. Use of a weather radar for the hydrology of a mountainous area. Part I: radar measurement interpretation. *Journal of Hydrology*, 193, pp. 1-25.
- ANTOINE, P., GIRAUD, A., MEUNIER, M., VAN ASCH, T.**, 1995. Geological and geotechnical properties of the "Terres Noires" in southeastern France: Weathering, erosion, solid transport and instability. *Engineering Geology*, 40, pp. 223-234.
- AVOCAT, C.**, 1970. Premiers résultats du recensement de 1968 en Ubaye. *Revue de Géographie Alpine* 58, pp. 435-451.
- BALLANDRAS, S.**, 1996. Contribution à l'étude de la torrentialité alpine. These de Doct. Geog., Univ. Savoie, en cours de rédaction.
- BENDA, L.**, 1990. The influence of debris flows on channels and valley floors in the Oregon Coast range, USA; *Earth surface processes and landforms*, Vol. 15, pp. 457-466.
- BENDA, L. E. & CUNDY, T. W.**, 1990. Predicting deposition of debris flows in mountain channels; *Canadian Geotechnical Journal*, Vol. 27, pp. 409-417.
- BENDA, L. & DUNNE, T.**, 1987. Sediment routing by debris flow; *Erosion and Sedimentation in the Pacific Rim* (Proceedings of the Corvallis Symposium, August, 1987), IAHS Publ. no. 165, pp. 213-223.
- BENISCHKE, R. & HARUM, T.**, 1990. Determination of discharge rates in turbulent streams by salt tracer dilution applying a microcomputer system. Comparison with current meter measurements. *Hydrology in mountainous regions I. Hydrological Measurements; the Water Cycle*. IAHS Publ. No. 193. pp. 215 – 221.
- BLIJENBERG, H.**, 1998. Rolling Stones? Triggering and Frequency of Hillslope Debris Flows in the Bachelard Valley, Southern French Alps. Faculteit Ruimtelijke Wetenschappen, Universiteit Utrecht.
- BOELHOUWERS, J.**, 1996. Geomorphology 321. Department of Earth Sciences, University of the Western Cape.
- BUNZA, G. & KARL, J.**, 1975. Erläuterungen zur hydrograpisch-morphologischen Karte der Bayerischen Alpen 1:25.000. Bayer. Landesamt Wasserwirtsch. S.-H.: 68 pp.
- BURROUGH, P.A.**, 1986. Principles of Geographical Information Systems for Land Resources Assessment. *Oxford University Press*. 194 pp.
- BRAAM, R.R., WEISS, E.E.J & BURROUGH, P.A.**, 1987. Spatial and temporal analysis of mass movement using dendrochronology; *Catena* 14, pp. 573-584.
- CAINE, N.**, 1980. The rainfall intensity-duration control of shallow landslides and debris flows; *Geografiska Annaler* 62A, pp. 23-27.
- CHAPMAN McGREW, J. & MONROE, C.**, 1993. An introduction to statistical problem solving in Geography, Wm. C. Brown, 305 pp.
- COOKE, R.U. & DOORNKAMP, J.C.**, 1990. Monitoring Geomorphological Change (Ch3) & Drainage Basins and Sediment Transfer (Ch7). In: *Geomorphology in Environmental Management*, second edition, Clarendon Press, Oxford, pp. 64-78, 179-200.
- COOLS, H. & DEN HOED, J.**, 1984. Legenda's voor karteringen in het bekken van Barcelonnette, veldwerk Alpes du Sud. Vakgroep Fysische Geografie, Rijksuniversiteit Utrecht, 58 pp.
- COUSSOT, P. & MEUNIER, M.**, 1996. Recognition, classification and mechanical description of debris flows. *Earth-Science Reviews*, 40, pp. 209-227.
- COSTA, J.E.**, 1984. Physical geomorphology of debris flows. In: J.E. Costa & P.J. Fleisher (Eds.): *Developments and Applications of Geomorphology*, Springer Verlag: Berlin/Heidelberg, pp. 268-317.
- DEBELMAS, J.**, 1970. Alpes Savoie et Dauphiné, *Guides géologiques régionaux*, Paris, Masson & Cie, pp. 193-204.

- DEBELMAS, J.**, 1974. *Geologie de la France*, Paris, Masson & Cie, 540 pp.
- DESCROIX, L.**, 1985. Contribution à l'étude de la dynamique érosive dans les Baronnies Orientales et les Pays du Buech Moyen; problemes d'aménagement. These de Illeme Cycle, Université de Lyon-II, 260 pp.
- DE VILLIERS, G DU T.**, 1990. Rainfall variations in mountainous regions. *Hydrology in mountainous regions I. Hydrological Measurements; the Water Cycle*. IAHS Publ. No. 193. pp.33-41.
- DIETRICH, W.E. & DUNNE, T.**, 1978. Sediment budget for a small catchment in mountainous terrain; *Zeitschrift für Geomorphologie Neue Folge Supplementband 29*, pp. 191-206.
- DIETRICH, W.E., KIRCHNER, J.W., IKEDA, H. & ISEYA, F.**, 1989. Sediment supply and the development of the coarse surface layer in gravel-bedded rivers. *Nature* 340 (6230) pp. 215-217.
- DOUGEDROIT, A.**, 1976. Les paysages Forestiers de Haute-Provence et des Alpes-Maritimes, Edisud, Aix-en-Provence, 550 pp.
- ELDER, K. & KATTELMAN, R.**, 1990. Refinements in dilution gauging for mountain streams. *Hydrology in mountainous regions I. Hydrological Measurements; the Water Cycle*. IAHS Publ. No. 193. pp. 247-254.
- ELLENBERG, H.**, 1986. *Vegetation Mitteleuropas mit den Alpen in ökologischer Sicht*. Ulmer, Stuttgart, 989 p.
- FAULKNER, H.**, 1994. Spatial and temporal variation of sediment processes in the alpine semi-arid basin of Alkali Creek, Colorado, USA. *Geomorphology*, 9, pp. 203-222.
- FAULKNER, H.**, 1995. Gully Erosion associated with the expansion of untterraced almond cultivation in the coastal Sierra de Lujar, S. Spain. *Land degradation and rehabilitation*, Vol. 6, pp. 179 – 200.
- GEES, A.**, 1990. Flow measurement under difficult conditions : field experience with the salt dilution method. *Hydrology in mountainous regions I. Hydrological Measurements; the Water Cycle*. IAHS Publ. No. 193. pp. 255 – 262.
- GEORGIEV, B.V.**, 1990. Reliability of bed load measurements in mountain rivers. *Hydrology in mountainous regions I. Hydrological Measurements; the Water Cycle*. IAHS Publ. No. 193. pp. 263-270.
- HENDERSON-SELLERS, A. & ROBINSON, P.J.**, 1994. *Contemporary Climatology*. Pub: Longman Scientific & Technical. 439 pp.
- HINGSTON, E.D.C. & JERMY, C.A.**, 1998. Shear testing and analysis of the standard joint roughness profiles. 8th International IAEG Congress. Balkema, Rotterdam.
- HUVIUS, N.**, 1990. Ontstaan van puinstromen. Een onderzoek naar de aard van ontstaansgebieden van puinstromen en naar de manier waarop puinstromen ontstaan, in het zuidelijk deel van de Franse Alpen. Unpublished report, Utrecht University, Department of Physical Geography.
- HUTCHINSON, J.N.**, 1988. General report: Morphological and geotechnical parameters of landslides in relation to geology and hydrogeology; *Proceedings of the 5th International Symposium on Landslides (Lausanne)1*, (Rotterdam: Balkema), pp. 3-35.
- I.G.N.**, 1982/1983. Carte topographique 1:10.000, feuilles 3539 O: Barcelonnette/Pra-Loup. Inst. Géogr. Nat., Paris.
- INNES, J.L.**, 1983. Debris flows; *Progress in Physical Geography* 7, pp. 469-501.
- JAHN, A.**, 1989. The soil creep of slopes in different altitudinal and ecological zones of Sudeten Mountains. *Geografiska Annaler*, 71A, pp. 161-170.
- JOHNSON, A.M.**, 1970. Rheological properties of debris, ice and lave; Debris flow in channels. In: A.M. Johnson (Ed): *Physical Processes in Geology*. Freeman Cooper, San Francisco, pp. 495-514.
- JOHNSON, R.C., BLACKIE, J.R. & HUDSON, J.A.**, 1990. Methods of estimating precipitation inputs to the Balquhiddar experimental, Scotland. *Hydrology in mountainous regions I. Hydrological Measurements; the Water Cycle*. IAHS Publ. No. 193. pp. 7 – 14.

- JOODE, A. DE**, 2000. A Sediment Budget for a Subcatchment of the Riou Bourdoux, France. Unpublished report, *Utrecht University, Department of Physical Geography*.
- JORDA, M.**, 1983. La torrentialite holocene des Alpes Françaises du Sud: Facteurs anthropiques et parametres naturels de son evolution.; *Colloque sur le Postglaciaire Mediterranee*, Toulouse 5-6 sept., pp. 1-18.
- JORDA, M.**, 1987. Morphogénèse postglaciaire des régions intra-alpines Françaises du Sud. Le bassin de Barcelonnette (Ubaye) du tardiglaciaire au subboreal.; *Premières communautés paysannes en méditerranée occidentale*. Colloque International du C.N.R.S., Montpellier, (Paris, 1987), pp. 61-69.
- JORDA, M.**, 1988. Modalités paléoclimatiques et chronologiques de la deglaciation würmienne dans les Alpes Françaises du Sud. *Bulletin de l'association français pour l'étude du Quaternaire*, pp 111 – 122.
- JORDA, M. & ROSIQUE, T.**, 1994. Le tardiglaciaire des Alpes Françaises du Sud: Rythme et modalités des changements bio-morphoclimatiques. *Quaternaire*, 5, (3-4), pp. 141 – 149.
- KARSENBERG, D.**, 1998. PCRaster manual. Department of Physical Geography, Utrecht University, The Netherlands.
- KERCKHOVE, CL.**, 1969. La "zone du flysch" dans les nappes de l'Embrunais-Ubaye (alpes occidentales), *Geol. Alpine*, t. 45, pp. 5 – 204.
- KESSLER, J. & OOSTERBAAN, R.**, 1974. Determining hydraulic conductivity of soils. In: *Drainage Principles and Applications*. International Institute for Land Reclamation and Improvement (ILRI), Publ. 16, Vol III, Wageningen, pp. 253-296.
- KHOWSROWSHAHI, F.B.**, 1990. Sediment transport in mountain streams. *Hydrology in mountainous regions II. Artificial Reservoirs; Water and Slopes*. IAHS Publ. No. 194. pp. 59-66.
- KUTILEK, M. & NIELSON, D.R.**, 1994. Soil Hydrology. *GeoEcology textbook*. Cremlingen-Destedt, Catena verlag. 370 pp.
- LEHRE, A.K.**, 1981. Sediment budget of a small coast range drainage basin in North-Central California. In: *Sediment budgets and routing in forested drainage basins*. U.S.D.A. Forest service technical report PNW-141.
- LUCKMAN, B.H.**, 1992. Debris flows and snow avalanche landforms in the Lairig Ghru, Cairngorm Mountains, Scotland; *Geografiska Annaler 74A*, pp. 109-121.
- MALIK, R.S., PHOGAT, V. & JHORAR, B.S.**, 1994. Design of a sensitive and practical constant head well permeameter. *Soil Science*, Vol. 157 (2), pp. 84-90.
- MESSING, I. & JARVIS, N.J.**, 1990. Seasonal variation in field-saturated hydraulic conductivity in two swelling caly soils in Sweden. *Journal of Soil Science*, 41, pp. 229-237.
- MORGAN, R.P.C.**, 1977. Soil erosion in the United Kingdom: Field studies in the Silsoe area, 1973-5; *National College of Agricultural Engineering, Silsoe, Occasional Paper*, 4.
- NEWSON**, 1994. Hydrology and the river environment. Clarendon Press, Oxford, 221 pp.
- OOSTWOUD WIJDENES, D.J. & BRYAN, R.B.**, 1994. Gully headcuts as sediment sources on the Njemps Flats and initial low-cost gully control measures. *Advances in GeoEcology*, 27, pp. 205 – 229.
- OOSTWOUD WIJDENES, D.J. & ERGENZINGER, P.**, 1998. Erosion and sediment transport on steep marly hillslopes, Draix, Haute-Provence, France; an experimental field study. *Catena*, 33, pp. 179-200.
- OROMBELLI, G. & PORTER, S.C.**, 1983. Lichen growth curves for the southern flank of the Mont Blanc Massif, western Italian Alps. In: *Arctic and Alpine Research*, Vol. 15, No. 2, pp. 193-200.
- PHILLIPS, J.D.**, 1991. Fluvial sediment budgets in the North Carolina Piedmont; *Geomorphology* 4, pp. 231-241.
- POSTMA, R.**, 1988. Model voor de initiatie van Debris flows; Unpublished report, Utrecht University, Department of Physical Geography.
- RIEZEBOS, H.Th. & DE ROO, A.P.J.**, 1996. Modelling systems in physical geography, Volume I, an introduction. college syllabus, Utrecht University, Department of Physical Geography.

- REID, L.M. & DUNNE, T.** 1996. Rapid evaluation of sediment budgets. *GeoEcology paperback*. Reiskirchen, Catena verlag. 164 pp.
- SALOMÉ, A.I. & BEUKENKAMP, P.C.**, 1989. Geomorphological mapping of a high-mountain area, in black and white. *Zeitschrift für Geomorphologie (Neue Folge)*, 33 (1), pp. 119-123.
- SELBY, M.J.**, 1993. Hillslope Materials and Processes; *Oxford University Press*: Oxford.
- SHAW, E.**, 1994. Hydrology in practice. Third edition, Chapman & Hall, 569 pp.
- SINGH, P. & KUMAR, N.**, 1997. Effect of orography on precipitation in the western Himalayan region. *Journal of Hydrology*, 199, pp 183-206.
- SMITH, R.E. & PARLANGE, J.Y.**, 1978. A parameter-efficient hydrologic infiltration model. *Water Resources Research*, 14, pp. 533-538.
- SPEE, P.J.M. & VISSER, S.M.**, 1999. Sediment Budget Analysis; Riou Bourdoux catchment. Unpublished report, Utrecht University, Department of Physical Geography.
- SUMMERFIELD, M.A.**, 1992. Global Geomorphology: An introduction to the study of landforms; John Wiley & Sons, Inc., New York.
- SUTHERLAND, R.A.**, 1990. Variability of in-channel sediment storage within a small semiarid drainage basin; *Physical Geography*, 11, pp. 75-93.
- SWANSON, J.F., JANDA, R.J., DUNNE, T. & SWANSTONS, D.N.**, 1982. Sediment budgets and routing in forested drainage basins; *General technical report, United States Department of Agriculture*.
- TAKAHASHI, T.**, 1981. Debris flow; *Annual Review of Fluid Mechanics* 13, pp. 57-77.
- TERRY, J.P.**, 1996. Erosion pavement formation and slope process interactions in commercial forest plantations, northern Portugal. *Zeitschrift für Geomorphologie*, 40, 1, pp. 97-115.
- VAN ASCH, Th.W.J.**, 1992. Landdegradatie, Deel 1: *Massabeweging*; college syllabus, Utrecht University, Department of Physical Geography.
- VAN ASCH, TH. W. J.**, 1996. Landdegradatie, Deel 2: *Bodemerosie*, college syllabus, Utrecht University, Department of Physical Geography.
- VAN ASCH, Th.W.J. & MULDER, H.F.H.M.**, 1988. Risicokartering van massabewegingen in alpiene bosgebieden; Een kwantitatieve aanpak. *Nederlandse Geografische studies*, 63, pp. 125-136.
- VAN ASCH, Th.W.J. & VAN STEIJN, H.**, 1991. Temporal patterns of mass movements in the French Alps; *Catena* 18, pp. 515-527.
- VAN DEN BERG, J.H. & VAN GELDER**, 1999. Sedimentary structures (syllabus). Utrecht University, Department of Physical Geography.
- VAN ZUIDAM & CANCELADO**, 1987. ITC Textbook of Photo-Interpretation, Vol. 3. Ch. 6, Enschede, ITC, 310 pp.
- VARNES, D.J.**, 1958. Landslide types and processes; *Highway research board, special report* (Washington, DC), 29:20-47.
- VARNES, D.J.**, 1975. Slope movements in the Western United States; In: *Mass wasting* (Norwich: Geo Abstracts), pp. 1-17.
- WARD, R.C. & ROBINSON, M.**, 1990. Principles of Hydrology. 3<sup>rd</sup> edition. McGraw-Hill, London. 365 pp.
- WHITTOW, J.**, 1984. Dictionary of physical geography. London, Penguin books. 591 pp.
- WOLMAN, M.G. & GERSON, R.**, 1978. Relative scales of time and effectiveness of climate in watershed geomorphology. *Earth Surface Processes*, Vol. 3, pp. 189-208.